

THE ROLE OF CHROMATIN STRUCTURE IN CELLULAR RESPONSES TO BACTERIAL  
CYTOLETHAL DISTENDING TOXIN IN SACCHAROMYCES CEREVISIAE MODEL



A Dissertation Submitted in Partial Fulfillment of the Requirements  
for the Degree of Doctor of Philosophy in Medical Microbiology  
Medical Microbiology, Interdisciplinary Program  
Graduate School  
Chulalongkorn University  
Academic Year 2019  
Copyright of Chulalongkorn University

บทบาทของโครงสร้างโครมาตินในการตอบสนองของเซลล์ต่อสารพิษไซโตลิติกเหน็ดงจาก  
แบคทีเรียในโมเดลยีสต์



วิทยานิพนธ์นี้เป็นส่วนหนึ่งของการศึกษาตามหลักสูตรปริญญาวิทยาศาสตรดุษฎีบัณฑิต  
สาขาวิชาจุลชีววิทยาทางการแพทย์ สหสาขาวิชาจุลชีววิทยาทางการแพทย์  
บัณฑิตวิทยาลัย จุฬาลงกรณ์มหาวิทยาลัย  
ปีการศึกษา 2562  
ลิขสิทธิ์ของจุฬาลงกรณ์มหาวิทยาลัย

Thesis Title THE ROLE OF CHROMATIN STRUCTURE IN CELLULAR RESPONSES  
TO BACTERIAL CYTOLETHAL DISTENDING TOXIN IN SACCHAROMY  
CES CEREVISIAE MODEL

By Mr. Siriyod Denmongkolchai

Field of Study Medical Microbiology

Thesis Advisor Associate Professor ORANART MATANGKASOMBUT, Ph.D.

---

Accepted by the Graduate School, Chulalongkorn University in Partial Fulfillment of the  
Requirement for the Doctor of Philosophy

..... Dean of the Graduate School  
(Associate Professor THUMNOON NHUJAK, Ph.D.)

DISSERTATION COMMITTEE

..... Chairman  
(Professor NATTIYA HIRANKARN, Ph.D.)

..... Thesis Advisor  
(Associate Professor ORANART MATANGKASOMBUT, Ph.D.)

..... Examiner  
(Assistant Professor PANIDA THANYASRISUNG, Ph.D.)

..... Examiner  
(Assistant Professor KANITHA PATARAKUL, Ph.D.)

CHULALONGKORN UNIVERSITY

ศิริยศ เต็มมงคลชัย : บทบาทของโครงสร้างโครมาตินในการตอบสนองของเซลล์ต่อสารพิษไซโตล็ดิโทลดิสเทนดิง จากแบคทีเรียโมเดลยีสต์. (

THE ROLE OF CHROMATIN STRUCTURE IN CELLULAR RESPONSES TO BACTERIAL CYTOLETHAL DISTENDING TOXIN IN SACCHAROMYCES CEREVISIAE MODEL) อ.ที่ปรึกษาหลัก : รศ. ทญ.อรนาฎ มาตังคสมบัติปร.ด.

สารพิษไซโตล็ดิโทลดิสเทนดิง (Cytotoxic distending toxin, CDT) เป็นสารพิษจากแบคทีเรียที่เป็นพิษต่อสารพันธุกรรม โดยหน่วยย่อย ซีดีทีบี (CdtB) มีลักษณะคล้ายเอ็นไซม์ดีเอ็นเอส ทำให้เกิดความเสียหายต่อดีเอ็นเออันนำไปสู่การหยุดชะงักของวัฏจักรเซลล์และทำให้เซลล์ตาย การศึกษาก่อนหน้านี้พบว่าประสิทธิภาพในการทำลายดีเอ็นเอของสารพิษนี้ค่อนข้างต่ำเมื่อทำปฏิกิริยาในหลอดทดลอง นอกจากนี้ยังพบว่า การกลายพันธุ์ที่ตำแหน่งที่มีการเติมหมู่ฟอสเฟตของฮิสโตนเฮกซ์2บี (histone H2B) (S10A) ซึ่งเป็นส่วนสำคัญของกรดนิวคลีอิกโครมาตินในระหว่างการเกิด apoptosis ทำให้ยีสต์มีความต้านทานต่อซีดีทีบีเพิ่มขึ้น ดังนั้นการศึกษานี้จึงตั้งสมมติฐานว่าโครงสร้างของโครมาตินอาจเกี่ยวข้องกับการทำงานของซีดีทีบี จึงตรวจสอบว่าหน้าที่ควบคุมโครมาตินใด จำเป็นต่อการออกฤทธิ์ของซีดีทีบีในโมเดลยีสต์ ผลการทดลองพบว่าเมื่อตัดยีนเหล่านี้ออก เช่น ส่วนประกอบของ SWR-complex (*SWR1*, *SWC2*, *SWC5*, *SWC6*, และ *ARP6*), INO80-complex (*ARP5*), SIR-complex (*SIR2*, *SIR3*), และ Htz1 ทำให้เกิดความต้านทานต่อซีดีทีบี จากนั้นจึงได้ศึกษาถึงกลไกที่ยีสต์กลายพันธุ์ดังกล่าวใช้เพื่อต้านทานฤทธิ์ของซีดีทีบี ผลการทดลองแสดงให้เห็นว่าซีดีทีบีเดินทางไปยังนิวเคลียสได้ลดลงเมื่อมีการตัดยีนใดยีนหนึ่ง เช่น *htz1Δ*, *swr1Δ*, *swc2Δ*, *swc6Δ*, *arp6Δ*, และ *arp5Δ*. การลดลงนี้อาจเกิดจากผลกระทบของการขนส่งโปรตีนผ่าน ER ตามที่ได้มีการรายงานก่อนหน้านี้ ดังนั้นนี้อาจเป็นสาเหตุให้ยีสต์กลายพันธุ์เหล่านี้ทนต่อซีดีทีบีได้มากขึ้น นอกจากนี้ยังได้ทดสอบว่าซีดีทีบีสามารถทำลายดีเอ็นเอได้หรือไม่ โดยใช้การตัดยีน *RAD50* ซึ่งสำคัญต่อการซ่อมแซมดีเอ็นเอเป็นตัวอย่าง การตัดยีน *RAD50* ออกจากยีสต์ที่ไม่มียีน *HTZ1*, *SWR1*, *SWC2*, *SWC6*, *ARP6*, *SIR2*, และ *SIR3* ทำให้เซลล์มีความไวอย่างมากต่อซีดีทีบี จึงอนุมานได้ว่า CdtB ยังสามารถทำให้ดีเอ็นเอเสียหายได้ในยีสต์กลายพันธุ์เหล่านี้ ดังนั้นการที่เซลล์รอดชีวิตได้มากขึ้นแม้จะมีดีเอ็นเอเสียหาย อาจเป็นเพราะมันมีกระบวนการซ่อมแซมดีเอ็นเอที่ดีกว่าปกติ เมื่อค้นหายีนที่เหล่านี้ พบว่ามีสามยีนที่มีการแสดงออกมากขึ้นในยีสต์กลายพันธุ์ที่ทนต่อซีดีทีบี ได้แก่ *ADA2*, *MRC1* และ *SSL2* โดยสรุปแล้วยีนที่ควบคุมโครมาตินอาจมีความเกี่ยวข้องกับหลายๆ กระบวนการในเซลล์ระหว่างการขนส่งและการออกฤทธิ์ของซีดีทีบี นอกจากนี้ผู้วิจัยยังได้ทำการวิเคราะห์ทั้งจีโนมเพื่อศึกษาไกลอื่นๆ ภายในเซลล์ที่อาจเกี่ยวข้องกับการทำงานของซีดีทีบี โดยค้นหายีนที่เมื่อตัดออกแล้วทำให้ยีสต์ทนต่อซีดีทีบีมากขึ้น การศึกษานี้พบยีนถึง 243 ยีนที่สัมพันธ์กับหลายๆ กระบวนการในเซลล์ โดยเมื่อวิเคราะห์หา Gene ontology term ที่พบบ่อยในรายชื่อยีนนี้ พบว่า Organic anion transport (16 ยีน) เป็นเทอมที่พบในรายชื่อยีนนี้ด้วยความถี่สูงกว่าในจีโนมอย่างมีนัยสำคัญ ซึ่งพบว่า ยีสต์กลายพันธุ์เหล่านี้ก็มีการลดลงของซีดีทีบีในนิวเคลียสเมื่อเทียบกับยีสต์ปกติ การศึกษาวิจัยนี้ได้แสดงให้เห็นถึงความสัมพันธ์ของกลไกภายในเซลล์และการออกฤทธิ์ของสารพิษซีดีทีบี ซึ่งเป็นข้อมูลพื้นฐานสำหรับนำไปต่อยอดการศึกษาถึงวิธีที่จะต่อสู้กับสารพิษนี้ รวมไปถึงอาจนำไปประยุกต์ใช้กับงานแขนงอื่น อย่างเช่น การรักษามะเร็ง เป็นต้น

|            |                        |                                  |
|------------|------------------------|----------------------------------|
| สาขาวิชา   | จุลชีววิทยาทางการแพทย์ | ลายมือชื่อนิสิต .....            |
| ปีการศึกษา | 2562                   | ลายมือชื่อ อ.ที่ปรึกษาหลัก ..... |

## 5587809720 : MAJOR MEDICAL MICROBIOLOGY

KEYWORD: Aggregatibacter actinomycetemcomitans; Cytolethal distending toxin; Cytotoxicity; Chromatin regulators; Chromatin structure; Saccharomyces cerevisiae

Siriyod Denmongkholchai :

THE ROLE OF CHROMATIN STRUCTURE IN CELLULAR RESPONSES TO BACTERIAL CYTOLETHAL DISTENDING TOXIN IN SACCHAROMYCES CEREVISIAE MODEL. Advisor: Assoc. Prof. ORANART MATANGKASOMBUT, Ph.D.

Cytolethal distending toxin subunit B (CdtB) is a DNase I-like bacterial genotoxin that causes DNA damage leading to cell cycle arrest and cell death. Previous reports demonstrated that CdtB has low level of DNase activity *in vitro*. Besides, a mutation at histone H2B phosphorylation site required for chromatin condensation during apoptosis (S10A) conferred partial resistance to CdtB in *Saccharomyces cerevisiae* model. Therefore, we hypothesized that chromatin structure may affect CdtB function. In this study, we identified chromatin regulators required for CdtB cytotoxicity in yeast. We found that deletions of certain components of SWR-complex (*SWR1*, *SWC2*, *SWC5*, *SWC6*, and *ARP6*), INO80-complex (*ARP5*), SIR-complex (*SIR2*, *SIR3*), and Htz1 led to CdtB resistance. We investigated the mechanisms by which these mutations could confer CdtB resistance. Our results showed that CdtB nuclear localization, as observed by confocal fluorescence microscopy, was reduced in several mutants such as *htz1Δ*, *swr1Δ*, *swc2Δ*, *swc6Δ*, *arp6Δ*, and *arp5Δ*. This may be due to their effects on protein transport through ER reported in a previous study. Therefore, reduced CdtB nuclear localization may lead to increased survival in these mutants. We also determined whether CdtB could induce DNA damages in these mutants by using *rad50Δ* as DNA damage indicator. Deletion of *RAD50* in strains lacking *HTZ1*, *SWR1*, *SWC2*, *SWC6*, *ARP6*, *SIR2*, and *SIR3* led to CdtB hypersensitivity, suggesting that CdtB could induce DNA damage. Thus, the increased survival despite DNA damage may be due to enhanced DNA repair. We showed that three DNA repair genes including *ADA2*, *MRC1* and *SSL2* were upregulated in certain mutants. Taken together, chromatin regulators may be involved in several cellular processes during CdtB transport and intoxication. In addition, we performed a genome-wide screen for gene deletions that confer CdtB resistance. A list of 243 genes related to various processes was identified in the screen. The Gene Ontology term organic anion transport (16 genes) was significantly enriched in the gene list. We found that these mutants also showed reduced nuclear localization of CdtB. The results from this study provide further insights into the complex interplay of multiple host factors with CdtB. This information will be useful for further investigation into strategies to combat CdtB genotoxins and/or to develop them in other applications such as targeting cancer cells.

Field of Study: Medical Microbiology

Student's Signature .....

Academic Year: 2019

Advisor's Signature .....

## ACKNOWLEDGEMENTS

I would like to express my deeply grateful thank to my advisor, Associate Professor Oranart Matangkasombut, D.D.S., Ph.D., Department of Microbiology, Faculty of Dentistry, Chulalongkorn University, for her valuable suggestion, guidance, kindness, encouragement and helps throughout this study. I am thankful to my examiners, Professor Nattiya Hirankarn, M.D., Ph.D., Associate Professor Kanitha Patarekul, M.D., Ph.D., Assistant Professor Panida Thanyasrisung, D.D.S., Ph.D. and Associate Professor Laran T. Jensen, Ph.D. for their support, marvelous ideas and meticulous methodology suggestion. In addition, I thank Professor Gerald R. Fink, Stephen Buratowski, Chuenchit Boonchird, and Michael-Christopher Keogh for kindly providing strains and plasmids.

Thankfulness would be given to all members of RU on Oral Microbiology and Immunology, especially Miss Sureeporn Muangsawat at Chulalongkorn University and Mrs. Sarocha Choochuay at biotechnology laboratory, Chulabhorn Research Institute for laboratory technique suggestions, encouragement and assistances. I also thank the Oral Biology Research Center, Faculty of Dentistry, Chulalongkorn University for facility support. Furthermore, I would like to thank the grant supported by the Royal Golden Jubilee Ph.D. Program (Grant No. PHD/0133/2554).

Thanks to all my friends and the deepest sincere gratitude to my parent and family for their love, support, understanding and encouragement.

Siriyod Denmongkholchai

## TABLE OF CONTENTS

|  | Page |
|--|------|
| .....  | iii  |
| ABSTRACT (THAI).....   | iii  |
| .....  | iv   |
| ABSTRACT (ENGLISH).....  | iv   |
| ACKNOWLEDGEMENTS.....  | v    |
| TABLE OF CONTENTS.....   | vi   |
| LIST OF TABLES.....  | x    |
| LIST OF FIGURES.....   | xii  |
| CHAPTER I: INTRODUCTION.....   | 15   |
| Background.....  | 15   |
| Hypothesis.....  | 16   |
| Objectives.....  | 16   |
| CHAPTER II: LITERATURE REVIEW.....   | 17   |
| 1. Cytolethal Distending Toxin.....  | 17   |
| 1.1. The discovery of cytolethal toxin.....                                  | 17   |
| 1.2. Sequences and holotoxin structure of cytolethal distending toxin.....   | 17   |
| 1.3. Functional residues of cytolethal distending toxin.....                 | 20   |
| 1.4. Biogenesis of cytolethal distending toxin.....                          | 23   |
| 1.5. Cellular internalization of cytolethal distending toxin.....            | 24   |
| 1.6. Cellular responses to cytolethal distending toxin.....                  | 24   |
| 1.7. The role of cytolethal distending toxin in the periodontal disease..... | 28   |

|   |    |
|---|----|
| 2. DNA Double-strand break damages and repair .....                             | 36 |
| 3. Chromatin structure and regulation.....                                      | 37 |
| 3.1. H2A.Z (Htz1) histone variant, SWR- and INO80-complexes .....               | 39 |
| 3.2. SIR complex.....   | 41 |
| 3.3. Histone modifying enzymes.....   | 42 |
| 4. <i>Saccharomyces cerevisiae</i> , a powerful model for molecular study ..... | 43 |
| 5. Chromatin structure and cytolethal distending toxin activity .....           | 44 |
| CHAPTER III: MATERIALS AND METHODS .....  | 46 |
| 1. Preparation and general protocols.....                                       | 46 |
| 1.1. Yeast strains and media.....   | 46 |
| 1.2. Confirmation of gene deletion of CdtB resistant mutants.....               | 50 |
| 1.3. Bacterial strains and media .....  | 51 |
| 1.4. E. coli competent cells preparation .....                                  | 51 |
| 1.5. Plasmids and transformation method .....                                   | 51 |
| 1.6. Yeast and bacterial frozen stocks .....                                    | 52 |
| 1.7. Plasmid extraction.....  | 52 |
| 1.8. Recombinant CdtB expression, purification and determination .....          | 52 |
| 1.9. Immunoblot for detection of CdtB expression.....                           | 54 |
| 1.10. Cell cycle analysis by flow cytometry .....                               | 54 |
| 2. CdtB susceptibility test.....  | 55 |
| 2.1. CdtB susceptibility and survival plating assay .....                       | 55 |
| 2.2. CdtB susceptibility in genome wide screening .....                         | 55 |
| 3. CdtB-Htz1 interaction testing.....   | 56 |
| 3.1. Immunoprecipitation of CdtB and Htz1 .....                                 | 56 |



|   |    |
|---|----|
| 3.2. Chromatin Immunoprecipitation (ChIP).....  | 56 |
| 4. CdtB localization study .....  | 57 |
| 4.1. Yeast cells fractionation.....   | 57 |
| 4.2. Immunofluorescence for CdtB localization .....   | 58 |
| 4.3. Nuclear localization of CdtB using CdtB-EGFP fusion protein .....                                      | 59 |
| 5. In vitro CdtB activity.....  | 62 |
| 5.1. Chromatin extraction.....  | 62 |
| 5.2. In vitro CdtB activity on plasmid.....   | 63 |
| 5.3. In vitro CdtB activity on chromatin .....  | 63 |
| 6. The investigation of upregulated-DNA repair genes in the mutants.....                                    | 64 |
| 6.1. Data mining for DNA repair genes upregulation.....   | 64 |
| 6.2. RNA extraction .....   | 65 |
| 6.3. Quantitative real-time PCR (qPCR).....   | 65 |
| 7. Screening molecular processes in CdtB resistant strains .....  | 67 |
| 7.1. Perspective of molecular processes that are required for CdtB cytotoxicity .....                       | 67 |
| CHAPTER IV: RESULTS.....  | 68 |
| Objective 1. To identify chromatin regulatory genes that are required for cytotoxicity of CdtB.<br>.....    | 69 |
| Objective 2. To examine the mechanisms how chromatin regulatory genes, facilitate CdtB<br>cytotoxicity..... | 81 |
| 2.1. Testing the physical interaction between CdtB and Htz1 protein.....                                    | 81 |
| 2.2. Reduction of CdtB nuclear localization could be a CdtB-resistant mechanism .....                       | 83 |
| 2.3. Investigation of DNA damage caused by CdtB in CdtB resistant mutants .....                             | 91 |
| 2.4. Investigating the CdtB on chromatin using <i>in vitro</i> DNase activity assay .....                   | 93 |

|   |     |
|---|-----|
| 2.5. DNA repair gene expression in CdtB resistant candidates .....                                    | 96  |
| Objective 3. To globally identify genes that are required for CdtB cytotoxicity.....                  | 101 |
| 3.1 Genome-wide screening of CdtB resistant yeast deletion strains .....                              | 101 |
| 3.2 Gene Ontology analysis of genes required for CdtB cytotoxicity .....                              | 101 |
| 3.3 CdtB localization in CdtB resistant candidates which involved in organic anion<br>transport ..... | 103 |
| CHAPTER V: DISCUSSION.....  | 118 |
| 1. Chromatin regulators and CdtB cytotoxicity .....   | 118 |
| 1.1. Interaction with Htz1 .....  | 120 |
| 1.2. CdtB nuclear localization.....   | 120 |
| 1.3. DNA damage.....  | 121 |
| 1.4. DNA repair.....  | 122 |
| 1.5. Other mechanisms.....  | 123 |
| 2. Genome-wide identification of host genes required for CdtB cytotoxicity. ....                      | 125 |
| CHAPTER VI: CONCLUSION .....  | 128 |
| REFERENCES .....  | 129 |
| VITA .....  | 163 |

## LIST OF TABLES

|  | Page |
|--|------|
| Table 1 Examples of CDT producers and possible contribution of CDT in pathology. ...   | 18   |
| Table 2 GenBank accession number of DNA sequences, protein sequences and protein data bank (PDB) identification of CdtB structure..... | 19   |
| Table 3 Comparison of the predicted amino acid sequences of three subunits of A. actinomycetemcomitans CDT .....                       | 20   |
| Table 4 Responses of fibroblasts to cytolethal distending toxins .....   | 29   |
| Table 5 Responses of epithelial cells to cytolethal distending toxins.....   | 31   |
| Table 6 Responses of hematopoietic cells to cytolethal distending toxins .....   | 33   |
| Table 7 C-module subunit requirement for SWR-C integrity. ....   | 40   |
| Table 8 Genes that are related to chromatin structure in this study .....  | 47   |
| Table 9 Synthetic amino acid and trace element components (Hopkins mixture) .....  | 49   |
| Table 10 Primers and annealing temperature for CdtB resistant strains confirmation. <sup>a</sup> .                                     | 50   |
| Table 11 Plasmids in this study .....  | 53   |
| Table 12 Primers and melting temperature of DNA repair gene expression.....  | 66   |
| Table 13 The summary of phenotype by CdtB susceptibility test and subunit functions  | 75   |
| Table 14 DNA content analysis of CdtB-treated yeast .....  | 78   |
| Table 15 List of upregulated genes in DNA damage conditions and upregulation in CdtB resistant candidates. ....                        | 97   |
| Table 16 List of 16 organic anion transport genes that showed CdtB resistant phenotype.....  | 105  |
| Table 17 CdtB resistant genes that associate with endoplasmic reticulum .....  | 109  |

Table 18 CdtB resistant genes that associate with transcriptional regulation.....113



## LIST OF FIGURES

|   | Page |
|---|------|
| Figure 1 Functional residues of CDT are conserved among CDT producers.....  | 21   |
| Figure 2 PCR-based gene deletion strategy. ....   | 49   |
| Figure 3 The sequence of CdtB-EGFP construction .....   | 61   |
| Figure 4 Growth curve analysis of CdtB induction in yeast.....  | 68   |
| Figure 5 CdtB resistant profile of chromatin regulatory gene mutants.....   | 73   |
| Figure 6 CdtB non-resistant profile of chromatin regulatory gene mutants.....   | 74   |
| Figure 7 Strain confirmation by the PCR technique.....  | 76   |
| Figure 8 CdtB expression in CdtB resistant mutants.....   | 76   |
| Figure 9 Cycloheximide sensitivity test.....  | 77   |
| Figure 10 Effect of CdtB on the G1 cell cycle phase of the mutants. ....  | 79   |
| Figure 11 Effect of CdtB on the S cell cycle phase of the mutants.....  | 79   |
| Figure 12 Effect of CdtB on the G2/M cell cycle phase of the mutants.....   | 80   |
| Figure 13 Physical interaction between recombinant CdtB and Htz1 protein in vitro.....  | 82   |
| Figure 14 Chromatin immunoprecipitation result of CdtB and Htz1 interaction.....  | 82   |
| Figure 15 Cell fractionation and an immunoblotting assay of WT yeast. ....  | 84   |
| Figure 16 CdtB localization by the immunofluorescent method.....  | 84   |
| Figure 17 The expression of CdtB (29 kD) and CdtB-EGFP (59 kD) protein.....   | 87   |
| Figure 18 Spot assay of serial dilutions of wild-type and rad50 $\Delta$ strains with pYES-CdtB and pYES-CdtB-EGFP in comparisons to pYES2 and pYES2-EGFP on glucose and galactose media..... | 87   |

|   |     |
|---|-----|
| Figure 19 Representative fluorescent images (at 600x magnification) of localization of CdtB-EGFP and EGFP control in wild-type yeast at various concentrations of galactose ..... | 88  |
| Figure 20 Quantification of nuclear localization of CdtB-EGFP relative to EGFP at the various galactose concentrations as in figure 19 is shown in log 2 scale. ....              | 88  |
| Figure 21 Localization of CdtB-EGFP and EGFP control were examined by confocal fluorescent microscopy. ....   | 89  |
| Figure 22 Mander's coefficient was used to calculate the relative CdtB nuclear localization ratio between CdtB-EGFP and EGFP control. ....  | 90  |
| Figure 23 The deletions of RAD50 gene were confirmed by PCR with A and D specific primer. ....  | 92  |
| Figure 24 CdtB susceptibility test of CdtB resistant mutants which are defective in a DNA repair process. ....  | 92  |
| Figure 25 CdtB susceptibility test of $swc5\Delta rad50\Delta$ and $sir3\Delta rad50\Delta$ which are defective in a DNA repair process. ....                                     | 93  |
| Figure 26 Preparation of in vitro DNase assay. ....   | 95  |
| Figure 27 In vitro DNase I-like activity of CdtB in SIR2 deletion strain. ....  | 95  |
| Figure 28 The responsiveness of DNA repair gene expression to DNA damage caused by CdtB. ....   | 100 |
| Figure 29 The upregulation of DNA repair gene in CdtB resistant candidates. ....  | 100 |
| Figure 30 Biological processes of 243 candidates from yeast genome-wide screening analyzed by GO slim mapper. ....  | 103 |
| Figure 31 Molecular function of 243 candidates from yeast genome-wide screening analyzed by GO slim mapper. ....  | 104 |

|   |     |
|---|-----|
| Figure 32 Cellular components of 243 candidates from yeast genome-wide screening analyzed by GO slim mapper. ....                 | 104 |
| Figure 33 CdtB nuclear localization was reduced in mutants associated with organic anion transport. ....                          | 116 |
| Figure 34 The ratio of nuclear localization of CdtB-EGFP relative to EGFP control was calculated using Manders' coefficient. .... | 117 |



## CHAPTER I: INTRODUCTION

### THE ROLE OF CHROMATIN STRUCTURE IN CELLULAR RESPONSES TO BACTERIAL CYTOLETHAL DISTENDING TOXIN IN *SACCHAROMYCES CEREVISIAE* MODEL

#### Background

Although there have been significant advances in modern medicine, infectious diseases still remain a major threat for public health. Several infectious diseases are caused by bacterial pathogens that possess many virulence factors, including endo- and exo-toxin productions. A critical milestone to fight against infectious diseases is the understanding of their virulence factor mechanisms.

Cytolethal distending toxin (CDT) is a bacterial toxin produced by plenty gram-negative pathogens. It is well-documented that variety of bacteria express CDT as the weapon to conquer the host involved in several chronic infection including diarrhea, chancroid, hepatitis, aggressive periodontitis and etc. Toxicity of CDT greatly captured interest of researcher since it is described as the genotoxin with the ability to induce cell cycle arrest and death in mammalian cells eventually which lead the host tissue damage and reinforce the infection by immune evasion. CDT structure is described as the heterotrimeric protein namely CdtA, CdtB and CdtC. It is reported that CdtA and CdtC are the binding subunit assisting the toxin internalization to the susceptible host. Meanwhile, CdtB appears to be dominantly responsible for the genotoxic activity of CDT since its structure is greatly homologous to DNase in eukaryotic cells. Particularly, the similarity of CdtB and mammalian DNase I are indicated at five conserved residues. Disruption of catalytic residues in CdtB will make it fail to induce DNA damage.

As CDT causes toxic via damage on DNA, there is certain study supporting translocation of CdtB from extracellular environment to host nucleus. It is described that nuclear localization signal on CdtB is important to maintain its genotoxic potential. CdtB acts as the catalytic enzyme to cleave DNA, resulting in DNA breaks. DNA damage response (DDR) will take an action to process the DNA damage caused by CdtB



consequently via ATM/ATR pathway, p53, p21 and cyclin-dependent kinases. As the result, cell cycle was inhibited which provide the time for DNA repair process. The process of caspase-dependent cell death will be activated if the damage cannot be recovered.

The action of CdtB mechanism on DNAs is interesting since the magnitude of CdtB function between *in vitro* and *in vivo* is not equal. It suggests that the environment of *in vivo* model is more optimized than *in vitro* providing some protein factors for CdtB action. *Saccharomyces cerevisiae* was used as the model for mode of cell death of CdtB. Surprisingly, fundamental apoptosis markers such as ROS production, the appearance of phosphatidylserine residues on the cell surface, and involvement of caspase gene level are not major roles for yeast apoptosis. However, our previous study showed that a defect in chromatin condensation led to a partial resistance to CdtB in *S. cerevisiae*. We hypothesize that chromatin structure might affect CDT function by controlling access to DNA. Here, we use *S. cerevisiae* as a model to analyze CdtB-susceptibility of yeast strains with mutations in chromatin-related genes. Mutant strains that show resistance to CdtB may interfere with CdtB-chromatin interaction. Investigation of CdtB resistant mechanism was performed including nuclear localization, appearance of DNA damage caused by CdtB, and direct interaction between CdtB and some host factor. This study helps to understand how host factors, particularly chromatin structure, affect CdtB cytotoxicity.

### Hypothesis

Chromatin structure has a role in CdtB cytotoxicity

### Objectives

- 1) To investigate chromatin regulatory genes that are required for CdtB cytotoxicity.
- 2) To examine the mechanism how chromatin regulatory genes, facilitate CdtB cytotoxicity.
- 3) To globally identify genes that are required for CdtB cytotoxicity.

## CHAPTER II: LITERATURE REVIEW

### 1. Cytolethal Distending Toxin

#### 1.1. The discovery of cytolethal toxin

In 1998, Johnson and Lior discovered a new heat-labile toxin in the bacterial culture media of certain serogroup of *Escherichia coli* and certain species of *Campylobacter* [1, 2]. The media was toxic to several epithelial cells including CHO, Vero, HeLa, and HEp-2 cells, but not Y-1, mouse adrenal tumor cells. Because Y-1 is commonly used to investigate heat-labile or heat-stable enterotoxin from bacteria, but it was not susceptible to CDT, CDT was classified as a new toxin. Cell distension and cytotoxicity were observed when CHO cells were exposed to the toxin for 24h and over the next 96h. Due to these properties, the toxin was named “Cytolethal Distending Toxin (CDT)”. Moreover, CDTs were produced by other Gram-negative pathogens [3, 4], while there has been no report in Gram-positive bacteria. Most of these Gram-negative bacteria are important pathogens that are responsible for global food- and water-borne diseases, diarrhea, aggressive periodontitis, and others as shown in **Table 1**.

#### 1.2. Sequences and holotoxin structure of cytolethal distending toxin

CDT is a part of AB-type toxin superfamily, which can be classified into many classes, including AB, AB<sub>2</sub>, AB<sub>5</sub>, AB<sub>7</sub>, and A<sub>2</sub>B<sub>7</sub> based on the assembly of toxin subunits. “A” stands for “active subunit” that contains the enzymatic activities, while “B” stands for “binding subunit” that assists in cell internalization of the A-chain. Besides CDT, the activity of A subunits of several AB toxins results in the inhibition of protein synthesis, cell distention and lethality, interruption of cell homeostasis, and neurotoxicity. Unlike others, CDTs are genotoxin and cyclomodulin that can cleave host DNA and induce cellular responses to the DNA damage such as cell cycle arrest and apoptosis. Interestingly, CDT is the only one amongst the AB-type toxins that can localize to the nucleus while others have targets in the cytosol [5].

**Table 1** Examples of CDT producers and possible contribution of CDT in pathology.

| CDT producers   | Pathology                | Possible contribution of CDT   | References  |
|---|--------------------------|--|-------------|
| <i>Aggregatibacter actinomycetemcomitans</i>          | Aggressive periodontitis | <ul style="list-style-type: none"> <li>● Tissue destruction and immune evasion</li> </ul>  | [6-9]       |
| <i>Campylobacter jejuni</i>                           | Inflammatory diarrhea    | <ul style="list-style-type: none"> <li>● Prolongation of symptoms</li> <li>● Persistence of infection</li> </ul>   | [1, 10-12]  |
| Colorectal cancer- associated <i>Escherichia coli</i> | Colorectal cancer        | <ul style="list-style-type: none"> <li>● Potential promotion of cancer initiation of progression</li> <li>● Potential promotion of carcinogenesis</li> </ul> | [13]        |
| <i>Haemophilus ducreyi</i>                            | Chancroid lesions        | <ul style="list-style-type: none"> <li>● Development of ulcers</li> <li>● Persistence of lesion</li> </ul>   | [6, 14, 15] |
| <i>Helicobacter hepaticus</i>                         | Hepatitis                | <ul style="list-style-type: none"> <li>● Inflammation induced carcinogenesis</li> </ul>  | [16, 17]    |
| <i>Salmonella enterica</i> serovar Typhi              | Diarrhea                 | <ul style="list-style-type: none"> <li>● Prolongation of symptoms</li> <li>● Persistence of infection</li> </ul>   | [18, 19]    |
| <i>Shigella dysenteriae/boydii</i>                    | Diarrhea                 | <ul style="list-style-type: none"> <li>● Role to be defined</li> </ul>   | [20, 21]    |

(This table was modified from [22])

The molecular blueprint of CDT was revealed by sequencing of CDT-encoding loci from enteropathogenic *E. coli* (EPEC) [23] and enterotoxigenic *E. coli* (ETEC) [24]. The mRNA of CDT was transcribed from the polycistronic operon, which includes *cdtA*, *cdtB*, and *cdtC*. CdtA and CdtC are binding subunits facilitating toxin internalization. CdtB is the active subunit with conserved-residues across different species, but the *cdt* operon structures vary (review in [25]; **Figure 1**). Published reference DNA sequences, protein sequences, and CdtB structures are listed in **Table 2**. CDT was observed in several pathogens. Examples include *A. actinomycetemcomitans* Y4 (b strain), a virulent strain associated with localized aggressive periodontitis with high leukotoxin expression [26]; *C. jejuni* strain 81-176 (CH5; Penner serotype 23/36) isolated from a

diarrheal patient with raw milk consumption [27]; and *H. ducreyi* strain 35000, a well-characterized isolate of chancroid pathogen that showed cytotoxicity in HeLa, CHO, and HEP-2 cells [28, 29]. *E. coli* produces various types of CdtB depending on their serotypes which can be distinguished by PCR [30]. For example, *cdt* type-I, II and III were identified from the O86:H34 EPEC strain E6468/62, O128:H<sup>-</sup> EPEC strain 91422-88, and the O78 calf strain 1404, respectively [31]. Among the various CDT species, the amino acid sequence of AaCDT is very close to that of HdCDT, but it shares less than 50% identity to CjCDT or EcCDT ([32]; Table 3). This suggests that CDT from *A. actinomycetemcomitans* may have similar mechanisms to that of *H. ducreyi*, but not to that of either *C. jejuni* or *E. coli*. These sequence similarities were analyzed using the protein accession numbers in Table 2 [32].

**Table 2** GenBank accession number of DNA sequences, protein sequences and protein data bank (PDB) identification of CdtB structure

| Toxin producers   | DNA sequences<br>(accession no.) | Protein sequences<br>(accession no.) | Structure<br>(accession no.) |
|---|----------------------------------|--------------------------------------|------------------------------|
| <i>Aggregatibacter actinomycetemcomitans</i><br>(Strain Y4)       | AB011405<br>[32]                 | BAA33486<br>[32]                     | 2F2F<br>[33]                 |
| <i>Campylobacter jejuni</i><br>(Strain CH5)                       | AF038283<br>[11]                 | AAF16679<br>[11]                     | no study                     |
| <i>Haemophilus ducreyi</i><br>(Strain 35000)                      | U53215<br>[28]                   | AAB57726<br>[28]                     | 1SR4<br>[34]                 |
| <i>Escherichia coli</i><br>(O86:H34/ <i>cdt</i> -I)               | U03293<br>[23]                   | AAD10622<br>[23]                     | no study                     |
| <i>Escherichia coli</i><br>(O128:H <sup>-</sup> / <i>cdt</i> -II) | U04208<br>[24]                   | AAA18786<br>[24]                     | 2F1N<br>[35]                 |
| <i>Escherichia coli</i><br>(Strain 1404/ <i>cdt</i> -III)         | U89305<br>[36]                   | AAC45443<br>[36]                     | no study                     |

**Table 3** Comparison of the predicted amino acid sequences of three subunits of *A. actinomycetemcomitans* CDT

| AaCDT gene product | % Identity with |        |         |       |       |
|--------------------|-----------------|--------|---------|-------|-------|
|                    | CDT-I           | CDT-II | CDT-III | CjCDT | HdCDT |
| CdtA               | 29              | 22     | 22      | 27    | 91    |
| CdtB               | 48              | 45     | 46      | 48    | 97    |
| CdtC               | 19              | 23     | 19      | 20    | 94    |

(This table was modified from [32])

### 1.3. Functional residues of cytolethal distending toxin

Since the CdtB-target cells suffer from DNA damage, comparative studies between CDT and DNA damaging agents have provided insights into CDT function [37-39]. Certain DNA damaging agents, such as ionizing radiation (IR) and etoposide, activated similar pathways to CDT [38]. This suggested that CDT likely causes DNA breaks. When the amino acid sequence of bovine deoxyribonuclease (EC 3.1.21.1) was compared to EcCdtB, conserved motifs were found [40]. Furthermore, the X-ray crystallographic structure of HdCdtB also showed the between catalytic sites of CdtB and an enzyme of the DNase I family [34].

Several conserved amino acid residues important for toxin functions have been identified, including DNase and phosphatase catalytic residues, nuclear transport residues, and substrate binding residues. The active site residues of bovine DNase I were determined as His134 and His252, which are conserved in HdCdtB and AaCdtB at His160 and His274 in both species [34, 41]. The catalytic residues in other CdtB species are different, for example, the conserved residues are His134 in CjCdtB, and for EcCdtB-I, and EcCdtB-II are His152, and His154, respectively [40, 42, 43]. CdtB requires divalent cation for its activity [44]. In an in vitro DNase assay, MgCl<sub>2</sub> and CaCl<sub>2</sub> at 50 mM, and MnCl<sub>2</sub> at 100 mM, were the optimal concentrations for plasmid digestion. CdtB cofactors, therefore, are not restricted to Mg<sup>2+</sup> [45]. The metal binding residues of AaCdtB were found at Asp199 and Asp273, which are conserved in DNase I-metal binding residues at Asp168 and Asp251 [41, 46]. For this reason, CdtB were classified as a metalloenzyme.

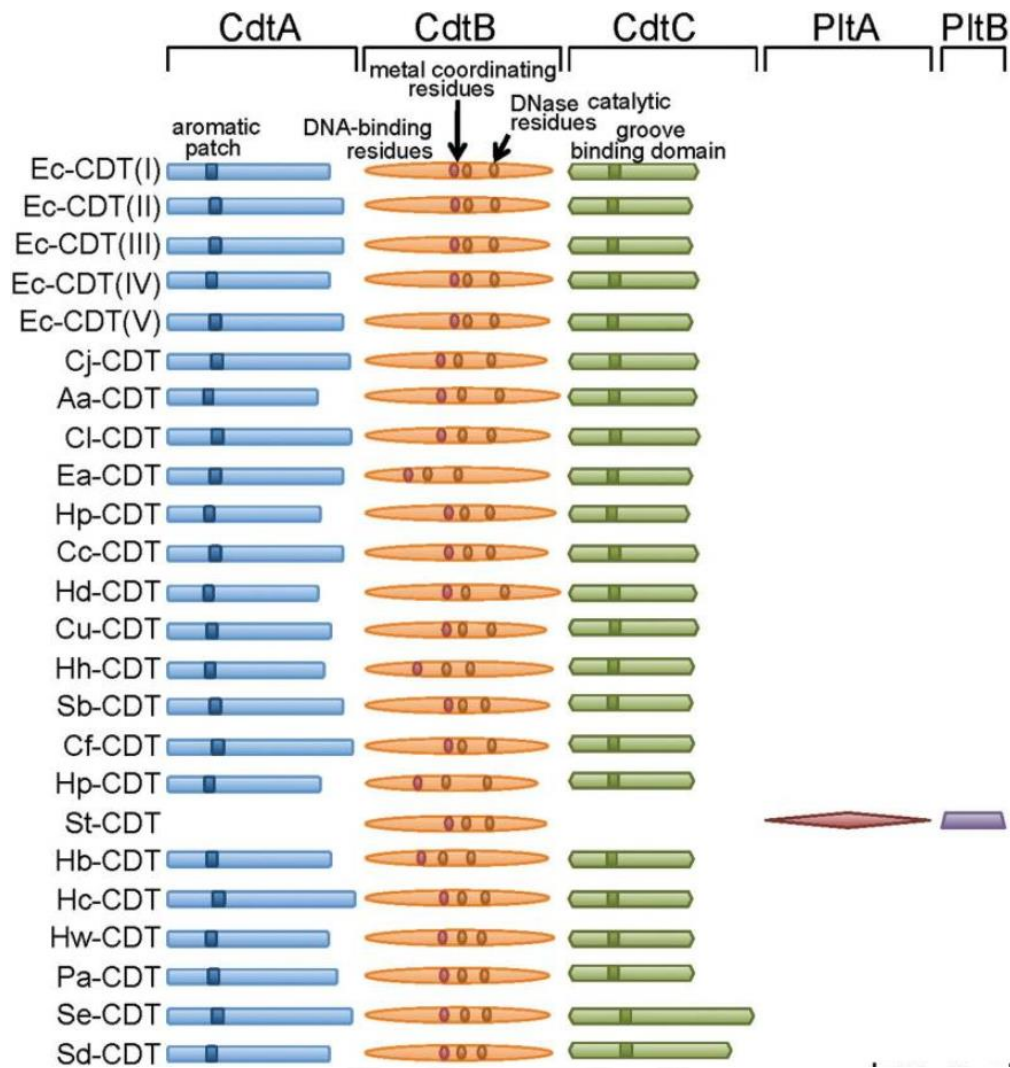


Figure 1 Functional residues of CDT are conserved among CDT producers.

[25]. The composition of CdtA, CdtB and CdtC was found in most of CDT, but not in *Salmonella typhi* which PltA and PltB assemble with CdtB to make the holotoxin. The several conserved residues were distributed to each subunit for example aromatic patch and groove binding domain are responsible for cell surface binding, whereas DNA-binding residues, metal coordinating residues, and DNase catalytic residues are responsible for toxin activity. Genuses and species are abbreviated as follows: Ec, *Escherichia coli*; Cj, *Campylobacter jejuni*; Aa, *Aggregatibacter actinomycetemcomitans*; Ci, *Campylobacter lari*; Ea, *Escherichia albertii*; Hp, *Haemophilus parasuis*; Cc, *Campylobacter coli*; Hd, *Haemophilus ducreyi*; Cu, *Campylobacter upsaliensis*; Hh, *Helicobacter hepaticus*; Sb, *Shigella boydii*; Cf, *Campylobacter fetus*; Hp, *Helicobacter pullorum*; St, *Salmonella typhi*; Hb, *Helicobacter bilis*; Hc, *Helicobacter cinaedi*; Hw, *Helicobacter winghamensis*; Pa, *Providencia alcalifaciens*; Se, *Salmonella enterica*; Sd, *Shigella dysenteriae*.

The metalloenzyme superfamily members are not only nucleases but also various phosphatases that dephosphorylate the lipid second messengers, including inositol polyphosphate 5-phosphate and sphingomyelin [47]. A novel function of AaCdtB was discovered as a phosphatidylinositol-3,4,5-triphosphate (PIP<sub>3</sub>) phosphatase [41]. The phosphatase catalytic residues were identified and were close to the DNase catalytic residues His160 and His274 of AaCdtB, including Phe156, Thr158, Tyr239, Ala240, Asp244, and His246 [48]. Phe156 and Thr158 are conserved in both CdtB and IP5P, the phosphoinositide 5-phosphatase, whereas the other four residues are conserved in both DNase I and IP5P. Intriguingly, when Ala163 residue, a putative active site, was substituted by arginine, the nuclease activity was eliminated while the phosphatase activity was decreased in half compared to WT CdtB. The DNase activity was restored and increased almost 4-fold when the Ala163Arg mutation was combined with Phe156Ile and Thr158Ala. Besides, Tyr239Arg mutation and the mutations of four DNase-I-IP5P conserved residues did not significantly change nuclease activity, but the phosphatase activity was over 50% decreased. Interestingly, all CdtB mutations on each or combined residues decrease CdtB toxicity, except for only Ala163Arg mutant whose toxicity is unchanged [48]. This result suggests that nuclease and phosphatase activity of CdtB cannot be clearly separated from each other, and both may contribute to CdtB toxicity. In addition, AaCdtB contains the cholesterol recognition amino acid consensus sequence (CRAC site), the VYIYYSR residues in positions 104-110 [49]. Proline substitutions at Val104, Tyr105 and Tyr107 reduced the cholesterol binding leading to suppressed toxin binding, internalization, cell cycle arrest, and apoptosis. Interestingly, CdtB also causes DNA damage and cell cycle arrest in budding yeast [50, 51] that lacks PIP<sub>3</sub> [52]. This suggests that only DNase activity is sufficient to cause cell toxicity.

The nuclear transport region was located at amino acid 48-124 in AaCdtB, which is different from EcCdtB that was designated as double loci of nuclear localization signals at amino acid 195-210 and 253-268 [53, 54]. Nuclear localization signal mutant (AaCdtB $\Delta$ 111aa) showed no toxicity in the yeast *Saccharomyces cerevisiae* model, suggesting the importance of the nuclear transport region to toxin activity [51].

DNA binding residues of CdtB also affected toxin efficiency. Alanine substitution of any Arg117, Arg144, and Asn201 or all of these residues in HdCdtB [34] and AaCdtB [41, 48, 55] led to reduced cell cycle arrest and inflammation. These three residues are conserved in DNase I at Arg41, Arg111, and Asn170. Interestingly, the HdCdtB (Asn201Ala) mutation decreased DNase activity on plasmid substrates [34], whereas the same mutant in AaCdtB increased the activity up to 3-fold higher than WT CdtB [48]. This phenomenon occurred when the alanine was substituted for Arg117 and Arg144 together with Asn201Ala in CdtB from both *A. actinomycetemcomitans* and *H. ducreyi*. Moreover, the three residue mutations decreased the phosphatase activity suggesting that these amino acids are not only responsible for nuclease activity, but also the phosphatase activity [48]. Furthermore, CdtB is cytotoxic in the *Saccharomyces cerevisiae* model. CjCdtB may have greater toxicity than AaCdtB, because it is highly toxic in haploid yeast, while AaCdtB was only moderately toxic [50].

#### 1.4. Biogenesis of cytolethal distending toxin

Biogenesis of AaCDT was studied using *E. coli* as a model [56, 57]. Each subunit was transcribed and translated from CDT operon as CdtA, CdtB, and CdtC. The holotoxin assembly occurred in the periplasmic space. The secretion of an unmodified CdtA, immature CdtB and immature CdtC via a sec-dependent secretory pathway have been proposed by a previous study [57]. Signal peptidase-I cleaved the immature CdtB and immature CdtC on the inner-cytoplasmic membrane to become mature proteins. On the other hand, unmodified CdtA was modified by lipoprotein-specific signal peptidase-II (lipo-CdtA) and translocated onto the outer membrane of the periplasm. Afterward, lipo-CdtA was rapidly N-terminally truncated (CdtA') after CdtC interaction. This is a key step of the holotoxin assembly process [56]. The complex of CdtA' and CdtC provided the docking site as cargo for CdtB to form the complete holotoxin. CDT may secrete out from bacteria with an unknown process or by outer membrane vesicles (OMVs) [58, 59].



### 1.5. Cellular internalization of cytolethal distending toxin

Molecular regions on the CDT molecule are important to recognize the host cell surface receptor. Several studies suggested that the internalization of CdtB is facilitated by the binding subunits CdtA and CdtC [60-62]. Localization of AaCDT has been investigated by live-cell imaging in Chinese hamster ovary cells (CHO cells) [46]. CdtA subunit contains the aromatic binding site (Tyr214) that was proposed to bind to a putative specific receptor on the target cell surface [46]. The cell surface binding of CdtC associated with the lipid raft [63]. The gangliosides, G protein-coupled receptor (TMEM181) and lipid rafts on the cell surface, are potential CDT receptors [62, 64, 65]. The binding of the AaCDT to membrane glycoproteins revealed that recombinant AaCDT binds to various type of gangliosides namely GM1 [Gal $\beta$ (1,3)GalNAc $\beta$ (1,4)[NeuAc $\alpha$ (2,3)]-Gal $\beta$ (1,4)Glc-ceramide], GM2 [GalNAc $\beta$ (1,4)[NeuAc $\alpha$ (2,3)]-Gal $\beta$ (1,4)Glc-ceramide], and GM3 [NeuAc $\alpha$ (2,3)]-Gal $\beta$ (1,4)Glc-ceramide] [62]. GM3 ganglioside is a component of the lipid rafts [65] and becomes a good candidate for the AaCDT receptor because the toxicity of the human macrophage cell line was observed when AaCDT was incubated with GM3 liposomes and infected to the cell line [62]. Moreover, CdtC provides the CRAC sequence (LIDYKGGK) to bind on the lipid rafts [63]. CdtB-CdtC heterodimer can be endocytosed via the endosomal vesicles and delivered to the Golgi apparatus in CHO cells, whereas CdtA remained on the cell surface [46]. The CdtB-CdtC containing vesicles travel to the nucleus via retrograde transport which passes through the Golgi apparatus and endoplasmic reticulum [46]. ER-associated degradation (ERAD) was proposed as a pathway for CdtC elimination [62]. Finally, CdtB was localized to the nucleus and targeted the host DNA.

### 1.6. Cellular responses to cytolethal distending toxin

CDT affects the target cells differently depending on cell types. The first cytopathic effects of CDT were reported in CHO cells, an epithelial cell line, which showed cell elongation and cytotoxicity [1, 2]. Subsequently, CDT effects on other cell types have been reported, including fibroblasts, endothelium, keratinocytes, and

hematopoietic cells, especially white blood cells. Cellular phenotypes upon exposure to various CDT species are shown in **Tables 4 - 6**.

Fibroblasts are the most common cells in connective tissues and play an important role in the wound healing process by producing extracellular matrix and collagen [66]. Several fibroblasts in oral cavity such as oral fibroblasts, periodontal ligament cells (PDLC) and gingival fibroblasts (GF), showed cellular elongation and distension with pseudopodia-like protrusion stretching towards neighboring cells when exposed to AaCDT [7]. AaCDT decreased cell proliferation of both PDLC and GF [7], which may reduce wound healing efficiency leading to chronic oral diseases. Moreover, similar phenotypes of fibroblast were observed after treatment with HdCDT [67].

The biphasic cell cycle arrest was found in other fibroblast cell lines including IMR-90, HFS, and HL [68, 69]. Cyclin dependent kinase (Cdc2), which controls both in G1→S and G2→M transitions, increased the phosphorylated Cdc2 (inactive form) accumulation, detected by immunoblotting assay after 24h treatment [68]. Moreover, Rad50 foci and  $\gamma$ -H2A.X formation were observed in fibroblasts indicating the induction of DNA damage caused by HdCDT [68, 69]. Enlargement of nuclei and nuclear fragmentation were observed as signs of apoptosis, while a low level of extracellular released lactate dehydrogenase (LDH), a marker for necrosis was observed [7]. However, caspase 3, an executioner caspase, decreased its activity [7], suggesting that apoptotic cell death caused by CDT in fibroblasts may be controlled by caspase-independent fashion.

The phenotype of cell cycle arrest in epithelial cells is different from fibroblasts. G2/M cell cycle arrest was observed in various epithelial cell types such as HeLa cells, human intestinal cells H407, HEP-2 cells, and Caco-2 cells [32, 37, 42, 67, 68, 70-74]. Interestingly, the G2/M synchronized cells were arrested at the next turn of the G2/M phase after EcCDT-I exposure [37]. Phosphorylated Cdc2 (inactive form) was accumulated in epithelial cells [37, 68] similarly to fibroblasts [68]. However, the biphasic cell cycle arrest was not observed in epithelial cells [75]. Several markers for DNA damage were also detected in epithelial cells, including  $\gamma$ -H2A.X formation [71, 76]

and Mre11 foci accumulation [76]. Epithelial cell death pathways include increased pro-apoptotic/anti-apoptotic (Bax/Bcl<sub>2</sub>) protein ratio, the release of cytochrome c, and the activation of general caspases 3/7/9 [71]. Therefore, caspase-dependent apoptosis may mediate epithelial cell death. The G2 arrest property of CDT was compared to several agents such as etoposide, a topoisomerase II inhibitor that blocks the G2 cell cycle phase [77]. Caffeine has the potential to override the G2 block caused by a variety of DNA damaging agents such as etoposide [77]. Whitehouse C.A. and colleagues demonstrated that caffeine could not break the cell cycle arrest through the G2 phase in the CjCDT-treated HeLa cells [74] suggesting that CdtB may have the different mode of function to etoposide. However, caffeine could partially override the G2 arrest in HdCDT-treated HEP-2 cells [68] implying that the mode of function of CdtB from different species may be different. Another remark is that HeLa cells have a defect in p53, a tumor suppressor protein that play a role in regulation through the cell cycle and apoptosis, but HEP-2 cells do not. Therefore, p53 may be involved in CDT function. However, both skin keratinocytes (HaCaT) and Normal foreskin keratinocytes (Ad3), which carry mutated p53 and normal p53, respectively, showed G2/M arrest and inactive Cdc2 (phosphorylated form) accumulation after HdCDT exposure [68]. Thus, the induction of G2 cell cycle arrest by HdCDT was not dependent on p53 status.

Cell responsiveness of various immune cells have been reported, including dendritic cells, macrophages, and lymphocytes. Dendritic cells are an antigen presenting cell (APC) that is important for T cell activation. DNA damage in dendritic cells was found after HdCDT treatment, supported by the detection of  $\gamma$ -H2A.X formation and Mre11 foci [76]. Cell distension and G2/M arrest were not observed, but HdCDT increased the sub-G<sub>0</sub> population, which is a signal of cell death [76]. Therefore, CDT responses in dendritic cells are different from those in fibroblasts and epithelial cells. This may be because dendritic cells are non-proliferating cells. The phenotypes between proliferating and non-proliferating monocytic cells after AaCDT exposure were compared to clarify this hypothesis [78]. Proliferating monocytic cell line, U937, showed G2/M arrest and increased apoptotic markers, including DNA fragmentation, % annexin

V positive cells and caspase 3 activations [78]. In contrast, differentiated non-proliferating U937 did not show accumulation of G2/M phase population and caspase 3 activation [78]. DNA fragmentation and the percentage of annexin V positive cells were increased to a smaller magnitude than in proliferating cells [78]. LDH-release assay confirmed that the mode of cell death was not necrosis. However, phosphatase inhibitor does not rescue non-proliferating cells from apoptosis.

Lymphocytes are also a target of CDT. Several studies demonstrated that CDT led to G2/M arrest in stimulated lymphocytes prepared from human peripheral blood mononuclear cells treated with phytohemagglutinin (PHA) [73, 79, 80]. The mode of cell death of stimulated lymphocytes is likely apoptosis based on several pieces of evidence, including annexin V and PI positivity, DNA fragmentation and the activation of both initiator caspases 8/9 and executioner caspase 3 [80, 81]. The p53-dependent apoptosis was a suspected mechanism to be investigated in T-lymphocytes. Jurkat cells, an acute T-cell leukemia cell line without p53 expression, is sensitive to Fas-mediated apoptosis. In contrast, MOLT-4, a mature T-lymphocyte cell line with functional p53, is resistant to Fas-mediated apoptosis. When these cell lines were exposed to AaCDT, both showed increased DNA fragmentation and chromatin condensation, but Jurkat cells showed less cell death than MOLT-4 cells [82]. Moreover, activation of initiator caspase 8 and executioner caspases 3/7 in AaCDT-treated Jurkat cells was less than in MOLT-4 cells [82]. Taken together, Jurkat cells were less sensitive to AaCDT than MOLT-4 cells, and thus p53 might control the apoptosis pathway of CDT-exposed T lymphocytes. Besides, MOLT-4 cell death was attenuated by *bcl-2* overexpression [82], suggesting that the mitochondrial outer membrane permeability may be involved in CDT-induced cell death. In contrast to T cells, the status of p53 in B cells may not be related to the susceptibility of CDT. B cell lines with functional p53 and mutated p53, JAC-B1 and BL41, respectively, showed a similar increase in the sub-G1 population after HdCDT exposure [68]. The ATM-deficient B cells (AT13LA) had a defect in DNA repair and failed to accumulate  $\gamma$ -H2A.X formation and delayed sub-G1 cell accumulation upon HdCDT treatment, suggesting that AT13LA may be more resistant to

HdCDT [68]. Moreover, *bcl-2* overexpression increased apoptotic resistance in B cells [80].

### 1.7. The role of cytolethal distending toxin in the periodontal disease

Periodontal disease is one of the most prevalent infectious diseases of mankind [83]. Periodontitis is a gingival inflammatory disease caused by the accumulation of pathogenic bacteria and bacterial toxins in periodontal pockets and the host inflammatory responses. This inflammation destroys the periodontal tissues that induce the alveolar bone loss leading to the loss of teeth [84]. *Aggregatibacter actinomycetemcomitans* (Aa) was shown to be associated with localized aggressive periodontitis [8, 85, 86]. Moreover, it affects not only oral health but also influences many non-oral infections, such as endocarditis, pericarditis, septicemia and urinary tract infection [87]. CDT was confirmed as a cytotoxic factor of *A. actinomycetemcomitans* Y4 strain [32]. AaCDT was studied in human periodontal ligament fibroblast cells. Interleukin (IL)-6 and receptor activator of nuclear factor kappa B ligand (RANKL), which play an important role in cell differentiation, proliferation and maturation, were upregulated after AaCDT challenge [88]. Besides, IL-6 upregulation was also found in the human gingival fibroblast cells [88, 89]. IL-6 is not only a multifunctional cytokine, but also stimulates osteoclast formation, leading to bone resorption [90]. Intriguingly, exposure of macrophages to AaCDT showed the increased levels of IL-1 $\beta$ , IL-10, IL-20, and TNF- $\alpha$ , but did not demonstrate CdtB-induced apoptosis [55]. The study suggested that the AaCDT may regulate the functions of macrophages by balancing between pro-inflammatory (IL-1 $\beta$ , IL-20) and anti-inflammatory (IL-10, TNF- $\alpha$ ) cytokines. Furthermore, AaCDT induces the detachment of rat junctional epithelium [91] and apoptosis in human T-lymphocytes [80] that may cause tissue destruction and promote immunoevasion of *A. actinomycetemcomitans*.

Table 4 Responses of fibroblasts to cytolethal distending toxins

| Cell lines | Cell details   | CDT species | Phenotypes  | References |
|------------|--|-------------|---|------------|
| IMR-90     | <ul style="list-style-type: none"> <li>Primary human fetal lung fibroblast cell line</li> </ul>            | CjCDT       | <ul style="list-style-type: none"> <li>Biphasic G1 and G2/M arrest</li> <li>Increased Rad50 foci and <math>\gamma</math>-H2A.X formation</li> <li>Failed to demonstrate phosphatidylserine externalization</li> </ul>   | [92]       |
| COS-1      | <ul style="list-style-type: none"> <li>SV40 transformed Grivet kidney cell lines</li> </ul>                | CjCDT       | <ul style="list-style-type: none"> <li>Nuclei enlargement and fragmentation</li> </ul>  | [42]       |
|            | <ul style="list-style-type: none"> <li>Contain Papovavirus</li> </ul>                                      | AaCDT       | <ul style="list-style-type: none"> <li>G2/M accumulation but less than HeLa cells</li> <li>Increased p21 protein expression</li> </ul>  | [72]       |
| HFS        | <ul style="list-style-type: none"> <li>Foreskin fibroblasts</li> <li>Functional p53</li> </ul>             | HdCDT       | <ul style="list-style-type: none"> <li>Biphasic G1 and G2/M arrest</li> </ul> Downregulation of Cdc2 protein  | [68]       |
| HL         | <ul style="list-style-type: none"> <li>Human embryonic lung fibroblasts</li> <li>Functional p53</li> </ul> |             | <ul style="list-style-type: none"> <li>Biphasic G1 and G2/M arrest and downregulation of Cdc2 protein</li> <li>Increased p21 protein expression but not p53</li> </ul>  | [68]       |
| PDLC       | Human periodontal ligament cells   | AaCDT       | <ul style="list-style-type: none"> <li>Decreased DNA synthesis and cell proliferation</li> <li>Low level of caspase 3 activity and LDH-release</li> <li>Elongated, distended cells with pseudopodia-like protrusion stretching towards neighboring cells</li> </ul> | [7]        |
|            |  | HdCDT       | <ul style="list-style-type: none"> <li>Biphasic G1 and G2/M arrest</li> </ul>   | [67]       |

| Cell lines | Cell details           | CDT species | Phenotypes  | References |
|------------|------------------------|-------------|---|------------|
| GF         | ● Gingival fibroblasts |             | <ul style="list-style-type: none"> <li>● Decreased DNA synthesis and cell proliferation</li> <li>● Low level of caspase 3 activity and LDH-release</li> <li>● Elongated, distended cells with pseudopodia-like protrusion stretching towards neighboring cells</li> </ul> | [7]        |
|            |                        | AaCDT       | <ul style="list-style-type: none"> <li>● Biphasic G1 and G2/M arrest</li> <li>● Phase arrest depended on toxin concentration (the more toxin, the more shift to G2 arrest)</li> </ul>   | [67]       |
|            |                        | HdCDT       | <ul style="list-style-type: none"> <li>● Biphasic G1 and G2/M arrest</li> </ul>   | [67]       |

Table 5 Responses of epithelial cells to cytolethal distending toxins

| Cell lines   | Cell details   | CDT species | Phenotypes  | References |
|--|--|-------------|---|------------|
| HeLa   | <ul style="list-style-type: none"> <li>● Contain HPV</li> <li>● Nonfunctional p53</li> </ul>         | EcCDT-I     | <ul style="list-style-type: none"> <li>● G2/M arrest (synchronized cells)</li> <li>● G2 and M phase cells arrested on the next G2/M phase</li> <li>● Did not affect progression through S-phase</li> <li>● Increased phosphorylated Cdc2 (inactive form)</li> </ul> | [37]       |
|  |  |             | <ul style="list-style-type: none"> <li>● G2/M arrest and increased phosphorylated Cdc2 (inactive form)</li> </ul>   | [68]       |
|  |  | HdCDT       | <ul style="list-style-type: none"> <li>● Increased <math>\gamma</math>-H2A.X formation and increased Mre11 foci</li> </ul>  | [76]       |
|  |  |             | <ul style="list-style-type: none"> <li>● G2/M arrest</li> </ul>   | [67]       |
|  |  | CjCDT       | <ul style="list-style-type: none"> <li>● G2/M arrest and failed to detect dephosphorylate Cdc2 (active form)</li> <li>● Caffeine has no effect to override a G2 arrest</li> </ul>   | [74]       |
|  |  |             | <ul style="list-style-type: none"> <li>● Accumulation of G2/M cells</li> </ul>  | [92]       |
| <ul style="list-style-type: none"> <li>● G2/M arrest and induce apoptosis</li> </ul> | [70]   |             |   |            |
| H407   | <ul style="list-style-type: none"> <li>● Human intestinal cells</li> <li>● Contain HPV-18</li> </ul> | AaCDT       | <ul style="list-style-type: none"> <li>● G2/M arrest and cell distension</li> </ul>   | [32, 73]   |
|  |  |             | <ul style="list-style-type: none"> <li>● G2/M arrest and increased p21 protein expression</li> </ul>  | [72]       |
|  |  | HhCDT       | <ul style="list-style-type: none"> <li>● G2/M arrest and activated caspase 3/7 and caspase 9</li> <li>● Increased <math>\gamma</math>-H2A.X formation, Bax/Bcl<sub>2</sub> ratio, and cytochrome c release</li> </ul>   | [71]       |
|  |  | CjCDT       | <ul style="list-style-type: none"> <li>● G2/M arrest and enlargement of cells and nuclei</li> </ul>   | [42]       |



| Cell lines  | Cell details  | CDT species | Phenotypes   | References |
|-------------|---|-------------|--|------------|
| HEp-2       | <ul style="list-style-type: none"> <li>Human epithelial type 2</li> <li>Functional p53</li> </ul>         | HdCDT       | <ul style="list-style-type: none"> <li>G2/M arrest</li> <li>Increased phosphorylated Cdc2 (inactive form)</li> <li>Increased p53 and p21 protein expression</li> <li>Caffeine partially overrides a G2 arrest</li> </ul> | [68]       |
| Caco-2      | <ul style="list-style-type: none"> <li>Human colorectal adenocarcinoma</li> </ul>                         | CjCDT       | <ul style="list-style-type: none"> <li>G2/M arrest</li> </ul>  | [74]       |
| CHO         | <ul style="list-style-type: none"> <li>Chinese hamster ovarian cell line</li> </ul>                       | EcCDT-I     | <ul style="list-style-type: none"> <li>Increased cellular distension</li> </ul>  | [23]       |
|             |   | EcCDT-II    | <ul style="list-style-type: none"> <li>Increased cellular distension</li> <li>Abundant toxin stress fibers</li> <li>Decreased cell proliferation and DNA synthesis</li> </ul>  | [93]       |
| HMVEC-d     | <ul style="list-style-type: none"> <li>Normal human microvascular endothelial cells</li> </ul>            | HdCDT       | <ul style="list-style-type: none"> <li>Increased cell death (MTT assay)</li> <li>G2/M arrest and increased phosphorylated Cdc2 (inactive form)</li> </ul>  | [14]       |
| HaCaT cells | <ul style="list-style-type: none"> <li>Skin keratinocytes</li> <li>p53 mutated</li> </ul>                 | HdCDT       | <ul style="list-style-type: none"> <li>G2/M arrest</li> <li>Increased phosphorylated Cdc2 (inactive form)</li> </ul>   | [68]       |
| Ad3 and Ad5 | <ul style="list-style-type: none"> <li>Neonatal foreskin keratinocytes</li> <li>Functional p53</li> </ul> | HdCDT       | <ul style="list-style-type: none"> <li>G2/M arrest</li> <li>Downregulation of Cdc2 protein</li> </ul>  | [68]       |

Table 6 Responses of hematopoietic cells to cytolethal distending toxins

| Cell lines      | Cell details   | CDT species | Phenotypes  | References |
|-----------------|--|-------------|---|------------|
| Dendritic cells | <ul style="list-style-type: none"> <li>Non-proliferating cells</li> </ul>                                    | HdCDT       | <ul style="list-style-type: none"> <li>Increase <math>\gamma</math>-H2A.X formation and Mre11 foci</li> <li>Increase sub-G0 population and fail to increase cell distension</li> </ul>  | [76]       |
| U937            | <ul style="list-style-type: none"> <li>Monocytic cell line</li> <li>Proliferating cells</li> </ul>           | AaCDT       | <ul style="list-style-type: none"> <li>G2/M arrest</li> <li>Increase DNA fragmentation, annexin v positive cell and caspase 3</li> </ul>  | [78]       |
| U937-PMA        | <ul style="list-style-type: none"> <li>Monocytic cell line</li> <li>Non-proliferating macrophages</li> </ul> | AaCDT       | <ul style="list-style-type: none"> <li>No population in G2/M phase</li> <li>Increase DNA fragmentation</li> <li>Did not increase caspase 3</li> <li>Low LDH release in 0.1% Triton (no sign for necrosis)</li> <li>Increase DNA fragmentation with phosphatase activity</li> <li>Phosphatase inhibitor does not affect apoptosis</li> </ul>                                       | [78]       |
| T lymphocytes   | <ul style="list-style-type: none"> <li>Prepared from human PBMCs</li> </ul>                                  | AaCDT       | <ul style="list-style-type: none"> <li>Show annexin V and PI positive, increase magnitude if PHA was added</li> </ul>   | [82]       |
| T lymphocytes   | <ul style="list-style-type: none"> <li>Prepared from human PBMCs</li> </ul>                                  | AaCDT       | <ul style="list-style-type: none"> <li>G2/M arrest if PHA was added</li> <li>Increase DNA fragmentation</li> <li>Induce apoptosis in activate T-cells with PHA, anti-CD3, and anti-CD28</li> <li>Increase Apo2.7 positive (sign for apoptosis)</li> <li>Decrease mitochondrial membrane permeability</li> <li>Increase superoxide anion</li> <li>Activate caspase8/9/3</li> </ul> | [80]       |

| Cell lines   | Cell details  | CDT species | Phenotypes   | References |
|--|---|-------------|--|------------|
| CD4 <sup>+</sup> T cells<br>CD8 <sup>+</sup> T cells | <ul style="list-style-type: none"> <li>Prepared from human PBMCs</li> </ul>                                     | AaCDT       | <ul style="list-style-type: none"> <li>Induce T-cell activation and arrest at G2/M phase</li> <li>Did not detect morphological changes</li> <li>Decrease in RNA and protein content in both G1 and G2/M phase</li> </ul>   | [73]       |
| Jurkat   | <ul style="list-style-type: none"> <li>Acute T-cell leukemia</li> <li>Non-sense mutation in p53 gene</li> </ul> | AaCDT       | <ul style="list-style-type: none"> <li>Increase DNA fragmentation, chromatin condensation and apoptosis</li> <li>Increase caspase3/7/8 activity less than MOLT-4</li> <li>Induce the activation of caspase-2 and caspase-7</li> </ul>  | [82]       |
|  |   | HdCDT       | <ul style="list-style-type: none"> <li>Decrease cell proliferation</li> <li>Increase DNA fragmentation and apoptosis</li> <li>Increase the redistribution of phosphatidylserine, loosen phospholipid packing</li> </ul>  | [94]       |
| MOLT-4   | <ul style="list-style-type: none"> <li>T lymphoblast</li> <li>p53 is not expressed</li> </ul>                   | AaCDT       | <ul style="list-style-type: none"> <li>Increase chromatin condensation and apoptosis</li> <li>Increase caspase3/7/8 activity</li> </ul>  | [82]       |
|  |   |             | <ul style="list-style-type: none"> <li>Induce G2/M arrest and induce apoptosis</li> <li>Caspase inhibitor can block apoptosis</li> <li>Increase apoptosis with caspase-independent fashion at 48h</li> <li>Cell death was attenuated by the overexpression of <i>bcl-2</i></li> <li>Increase PI positive cells, even if caspase inhibitor was added</li> </ul> | [81]       |

| Cell lines       | Cell details   | CDT species | Phenotypes  | References |
|------------------|--|-------------|---|------------|
| SN-B1            | <ul style="list-style-type: none"> <li>● B lymphocyte</li> <li>● Functional p53</li> </ul>   | HdCDT       | <ul style="list-style-type: none"> <li>● Increase sub-G1 population (apoptosis)</li> <li>● Increase p53 protein expression</li> <li>● Increase <math>\gamma</math>-H2A.X formation</li> </ul>   | [68]       |
| JAC-B1           | <ul style="list-style-type: none"> <li>● B lymphocyte</li> <li>● Contain EBV</li> <li>● Functional p53</li> </ul>  | HdCDT       | <ul style="list-style-type: none"> <li>● Increase sub-G1 population (apoptosis)</li> </ul>  | [68]       |
| BL41             | <ul style="list-style-type: none"> <li>● Burkitt's lymphoma-derived cell line</li> <li>● p53 mutated</li> </ul>  | HdCDT       | <ul style="list-style-type: none"> <li>● Increase sub-G1 population (apoptosis)</li> </ul>  | [68]       |
| AT13LA           | <ul style="list-style-type: none"> <li>● B lymphocyte</li> <li>● M deficient</li> </ul>  | HdCDT       | <ul style="list-style-type: none"> <li>● Delay the sub-G1 accumulation (more resistant to toxin effect)</li> <li>● Very slightly increase p53 protein expression</li> </ul>   | [68]       |
| HS-72-EBV        | <ul style="list-style-type: none"> <li>● Murine B-cell hybridoma cell line</li> <li>● Contain E6/E7 gene of HPV-16</li> <li>● Suppressed endogenous p53</li> </ul> | AaCDT       | <ul style="list-style-type: none"> <li>● Fail to accumulate <math>\gamma</math>-H2A.X formation</li> <li>● G2/M arrest</li> <li>● Increase cellular distension</li> <li>● Increase p21 protein expression with p53-independent fashion</li> </ul> | [76]       |
| JY/ <i>bcl-2</i> | <ul style="list-style-type: none"> <li>● B lymphoblastoid cell line</li> <li>● Human <i>bcl-2</i> gene overexpression</li> </ul>                                   | AaCDT       | <ul style="list-style-type: none"> <li>● Increase resistant to apoptosis</li> </ul>   | [72]       |
|                  |  |             | <ul style="list-style-type: none"> <li>● Increase resistant to apoptosis</li> </ul>   | [80]       |

## 2. DNA Double-strand break damages and repair

Genomic integrity is very important to maintain fidelity of genetic information. Cells have several mechanisms for detection, signal transduction, and repair of DNA damages to survive. These processes also tightly linked to cell cycle control. The DNA is synthesized during the S phase and segregate at the mitosis (M) phase. The gap (G) phase between M and S phase is called G<sub>1</sub>, while G<sub>2</sub> is between S and M phases.

The cell cycle progression at G<sub>1</sub> and G<sub>2</sub> phase was controlled by cyclin-dependent kinase 2 (Cdk2)/cyclin E and Cdk1/cyclin B, respectively. Cdk1 and Cdk2 are encoded by the *CDC2* gene [95] and *CDK2* gene [96], in humans. The activity of Cdk1/Cyclin B complexes is regulated by Myt1 and Wee1 protein kinases. Myt1 and Wee1, respectively, phosphorylate Cdk1 at Tyr14 and Tyr15 to generate an inactive form of Cdk1/cyclin B complex [97]. Cdc25 activates the active form of Cdk1/cyclin B kinase by its phosphatase function on Tyr14 and Tyr15 to drive to the mitosis phase [98]. The active form of Cdc25 is regulated by the Chk1 protein kinase or Chk2 serine kinase at Ser-216 position [99].

Several factors can cause DNA double-strand breaks (DSBs), including exogenous agents such as  $\gamma$ -irradiation and chemical agents, and endogenous processes such as replication fork collapse [100]. Non-homologous end-joining (NHEJ) and homologous recombination (HR) are the two conserved DNA DSB repair mechanisms [101]. DNA damage surveillance proteins (MRN complex) are recruited to DSBs [102] following CDT exposure. This complex initiates the ATM (ataxia telangiectasia mutated) and ATR (ATM and Rad3-related) activation [99] leading to the accumulation of  $\gamma$ H2A.X foci, a DSB marker [76]. Moreover, ATM and ATR trigger several DNA-damage signaling pathways, such as p53 (tumor suppressor protein), Chk1 and Chk2 kinases. Arrest at the G<sub>1</sub> phase is an effect of p21 upregulation mediated by phosphorylated p53. The p21 inhibits the active form of Cdk2/cyclin E leading to G<sub>1</sub> arrest and also binds to PCNA (proliferating cell nuclear antigen) resulting in an inhibition of DNA duplication [103]. In the case of G<sub>2</sub> arrest, ATM and ATR activate Chk2 and Chk1 to phosphorylate Cdc25 phosphatase. Phosphorylation of Cdc25

renders it inactive and unable to dephosphorylate Cdk1/cyclin B, blocking the activation of G2 progression. The accumulation of phosphorylated p53 caused by ATM-induced Chk2 kinase can lead to apoptosis [104] by stimulating pro-apoptotic proteins, such as BAX and BAK that affect cytochrome C release.

In yeast, homologous recombination and sensors responded to AaCdtB toxicity together with the role of Chk2 (Rad53 in yeast) in the survival [51]. CdtB is translocated into host nuclei, induces DNA damages and triggers DNA damage response [75]. However, it remains unclear whether CdtB generates single-strand (SSB) or double strand breaks. The low dose of EcCDT (50 pg/ml) has been shown to induce DNA SSB in S-phase in HeLa [105]. This suggests that CdtB induces single-strand breaks, which are then converted into double-strand breaks during the S-phase. This finding is consistent with the report in yeast that Rad53, a major S-phase checkpoint kinase, is required for yeast survival from CdtB damage [51]. Besides, HR plays a more important role than NHEJ in the case of AaCdtB-induced damages in yeast [51].

If DSB lesions are not repaired within approximately 15 hours, the cell cycle will progress with an unrepaired chromosome [106]. This is called checkpoint adaptation. Persistent DSBs are localized to the nuclear periphery, and this requires a single strand-DNA binding protein Cdc13, Rad51 recombinase, and Mps3; an inner nuclear membrane protein. Peri-nuclear localization associated with the delay of DSB repair [107]. The reason why DSBs localized to the nuclear periphery is unclear, but it might protect the inappropriate recombination repair as in telomeric regions [108].

### 3. Chromatin structure and regulation

Eukaryotes pack their genome into the complex chromatin structure to fit into the nucleus. Chromatin organization is a dynamic process that not only arranges the entire eukaryotic genome into the limited space but also controls the DNA accessibility for gene transcription, DNA replication, DNA repair and others [109].

The basic building block of chromatin is the nucleosome which consists of octameric histone proteins, including two copies of histone H2A, H2B, H3 and H4 [110]. The two sets of H3-H4 proteins heterodimerized before the assembly of double H2A-

H2B dimers [111]. Moreover, histone H1 stabilizes the zig-zag structure of compact chromatin [112]. Histones can be removed, replaced and exchanged from the nucleosomes. Previous studies revealed that the inter-bonding of H2A-H2B dimers to the nucleosome is more easily removed than the stable H3-H4 [113-115]. Furthermore, there are several histone variants or non-canonical histones that function in various cellular processes. For example, H2A.Z is involved in transcription [116], H3.1 is incorporated during replication [117], and CenH3 is essential for kinetochore assembly at M phase [118].

The dynamic chromatin structure is regulated by several processes, such as histone exchange, chromatin remodeling and post-translational modifications on histone. Histone exchange may enhance DNA accessibility to enzymes, such as RNA polymerase II leading to increased gene expression [119]. Chromatin remodelers and post-translational modifications on histone play a crucial role to control histone exchange and chromatin dynamics. Chromatin remodeling complexes regulate chromatin structure via nucleosome spacing, nucleosome sliding and nucleosome eviction (reviewed in [120]). They also cooperate with other chromatin regulatory processes. For example, SWR-complex is required for H2A.Z histone exchange into the nucleosome at transcription start site to activate the gene transcription, while INO80-complex is required for removal of H2A.Z from the nucleosome [121-123]. Histone modifying enzymes also contribute to transcriptional regulation. For example, histone acetyltransferases (HATs) allow transcription factors recruitment to transcription start sites [124]. Histone deacetylases (HDACs) remove the acetyl-group from the histones leading to heterochromatin formation and inactivation of gene transcription. Besides, the SIR complex, the Silent Information Regulator, has HDAC activity and regulates heterochromatin at the telomere [125], ribosomal DNA [126], and mating type loci in yeast [127]. Accumulating pieces of evidence suggest that several chromatin regulatory factors work in harmony to control chromatin dynamics and DNA metabolism.

### 3.1. H2A.Z (Htz1) histone variant, SWR- and INO80-complexes

H2A.Z, Htz1 in yeast, is an H2A variant that is highly conserved across eukaryotic species [128]. It forms a heterodimer with H2B that can replace H2A-H2B in the nucleosome. The binding between Htz1-H2B dimers and H3-H4 tetramers is not stable [129]. These physical properties contribute to transcription activation, DNA repair and chromosomal domain segregation [130]. The exchange of Htz1 into and out of the nucleosome is regulated by chromatin remodelers, histone post-translational modification and histone chaperones [119].

The major function of chromatin remodelers is to modify the chromatin structure into an open or closed chromatin structure using the energy from ATP hydrolysis. SWR and INO80 complexes, for example, are associated with H2A.Z exchange, nucleosome sliding, and eviction [123, 131, 132]. Htz1-H2B is incorporated to replace H2A-H2B at the upstream promoter region by the SWR complex for transcription initiation [133]. On the other hand, the INO80 complex removes the H2A.Z variant, in opposition to the SWR function [122]. The SWR complex is comprised of four modules including Swr1, N-module (Swc7), C-module (Swc2, Swc3, Swc6, and Arp6) and RvB assembly platform (reviewed in [120]). The integrity of SWR-C has been studied using co-immunoprecipitation in strains that lack each subunit. The results are summarized in Table 7.



**Table 7** C-module subunit requirement for SWR-C integrity.

| Yeast strains | Swc2 | Swc3 | Swc6 | Arp6 | Swc5 | Complex organization | Histone exchange function |
|---------------|------|------|------|------|------|----------------------|---------------------------|
| WT            | ✓    | ✓    | ✓    | ✓    | ✓    | Normal               | Normal                    |
| <i>swc2Δ</i>  | ×    | ×    | ✓    | ✓    | ✓    | Cannot form          | Impair                    |
| <i>swc3Δ</i>  | ✓    | ×    | ✓    | ✓    | ✓    | Normal               | Normal                    |
| <i>swc6Δ</i>  | ×    | ×    | ×    | ×    | ✓    | Cannot form          | Impair                    |
| <i>arp6Δ</i>  | ×    | ×    | ×    | ×    | ✓    | Cannot form          | Impair                    |
| <i>swc5Δ</i>  | ✓    | ✓    | ✓    | ✓    | ×    | Normal               | Impair                    |

(This table was modified from [134])

✓ = A subunit that was found in each mutant determined by co-immunoprecipitation.

×

Flag-tagged Swr1 was used as background for every mutant. Anti-Flag tag antibody was used for immunoprecipitation.

Swr1 is the important ATP-dependent catalytic subunit of the SWR complex. [123]. Swc2 plays a role in complex integrity and allows the complex to selectively bind on the +1 nucleosome next to the DNA binding protein Reb1 [134, 135]. Besides, Swc2 binds and serves Htz1 to Swr1 to be inserted into the nucleosome [134]. Swr1 and Swc2 are required for Htz1 exchange [120, 136]. The deletion of either *SWC6* or *ARP6* results from the loss of all subunits, indicating the complex's scaffold function. This suggested that Swc6 and Arp6 are essential for subunit assembly. Although Swc5 is not pivotal to the complex assembly it is required for SWR-ATPase activation for histone replacement [134, 137]. The deletion of *SWC3* and *SWC7* did not interfere with the complex organization and histone exchange (**Table 7**) [134, 138].

The four modules of the INO80 complex include RvB1/2 (head module), Arp5 (neck module), Nhp10 (body module) and Arp8 (foot module). INO80 subunit is an ATPase and nucleosome spacing factor [139]. Arp5 subunit involves histone exchange and nucleosome remodeling. Nhp10 and Arp8 subunits are associated with nucleosome binding [120].

Besides transcription activation, Santisteban and colleagues found that *htz1Δ* is hypersensitive to drugs that inhibit elongation when elongation genes, namely *SPT5* and *SPT16*, are mutated [140]. This suggests that Htz1 also involves in transcription elongation process. SWR- and INO80- complexes function to exchange Htz1 at both the +1 nucleosomes and the telomeres [141, 142]. Htz1 deposition at the sub-telomeric region prevents heterochromatin spreading from the telomere to euchromatin [130].

In addition, chromatin remodelers, including SWR- and INO80-complexes, are involved in the DNA repair process. ATM phosphorylates H2A.X resulting in  $\gamma$ -H2A.X;  $\gamma$ -H2A in yeast when DSB occurred, leading to the recruitment of INO80- and SWR-complexes to the break sites [143]. INO80 complex removes or slides the nucleosome away from the end of the break providing 3'-end for homologous recombination repair [144, 145]. SWR-complex also replaces  $\gamma$ -H2A.X with H2A.Z, which prevents the hyperactivation of DNA repair [143]. Moreover, the localization of DSB to the nuclear periphery requires SWR-C-dependent H2A.Z incorporation [146]. SWR-Complex activity is required for the recruitment of DSBs to nuclear pores in the G1 phase for NHEJ repair [146], but not in *arp8Δ* [147].

### 3.2. SIR complex

Silencing Regulator (SIR) complex contains three major subunits Sir2, Sir3, and Sir4. This complex regulates several processes including recombination, genomic stability, and cellular aging [148, 149]. The NAD<sup>+</sup>-dependent deacetylase enzymatic component of the SIR complex is Sir2, while Sir3 and Sir4 bind to chromatin leading to heterochromatin formation [150, 151]. Sir2 facilitates heterochromatin formation at telomeres, mating type loci (HML and MHR), and rDNA loci [127, 152-154]. Although Sir2 is not essential for cell viability, the lack of Sir2 function increases the rate of rDNA recombination, increases chromosome instability, causes a partial loss of heterochromatin formation, and decreases lifespan [148, 149, 154-156]. The yeast life span was extended when Sir2 was overexpressed in a dose-dependent fashion, but it can be toxic to the cells because it decreased chromosome stability indicating by

fluctuation analysis of the non-essential chromosome [148, 149]. Sir2 activity can be increased by caloric restriction but inhibited by nicotinamide [157, 158]. The Sir complex does not directly bind to DNA, but to other proteins, such as Rap1, Abf1, and Sir1 proteins [159-161]. Sir4 binding is a key initial step to initiate silencing and recruits Sir2 to the silencing sites [162]. Sir2 removes the acetyl group from histone tails, which in turn recruit Sir3 and Sir4 to start the chain reaction of heterochromatin formation. The distance of heterochromatin spreading is counteracted by Htz1 [130]. Another function of the SIR complex is to silence the mating type and rDNA loci [127, 163]. Sir2, but not other Sir proteins, together with Net1 and Cdc14 phosphatase comprise the RENT nucleolar complex [164, 165]. RENT is recruited to rDNA through interaction with Fob1 and RNA polymerase I [166]. rDNA silencing negatively regulates the rDNA recombination [167], thus Sir2 may delay yeast aging by preventing extrachromosomal rDNA circle (ERC) produced by homologous recombination within the rDNA region [168]. Sir3 and Sir4 may also play a role in yeast aging. The null mutation of *SIR3* is associated with a shortened lifespan, while the *sir4* mutant extended lifespan. Moreover, the redistribution of Sir3 from telomere to nucleolus was found in the *SGS1* or *RAD52* mutants, which shortens yeast lifespan [169, 170]. In the *sir4* mutant, a longer lifespan was explained by the increase in rDNA silencing [163, 171]. The defect of ERC formation has been proposed for extended lifespan in the case of rDNA silencing [168].

CHULALONGKORN UNIVERSITY

### 3.3. Histone modifying enzymes

Histone tails are the targets of several posttranslational modifications (PTMs), including acetylation, phosphorylation, and methylation. PTMs affect nucleosome stability [172, 173] and control the accessibility of chromatin remodelers or modifiers to the target DNA. In this study, a few histone modifying enzymes were selected for investigation.

Gcn5 is the catalytic subunit of ADA, SAGA and SLIK/SALSA histone acetyltransferase that acetylate histone H2B, H3 tails and Htz1 [174]. These three chromatin-modifying complexes are involved in the retrograde response and

transcriptional regulation of several genes [175, 176]. The retrograde response is a series of molecular signals that form a communication pathway from mitochondria to the nucleus and initiates a cellular response to changes in mitochondrial function. Acetylation of H2A.Z prevents its removal from transcription start sites by INO80, resulting in active transcription [122]. Ste20 is a kinase of p21-activated kinase (PAK) that phosphorylates the Ste11p mitogen-activated protein kinase kinase kinase (MAPKKK) [177, 178] which has been found to be involved in regulation of osmosensing [179], filamentous growth [180], bud site selection [181], polarization growth [182, 183], actin organization [184, 185], regulation of exit from mitosis [186], and apoptosis [187]. Furthermore, Ste20 associated with chromatin condensation during apoptosis. In the case of hydrogen peroxide-induced cell death in *S. cerevisiae*, Ste20 translocates to the nucleus and phosphorylates serine 10 of histone H2B which is required for chromatin condensation [188]. Dot1 is a histone methyltransferase that methylates at lysine 79 of histone H3. Dot1 can also inhibit the activation of Cdc25 and p53 resulting in cell cycle arrest [189]. Moreover, methylation of histone H3-Lys79 affects the binding of SIR proteins to telomere [190].

#### 4. *Saccharomyces cerevisiae*, a powerful model for molecular study

The budding yeast, *Saccharomyces cerevisiae*, is a powerful eukaryotic model with highly conserved fundamental biological processes, such as DNA replication, transcription, DNA repair, cell cycle regulation, chromatin regulation, and cell signaling [191]. Since the yeast genome sequencing project, the first eukaryotic genome sequencing, was completed in 1996, it had two impacts on the field of molecular study. First, we discovered new predicted proteins from the DNA sequences [192] and the genes that highly conserved among higher eukaryotes including humans [193]. Many tools allow for molecular studies, including targeted gene deletion for phenotypic testing, GFP fusion for subcellular localization, and others due to the easy genetic manipulation and the less complexity of the yeast genome. This benefit allowed us to create yeast null mutant with the PCR-based method, homologous recombination [194].

Furthermore, the *S. cerevisiae* Deletion library was constructed by targeted deletions of virtually every open reading frame in the yeast genome [195]. This deletion library has been applied to the genome-wide analysis assays purposed to increase the understanding of biological function, yeast stress response, and drug mechanism. Moreover, the large-scale phenotypic screens of yeast mutants from the experimental data were curated and described the gene function by the *Saccharomyces* Genome Database (SGD). Because of the many advantages of using *S. cerevisiae* for molecular biology study, we used the budding yeast as a model in our study.

### 5. Chromatin structure and cytolethal distending toxin activity

The activity of CDT as a genotoxin requires internalization and translocation of CdtB into the nucleus and interaction with host DNA. We have a poor understanding of how CdtB targets the host DNA. Although CdtB contains the nuclease activity, its activity is low *in vitro* comparing to its activity *in vivo* [42]. We hypothesize that CdtB may require some host factors for its activity. The eukaryotic genome is packed in chromatin structure, which controls access to DNA. Because CdtB requires interaction with DNA, the chromatin structure may play a role in regulating CdtB activity in eukaryotes.

Our previous study showed that mutation of H2B histone phosphorylation site (S10A), which is required for chromatin condensation during apoptosis, conferred partial resistance to AaCdtB in yeast [51]. Thus, AaCdtB toxicity in eukaryotic cells may depend on the chromatin structure. In this study, we proposed that chromatin structure or regulators may be involved in regulating CdtB activity. In this study, we identified genes that are required for CdtB cytotoxicity by screening for the CdtB resistant phenotype using plate sensitivity and survival plating assay in yeast strains with deletions in genes important in the regulation of chromatin structure. The potential CdtB resistant mechanisms were examined based on several hypotheses, including nuclear localization, DNA damage, the interaction of CdtB with chromatin/chromatin component and DNA repair gene upregulation. Besides, we performed a genome-wide screen using the yeast deletion library to identify genes that are required for CdtB. Gene lists

were analyzed based on gene ontology (GO) terms to define the major cellular processes that are required for the CdtB function. The results provided information regarding the role of host factors in CdtB cytotoxicity.



## CHAPTER III: MATERIALS AND METHODS

### 1. Preparation and general protocols

#### 1.1. Yeast strains and media

*Saccharomyces cerevisiae* BY4741 (MATa *his3Δ1 leu2Δ0 met15Δ0 ura3Δ0*) was used as the wild-type control. Isogenic deletion mutants of selected genes were obtained from the yeast deletion library (Invitrogen/Open Biosystems, USA) (**Table 8**). The complete yeast deletion library was also used for the genome-wide screen. To generate double deletion yeast, PCR-based strategy was used to knock-out the *RAD50* gene in mutant candidates (**Figure 2**). *LEU2* gene in pRS315 was used as a template and amplified using a couple of 45 nucleotides of *RAD50*-overhanging upstream primer (5'-AACCATGAGAGGCAAAAACAAGGGAACGACGGAAAGCAGGCATGAGATTGTAAGAGAGTGAC-3'; T<sub>m</sub> = 85.0°C) and downstream primer (5'-ATCAATCAAAGTCTATCCCTTCGTAGATATTATGGGGTCTTTCACTGTGCGGTATTTCA CACCG-3'; T<sub>m</sub> = 83.3°C), then *RAD50*-flanking *LEU2* PCR product was transformed into wild-type and mutant candidates. Positive colonies were selected using synthetic complete media without leucine and verified the deletion of the *RAD50* gene by PCR. The PCR product sizes were generated by A couple of primers A and D at *RAD50* locus. The forward A primer is 5'-ATAACCATGCATCTTGCAATACTTT-3' (T<sub>m</sub> = 59.2°C) and the reverse D primer is 5'-ATATGATGGGTATCAAAGGTGCTTA-3' (T<sub>m</sub> = 60.9°C). If *RAD50* was replaced by *LEU2*, the product size should be 2,728 bp whereas 4,548 bp is the result if *RAD50* was not replaced by *LEU2*. Subsequently, pYES2 and pYES2-CdtB were individually transformed into double deletion strains.

YPD media (1% yeast extract; 2% peptone; 2% dextrose) was used as normal yeast culture. The drop-out media include 0.15% Difco Yeast Nitrogenous Base w/o AA; 0.5% ammonium sulfate; 1.49 g/L of drop-out amino acid powder and 2% carbon source. The ingredients of the amino acid mix are shown in **Table 9**; an appropriate drop out of certain ingredients was used for the selection of the corresponding auxotrophic marker. Glucose and galactose were used for repression and induction of CdtB,

respectively. Sucrose was used for log phase culture before galactose induction of CdtB expression.

**Table 8** Genes that are related to chromatin structure in this study

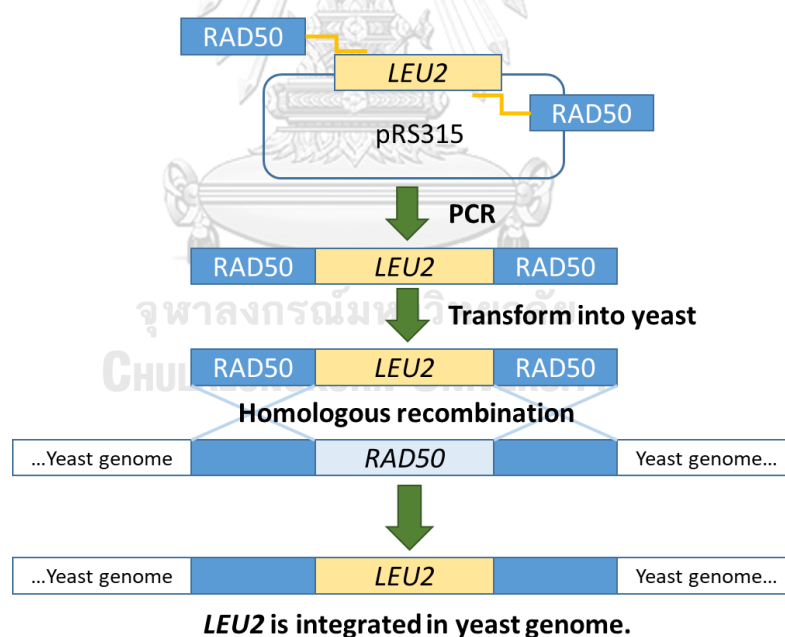
| Classification                | Systematic name | Standard name                   | Description from SGD   |
|-------------------------------|-----------------|---------------------------------|--|
| Histone proteins              | <i>YPL127C</i>  | <i>HHO1</i>                     | Histone H1, a linker histone required for nucleosome packaging at restricted sites; suppresses DNA repair involving homologous recombination; not required for telomeric silencing, basal transcriptional repression, or efficient sporulation   |
|                               | <i>YOL012C</i>  | <i>HTZ1</i>                     | Histone variant H2AZ, exchanged for histone H2A in nucleosomes by the SWR1 complex; involved in transcriptional regulation through prevention of the spread of silent heterochromatin  |
| SWR complex (unique subunits) | <i>YDR334W</i>  | <i>SWR1</i>                     | Swi2/Snf2-related ATPase that is the structural component of the SWR1 complex, which exchanges histone variant H2AZ (Htz1p) for chromatin-bound histone H2A  |
|                               | <i>YDR485C</i>  | <i>SWC2</i><br>( <i>VPS72</i> ) | Htz1p-binding component of the SWR1 complex, which exchanges histone variant H2AZ (Htz1p) for chromatin-bound histone H2A; required for vacuolar protein sorting   |
|                               | <i>YAL011W</i>  | <i>SWC3</i>                     | Protein of unknown function, component of the SWR1 complex, which exchanges histone variant H2AZ (Htz1p) for chromatin-bound histone H2A; required for formation of nuclear-associated array of smooth endoplasmic reticulum known as karmellae. |
|                               | <i>YBR231C</i>  | <i>SWC5</i>                     | Protein of unknown function, component of the SWR1 complex, which exchanges histone variant H2AZ (Htz1p) for chromatin-bound histone H2A   |
|                               | <i>YML041C</i>  | <i>SWC6</i><br>( <i>VPS71</i> ) | Nucleosome-binding component of the SWR1 complex, which exchanges histone variant H2AZ (Htz1p) for chromatin-bound histone H2A; required for vacuolar protein sorting  |
|                               | <i>YLR385C</i>  | <i>SWC7</i>                     | Protein of unknown function, component of the Swr1p complex that incorporates Htz1p into chromatin   |
|                               | <i>YLR085C</i>  | <i>ARP6</i>                     | Actin-related protein that binds nucleosomes; a component of the SWR1 complex, which exchanges histone variant H2AZ (Htz1p) for chromatin-bound histone H2A  |



| Classification                           | Systematic name | Standard name | Description from SGD  |
|--|-----------------|---------------|---|
| INO80 complex (unique subunits)          | <i>YNL059C</i>  | <i>ARP5</i>   | Nuclear actin-related protein involved in chromatin remodeling, component of chromatin-remodeling enzyme complexes  |
|  | <i>YOR141C</i>  | <i>ARP8</i>   | Nuclear actin-related protein involved in chromatin remodeling, component of chromatin-remodeling enzyme complexes  |
|  | <i>YDL002C</i>  | <i>NHP10</i>  | Protein related to mammalian high mobility group proteins; preferentially binds DNA ends, protecting them from exonucleatic cleavage; likely component of the chromatin-remodeling complex INO80 complex; proposed to be involved in DNA repair                     |
| SIR complex (hetero-chromatin formation) | <i>YDL042C</i>  | <i>SIR2</i>   | Conserved NAD <sup>+</sup> dependent histone deacetylase of the Sirtuin family involved in regulation of lifespan; plays roles in silencing at HML, HMR, telomeres, and the rDNA locus; negatively regulates initiation of DNA replication                          |
|  | <i>YLR442C</i>  | <i>SIR3</i>   | Silencing protein that interacts with Sir2p and Sir4p, and histone H3 and H4 tails, to establish a transcriptionally silent chromatin state; required for spreading of silenced chromatin; recruited to chromatin through interaction with Rap1p                    |
|  | <i>YDR227W</i>  | <i>SIR4</i>   | Silent information regulator that, together with SIR2 and SIR3, is involved in assembly of silent chromatin domains at telomeres and the silent mating-type loci; potentially phosphorylated by Cdc28p; some alleles of SIR4 prolong lifespan                       |
| Other histone modifying enzymes          | <i>YGR252W</i>  | <i>GCN5</i>   | Histone acetyltransferase, acetylates N-terminal lysines on histones H2B and H3; catalytic subunit of the ADA and SAGA histone acetyltransferase complexes; founding member of the Gcn5p-related N-acetyltransferase.   |
|  | <i>YHL007C</i>  | <i>STE20</i>  | Cdc42p-activated signal transducing kinase of the PAK (p21-activated kinase) family; involved in pheromone response, pseudohyphal/invasive growth, vacuole inheritance, down-regulation of sterol uptake; GBB motif binds Ste4p; histone H2B serine kinase activity |
|  | <i>YDR440W</i>  | <i>DOT1</i>   | Nucleosomal histone H3-Lys79 methylase; methylation is required for telomeric silencing, meiotic checkpoint control, and DNA damage response  |

**Table 9** Synthetic amino acid and trace element components (Hopkins mixture)

| Components                    | mg/L | Components      | mg/L  |
|-------------------------------|------|-----------------|-------|
| Adenine                       | 21   | L-methionine    | 85.6  |
| Para-aminobenzoic acid (PABA) | 8.6  | L-phenylalanine | 85.6  |
| Glutamine                     | 85.6 | L-proline       | 85.6  |
| Glycine                       | 85.6 | L-serine        | 85.6  |
| Myo-inositol                  | 85.6 | L-threonine     | 85.6  |
| L-alanine                     | 85.6 | L-tyrosine      | 85.6  |
| L-arginine                    | 85.6 | L-valine        | 85.6  |
| L-asparagine                  | 85.6 | L-leucine       | 173.4 |
| L-aspartic acid               | 85.6 | L-histidine     | 85.6  |
| L-cysteine                    | 85.6 | L-lysine        | 85.6  |
| L-glutamic acid               | 85.6 | L-tryptophan    | 85.6  |
| L-isoleucine                  | 85.6 | Uracil          | 85.6  |

**Figure 2** PCR-based gene deletion strategy.

The method was used to generate ORF deletion in the yeast genome. The disruption cassette was amplified by PCR using a couple of primers that uniquely RAD50 tagged (45 nucleotides) with its flanking sequences. LEU2 gene was selected as an auxotrophic marker for the positive clones. The disruption cassette was transformed into yeast and integrated into the genome via mitotic homologous recombination. Positive clones could grow on leucine-depleted synthetic complete media.

## 1.2. Confirmation of gene deletion of CdtB resistant mutants

Overnight culture of yeast was harvested and resuspended in lysis buffer (10mM Tris-HCl pH8.0, 100mM NaCl, 1mM EDTA, 1% SDS and 2% Triton X-100). Yeast genomic DNA was extracted by the glass beads disruption method [196]. Samples were treated with 100 µg/ml of RNase A followed by phenol-chloroform-isoamyl alcohol (PCI) extraction to eliminate RNA and protein contaminants, respectively. Ethanol precipitation was used for DNA precipitation. The concentration of genomic DNA was measured and used for PCR. Primer A for respective gene deletion strain and *KanB* primer were used to check for the integration of the KanMX marker cassette at appropriate loci as described [197]. Annealing temperature and MgCl<sub>2</sub> concentration of PCR reaction was 54°C and 3mM MgCl<sub>2</sub> for *swc6Δ*; 55°C and 1.5mM MgCl<sub>2</sub> for *swc2Δ*; and 57°C and 1.5mM MgCl<sub>2</sub> for others. The expected sizes of PCR products are shown in Table 10.

Table 10 Primers and annealing temperature for CdtB resistant strains confirmation. <sup>a</sup>

| Test on mutants | Primer sequences                 | Melting temperature (°C) <sup>b</sup> | Product size (bp) |
|-----------------|----------------------------------|---------------------------------------|-------------------|
| <i>htz1Δ</i>    | 5' -TCCATGCTAGATTAGCACACAGTAA-3' | 57.4                                  | 589               |
| <i>swr1Δ</i>    | 5' -CCTCTATACGATTATTAAGGGAGGG-3' | 56.1                                  | 652               |
| <i>swc2Δ</i>    | 5' -CATTAGGTAACGATATGCCAGTTA-3'  | 56.2                                  | 596               |
| <i>swc5Δ</i>    | 5' -TTACAGAAAGATTATTTAATGCCGC-3' | 53.6                                  | 621               |
| <i>swc6Δ</i>    | 5' -TTGGAGTATTACAAAACGACCATT-3'  | 54.3                                  | 596               |
| <i>arp6Δ</i>    | 5' -GCTTAGGTTAACTCGGTTTTCTACC-3' | 57.9                                  | 674               |
| <i>arp5Δ</i>    | 5' -GGAAGGTGACAATATAGAAGGGTCT-3' | 58.0                                  | 614               |
| <i>sir2Δ</i>    | 5' -CTTTTCCAAGCTACATCTAGCACTC-3' | 57.7                                  | 613               |
| <i>sir3Δ</i>    | 5' -GCAATGACTGATACACAAAGAAATG-3' | 54.4                                  | 640               |
| <i>KanB</i>     | 5' -CTGCAGCGAGGAGCCGTAAT-3'      | 62.9                                  | -                 |

<sup>a</sup> Confirmatory primer sequences are provided on Saccharomyces Genome Deletion Project website.

([http://www-sequence.stanford.edu/group/yeast\\_deletion\\_project/strain\\_a\\_mating\\_type.txt](http://www-sequence.stanford.edu/group/yeast_deletion_project/strain_a_mating_type.txt))

<sup>b</sup> Melting temperatures were calculated by Thermo Fisher Scientific Tm calculator

(<https://www.thermofisher.com/th/en/home/brands/thermo-scientific/molecular-biology/molecular-biology-learning-center/molecular-biology-resource-library/thermo-scientific-web-tools/tm-calculator.html>)

### 1.3. Bacterial strains and media

*Escherichia coli* (DH5-Alpha and BL21(DE3)) were used for cloning and recombinant protein production, respectively. *E. coli* was cultured in Luria-Bertani broth (LB, 1% tryptone, 1% NaCl, and 0.5% yeast extract). Antibiotic (100 µg/ml Ampicillin or 30 µg/ml Kanamycin) was added for a selection of plasmids with antibiotic-resistant markers.

### 1.4. *E. coli* competent cells preparation

*E. coli* log phase culture in LB broth (25 ml) was harvested by centrifugation (5,000g, 4°C, 5 min) and resuspended in 25ml of 80mM MgCl<sub>2</sub>/20mM CaCl<sub>2</sub> then incubated on ice for 1h. The cells were washed and resuspended in 2ml of 0.1M CaCl<sub>2</sub> and 2ml of 0.1M CaCl<sub>2</sub>/30%glycerol. One hundred µl aliquots were stored at -80°C.

### 1.5. Plasmids and transformation method

Plasmids used in this study are shown in Table 11. For bacterial transformation, plasmids were transformed by heat shock method [198]. Competent cells (50µl per reaction) were thawed on ice and incubated with 100 ng of plasmid DNA on ice for 1 hour followed by heat shock at 42°C for 90 seconds. The cells were immediately put on ice and resuspended in 1 ml SOC broth (2% tryptone; 0.5% yeast extract; 10 mM NaCl; 2.5 mM KCl; 10 mM MgSO<sub>4</sub> and 20 mM glucose) and incubated at 37°C for 1 hour. Transformants were plated on appropriate selective media.

For yeast transformation, plasmids were transformed by the lithium acetate/single-stranded carrier DNA/ polyethylene glycol (LiAc/SS-carrier DNA/PEG) transformation protocol as described [199]. Briefly, a log phase culture of 10<sup>8</sup> yeast cells was resuspended in 360 µl transformation mixture (33% PEG-3350; 0.1M lithium acetate; 0.28 mg/ml boiled SS-Carrier DNA; 1 µg of plasmid). The transformation reactions were incubated at 42°C for 40 min. Cells were collected by centrifugation (15,000 xg at room temperature for 30 sec) and resuspended with 1ml of sterile deionized distilled water. Transformation mix was plated on selective media and incubated at 30°C for 2-4 days.

For the large scale transformation, samples that resuspended in 50  $\mu$ l transformation mixture (LiAc/SS-Carrier DNA/PEG/plasmid) were incubated for 3 h at 30°C, then subjected to 45 min incubation at 42°C. Transformant selection was performed using synthetic complete media without uracil (SC-Ura). pYES2-CdtB contains the *GAL1* promoter, which expresses CdtB conditionally upon the induction with galactose.

#### 1.6. Yeast and bacterial frozen stocks

A single colony of yeast or *E. coli* was inoculated in suitable media and incubated at 30°C for yeast or 37°C for bacteria overnight with shaking. The overnight culture was mixed with an equal volume of 30% glycerol and stored at -80°C.

#### 1.7. Plasmid extraction

Mini-preparation of plasmid was done by the NucleoSpin<sup>®</sup> kit (Macherey-Nagel) according to the manufacturer's instructions. Briefly, a 5 ml log phase culture was centrifuged in the microcentrifuge tube at 8,000  $\times$ g for 5 min. Resuspension buffer was added into the tube following by lysis buffer. Protein precipitated buffer was added after 5 minutes of incubation. The supernatant was collected by centrifugation at 11,000  $\times$ g for a minute and was loaded into a silica spin column. Ethanol buffer was used to wash the column, and then the plasmid was eluted. Plasmid concentration was measured by Nanodrop using an appropriate diluent for a control.

#### 1.8. Recombinant CdtB expression, purification and determination

The plasmid pET28a carrying CdtB with a 6-histidine tag was transformed into *E. coli* BL21(DE3) competent cells by heat shock transformation and plated on LB agar supplemented with 30  $\mu$ g/ml kanamycin. CdtB expression was induced by adding 250  $\mu$ M IPTG in the mid-log phase culture for 4h at 37°C. Cells were lysed by sonication and the soluble fraction was collected. Immobilized metal affinity chromatography method (IMAC with Ni-NTA beads) was used to purified 6xHis-CdtB protein. Samples were washed and eluted with various concentrations of imidazole in purification buffer (50mM NaH<sub>2</sub>PO<sub>4</sub>, 300mM NaCl, proteinase inhibitors). Protein samples were analyzed using SDS-PAGE and Coomassie blue staining.

Table 11 Plasmids in this study

| Plasmids                   | Selectable markers  | Promotor | Purposes and details  | Source or references |
|----------------------------|---|----------|---|----------------------|
| pYES2                      |   |          | <ul style="list-style-type: none"> <li>● A high-copy yeast vector for expression of protein under Galactose-inducible promoter</li> </ul> | [51]                 |
| pYES2-CdtB                 |   |          | <ul style="list-style-type: none"> <li>● Using as a control</li> <li>● Galactose-inducible CdtB expression in yeast</li> </ul>            |                      |
| pYES2-CdtB( $\Delta$ 11aa) | <ul style="list-style-type: none"> <li>● Ampicillin resistant gene</li> <li>● <i>URA3</i> auxotrophic marker</li> </ul> | GAL1     | <ul style="list-style-type: none"> <li>● Expression of CdtB mutant lacking NLS sequence</li> </ul>  |                      |
| pYES2-EGFP                 |   |          | <ul style="list-style-type: none"> <li>● EGFP expression under galactose-inducible promoter in yeast.</li> </ul>                          |                      |
| pYES-CdtB-EGFP             |   |          | <ul style="list-style-type: none"> <li>● Galactose-inducible expression of EGFP-tagged CdtB used for CdtB localization study</li> </ul>   | This study           |
| pET-28a (+) CdtB           | <ul style="list-style-type: none"> <li>● Kanamycin resistant gene</li> </ul>  |          | <ul style="list-style-type: none"> <li>● Recombinant His-tagged CdtB expression in <i>E. coli</i></li> </ul>                              | [32]                 |
| pRS315                     | <ul style="list-style-type: none"> <li>● Ampicillin resistant gene</li> </ul>   | T7       | <ul style="list-style-type: none"> <li>● A yeast centromeric plasmid with <i>LEU2</i> marker</li> </ul>                                   | -                    |
| pBluescriptKS(-)           |   |          | <ul style="list-style-type: none"> <li>● A cloning plasmid used as substrate for CdtB activity</li> </ul>                                 | -                    |

### 1.9. Immunoblot for detection of CdtB expression

Yeast transformants were grown in SC-Ura with 2% glucose overnight at 30°C with 200 rpm shaking. Yeasts were grown to log phase yeast in SC-Ura with 2% sucrose until OD<sub>600</sub> was between 0.4 to 0.8. CdtB expression was induced in SC-Ura with 2% galactose for 6h; then cells were harvested by centrifugation. Whole-cell lysates were extracted by glass beads disruption method [200]. Briefly, yeast pellet was resuspended in lysis buffer (20mM HEPES pH7.6; 200 mM potassium acetate; 10% glycerol; 1mM EDTA; and proteinase inhibitors) with the glass beads and vortexed. Protein samples were separated by SDS-PAGE and transferred on to nitrocellulose membranes according to the standard protocol [201]. Rabbit anti-Aa-CdtB serum [32] and goat anti-rabbit IgG conjugated with HRP (ENZO, ADI-SAB-300) were used to detect CdtB expression.

To detect the CdtB expression of the mutants in genome-wide screening, protein lysates were extracted using glass beads and trichloroacetic acid method [202]. Protein samples were separated using SDS-PAGE and transferred onto nitrocellulose membranes. Rabbit anti-AaCdtB serum coupled with goat anti-rabbit IgG antibody conjugated with HRP was used to analyze the AaCdtB expression.

### 1.10. Cell cycle analysis by flow cytometry

Yeast cells were collected after the induction of CdtB expression at 0h, 12h, and 24h and fixed with 70% ethanol at 4°C overnight. Samples were collected (6,000 ×g, 5min, RT) and rehydrated by 1 ml of 50 mM sodium citrate. Triton X-100 (0.2%) and 0.25 mg/ml RNase A were added before propidium iodide staining (16 µg/ml in 50 mM sodium citrate) at 4°C for 10 min, then remove the excess propidium iodide by the same centrifugation condition. Flow cytometry was performed with a Beckman Coulter FC500 series and analyzed with ModFitLT software.

## 2. CdtB susceptibility test

### 2.1. CdtB susceptibility and survival plating assay

A single colony of yeast culture from the frozen stock was inoculated into uracil-dropout SC (SC-Ura) supplemented with 2% glucose and incubated at 30°C for overnight. Afterward, samples were grown to log phase ( $OD_{600}$  0.4 to 0.8) in SC-Ura with 2% sucrose. CdtB susceptibility test was performed by spotting ten-fold serial dilutions of log-phase culture on SC-Ura plate with 2% glucose and with 2% galactose and incubated at 30°C for 2-3 days.

For survival plating assay, approximately 500 cells/sample was plated on both types of agars, incubated for 3-4 days, and the colony-forming units (CFUs) were counted. Survival percentage of yeast under the CdtB expression condition was calculated from the ratio of CFU on CdtB-inducing media (galactose) and CdtB-repressing media (glucose). The ratio of CFUs on galactose and glucose media of the corresponding strain carrying the empty pYES2 vector was used to normalize for comparisons among different strains. The difference of each deletion candidate was compared to wild-type using the Mann-Whitney U test (SPSS Statistics 20).

### 2.2. CdtB susceptibility in genome wide screening

The transformed yeast library was growth overnight in SC-Ura supplemented with 2% glucose. The cultures were serially diluted and inoculated with a 96-pin floating pin replicator (V&P Scientific, Inc., United States) on SC-Ura media containing 2% galactose (inducing media) and on that containing 2% glucose (repressing media) as a control. Mutants showing significant growth on galactose plates, in the dilutions where the wild-type yeast strain BY4741 did not growth, were selected for further confirmatory screening.

Subsequently, the mutants selected in the primary screen were compiled in 96-well plates and rescreened by spotting dilutions of cultures onto glucose and galactose plates. Mutants that grew well on galactose plates were further analyzed by spot tests as described [51]. Briefly, log phase cultures were serially diluted and spotted on inducing and repressing media. After 40-48 h of incubation at 30°C, yeast growth was



observed. Mutants that showed better growth than wild-type on the galactose plate were selected for rescreening. After at least four repeats, mutants that consistently show resistance to CdtB were classified as CdtB resistant mutants.

### 3. CdtB-Htz1 interaction testing

#### 3.1. Immunoprecipitation of CdtB and Htz1

Recombinant 6-histidine-tagged CdtB was captured on protein A beads by rabbit anti-CdtB serum in binding buffer (20mM Na<sub>3</sub>PO<sub>4</sub> pH7.0, 50mM Tris-Cl pH7.0). Whole cell lysate of HA-tagged Htz1 yeast strain was co-incubated with CdtB-protein A bead complex in buffer (20mM HEPES pH7.6, 10% Glycerol, 200mM potassium acetate, 1mM EDTA, and protease inhibitors; modified from [203]) for overnight with gentle agitation at 4°C. The immunoprecipitated samples were examined by SDS-PAGE and immunoblotting using 1:5,000 rabbit anti-CdtB serum and 1:5,000 anti-HA antibody (Abcam ab9110). The secondary antibody was 1:10,000 goat anti-rabbit IgG conjugated with HRP (ENZO SAB-300).

#### 3.2. Chromatin Immunoprecipitation (ChIP)

Yeast containing Htz1:HA tag with or without CdtB expression were used in this experiment. Keogh et al. provided the ChIP method that we modified to use in our experiment. Briefly, Protein A beads were coated with 1:1,000 anti-CdtB antibody or 1:1,000 anti-HA antibody (Abcam ab9110). Pre-cleared whole-cell extract samples were precipitated with anti-CdtB beads or anti-HA beads at 4°C overnight. CdtB was induced by 2% galactose for 8 hours before 1% formaldehyde final concentration was added to crosslink the samples. Formaldehyde solution was prepared in the diluent (final concentration 100mM NaCl, 1mM EDTA, 50mM HEPES-KOH pH7.5). Samples were resuspended in the lysis buffer (20mM HEPES-KOH, pH7.5, 1mM EDTA, 2% Triton X-100, 10mM potassium acetate, and proteinase inhibitors), then glass beads and vortexing were applied for yeast extraction. Supernatants were sonicated twice by 10% output with a 2-sec pulse cycle for 40 sec. Samples were incubated with anti-CdtB and anti-HA coated beads at 4°C under rotary agitation for 4h. The immunoprecipitated

samples were examined by SDS-PAGE and immunoblotting using 1:5,000 rabbit anti-CdtB serum and 1:5,000 anti-HA antibody (Abcam ab9110). The secondary antibody was 1:10,000 goat anti-rabbit IgG conjugated with HRP (ENZO SAB-300).

#### 4. CdtB localization study

##### 4.1. Yeast cells fractionation

Chromatin fractionation procedure was modified from the method previously described by Keogh and colleagues [202]. Briefly, 500 mg of CdtB-expressing yeasts was washed in pre-spheroplast buffer containing 20mM Tris-Cl pH7.4, 1M sorbitol, 2mM EDTA, 100mM NaCl, 10mM DTT and various proteinase inhibitors including 200  $\mu$ M PMSF, 200  $\mu$ M phenanthroline, 10  $\mu$ M E-64 and 1  $\mu$ M Pepstatin A. Samples were resuspended in the same buffer and incubated on ice for 10 min. Lyticase (Sigma L4025) was added for 20U/ml final concentration. Samples were placed at 30°C for 90 min to change into spheroplast. The spheroplasts were determined by OD<sub>600</sub> measurement in a 1% SDS solution. Samples should be lysed by more than 80%. Spheroplasts were washed by light spin centrifugation (400  $\times$ g, 3 min, 4°C) with spheroplast buffer containing 1M sorbitol, 20mM Tris-Cl pH7.4 and proteinase inhibitors as described. Lysis buffer (20mM Tris-Cl pH7.4, 100mM NaCl, 0.5% Triton X-100, 10mM DTT and proteinase inhibitors) was added into the samples together with 0.005% phenol red. Samples were placed on ice for 10 min and aliquoted the samples for the total fraction. Afterward, 1ml of nuclear isolating buffer was overlaid by the lysates. Samples were centrifuged at 15,000  $\times$ g, 15 min, 4°C. The cloudy reddish parts were aliquoted for the cytosolic fraction. All supernatants were removed, and nuclear pellets were collected and resuspended in nuclei lysis buffer containing 20mM Tris-Cl pH7.4, 100mM NaCl, 1% Triton X-100, 10mM DTT and proteinase inhibitors. Samples were placed on ice for 10 min and used as the nuclear fraction. Besides, the protein precipitation protocol was applied for a protein concentration of cytosolic fraction [204]. Briefly, three volumes of the chilled 13.3% w/v TCA in acetone was added to the samples together with 0.2% w/v DTT. After mixing by inverting tube, samples were incubated overnight,

then centrifuge at 20,000  $\times$ g, 10 min, 4°C and remove all supernatant. Pellets were breaking up using a glass rod in 1 ml of -20°C acetone containing 0.2% DTT and centrifuged to remove supernatant. Air drying the pellet for 5 min is recommended. Pellets were resuspended in 20mM Tris-Cl pH7.4. The fractionated samples were analyzed by SDS-PAGE and immunoblotting assay. CdtB protein was detected by 1:5,000 rabbit-anti CdtB serum [32] and 1:10,000 goat anti-rabbit IgG with HRP-conjugated (ENZO SAB-300). For cytosolic and nuclear markers were observed by 1:5,000 mouse anti-PGK1 IgG (Abcam ab113687) together with 1:5,000 rabbit anti-mouse IgG with HRP conjugated (Merck AP160P) and 1:5,000 rabbit anti-histone H3 IgG (Abcam ab1791), respectively.

#### 4.2. Immunofluorescence for CdtB localization

Immunofluorescence protocol was modified from the method previously described [205]. Briefly, a one-tenth gram of CdtB-8h induced yeasts was collected and fixed in 3.7% formaldehyde solution for 30 min. Samples were washed by 1  $\times$  PBS buffer pH7.4, resuspended in spheroplast buffer containing 1.2M sorbitol, 0.1M  $\text{KH}_2\text{PO}_4$ , and 10mM DTT, and placed on ice for 10 min. Lyticase (Sigma L4025) was added for 4U/ml final concentration. Samples were placed at 30°C for 90 min to change into spheroplast. The spheroplasts were determined by  $\text{OD}_{600}$  measurement in a 1% SDS solution. Samples should be lysed by more than 80%. Samples were washed with 1.2M cold-spheroplast buffer (500  $\times$ g, 1min, 15°C) and adjusted to  $5 \times 10^5$  cells/ $\mu\text{l}$ . Poly-L-lysine coated slides can be prepared during the sample preparation. After cleaning the glass slides with 70% ethanol, 500  $\mu\text{l}$  0.1% poly-L-lysine (Sigma P8920) was laid on the slides. Leave the solution for 10 min at room temperature, then rinse it off with sterilized distilled water and allow for air dry. The 20  $\mu\text{l}$ ,  $2 \times 10^6$  cells, of spheroplasts were dropped on the coated slides and air-dried at room temperature. The slides were fixed in -20°C chilled methanol for 5 min and washed in acetone for 30 sec and allow to completely air-dry. Optionally, a circular line for a reagent dam can be drawn using a correction pen. A humidity chamber is recommended for the process of antibody staining. Two-percent skim milk in PBST buffer was added to cover the area of the cells for blocking space,

then add 1:200 rabbit anti-CdtB serum on to the samples and incubate for 1h at room temperature on a rocket shaker. CdtB antibody was captured by 1:200 goat anti-rabbit IgG with rhodamine-conjugated (Merck AP132R) after 4x times washing the slides with 2% skim milk in PBST. DAPI at 1:1,000 concentration was used to stain the yeast nuclei. Mounting media (Thermo; SlowFade™ Gold antifade mountant S36940) was dropped on the cell area, then seal the coverslip above that with nail polish. CdtB localization was investigated under fluorescence microscopy.

#### 4.3. Nuclear localization of CdtB using CdtB-EGFP fusion protein

The wildtype CdtB gene of *Aggregatibacter actinomycetemcomitans* in the pYES2 vector was used as a template for the CdtB gene [51]. The plasmid contains the *KpnI*-Kozak sequence at 5'-end of the CdtB open reading frame. The template was amplified using T7 forward primer, *EcoRI*-site integrated reverse primer (5'-CCTTAGCGAGAAT TCACAAAAC-3') and high fidelity *pfu* DNA polymerase. *KpnI*-Kozak-CdtB-*EcoRI* PCR product was cloned into *KpnI*-*EcoRI* site of the pYES plasmid, then plasmid was linearized using *NotI* and *XbaI* restriction enzyme. pYES2-EGFP, a gift from Boonchird C. and colleagues, Mahidol university, was digested with *BamHI* and *XbaI* enzymes. Linearized pYES2-CdtB and EGFP fragment were treated with Klenow fragment to create blunt-end at *NotI* and *BamHI* sites, but not *XbaI* site, subsequently, EGFP fragment was ligated to form pYES2-CdtB-EGFP plasmid. The sequences of CdtB-EGFP construction as shown in **Figure 3**. CdtB-EGFP protein was expressed and checked for the protein expression and CdtB cytotoxicity by immunoblotting and susceptibility assay.

pYES2-CdtB-EGFP containing yeast were grown to mid-log phase and induced CdtB expression using galactose for 8h. Samples were fixed in 3.7% formaldehyde in PBS buffer (pH7.4) for 15 min and were permeabilized with 1% Triton X-100 at 42°C for 30 min. Samples were incubated with 0.1 µg/ml DAPI for 5 min avoiding light for yeast nuclei staining. Cells were washed twice with PBS, then drop on 1% agarose patched prepared glass slides. Fluorescent images were captured by a confocal fluorescent microscope (Olympus, FV10i-ASW model) at 60x optical magnification.

Fluorescent images were analyzed by Mander's coefficient function provide from Just Another Co-localization Plug-in (JACoP) in the ImageJ program [206]. The mean fluorescent intensity and standard deviation (SD) for each cell were calculated for DAPI and EGFP channels. The threshold level for positive signal of DAPI was set at  $\geq$  mean+1SD while that of EGFP was set at  $\geq$  mean+2SD. For each cell, we first defined the DAPI-positive area as the nucleus and counted the pixel number with EGFP signal above the threshold. Then, we calculated the relative percentage of nucleus localization of CdtB by comparing the percentage of EGFP-positive pixel numbers in nucleus over the total in yeast cells expressing CdtB-EGFP vs. EGFP control. The formula calculating the percentage of CdtB compare to EGFP alone in the yeast nucleus is shown here (Equation 1 - 3). The data was analyzed using Mann-Whitney U test with  $p < 0.05$  considered statistically significant.

$$\% \text{ EGFP in nucleus} = \frac{\text{Pixel number of EGFP in nucleus}}{\text{Total pixel number of EGFP}} \times 100$$

Equation 1 Percentage of EGFP in yeast nucleus calculation

$$\% \text{ CdtB in nucleus} = \frac{\text{Pixel number of CdtB in nucleus}}{\text{Total pixel number of CdtB}} \times 100$$

Equation 2 Percentage of CdtB in yeast nucleus calculation

$$\text{CdtB localization in yeast nucleus} = \frac{\% \text{ CdtB in nucleus}}{\% \text{ EGFP in nucleus}}$$

Equation 3 CdtB localization in yeast nucleus calculation



## 5. In vitro CdtB activity

### 5.1. Chromatin extraction

This chromatin extraction method was previously described elsewhere [207] and modified for our study. Briefly, there are four buffers for this method namely (i) **Sorbitol buffer** (1.4M sorbitol, 40mM Tris-Cl pH7.5, 0.5mM MgCl<sub>2</sub>), (ii) **Sucrose buffer** (16%(w/v) sucrose, 20mM Tris-Cl pH6.5, 0.5mM MgCl<sub>2</sub>), (iii) **Glycerol-sucrose buffer** (7%(w/v) sucrose, 20%(v/v) glycerol, 20mM Tris-Cl pH6.5, 0.5mM MgCl<sub>2</sub>) and (iv) **Nuclei lysis and MNase digestion buffer** (10mM Tris-Cl pH7.5, 0.5mM MgCl<sub>2</sub>, 0.05mM CaCl<sub>2</sub>). Note that, proteinase inhibitors such as 0.1mM PMSF and 1μM Pepstatin A were freshly added to all buffers. Overnight yeast culture in YPD was grown from 0.1 OD<sub>600</sub> to mid-log phase in 250ml YPD and its weight should be 1 gram per this culture. Samples were harvested, washed once and resuspended with 4ml **sorbitol buffer**. Spheroplast cells were generated by adding 40U/ml lyticase and incubate at 30°C for 90 min. Spheroplast efficiency should be more than 70% that was monitored in a 1%SDS solution. Samples were washed once with sorbitol buffer and gently resuspended with **sucrose buffer**, afterward, overlaid on the **glycerol-sucrose buffer** and spun at 21,500 ×g at 4°C for 30 min to eliminate ghost cells. Pellets were resuspended with **sucrose buffer** completely and vortex at the top speed for 5 min. Samples were centrifuged at 3,300 ×g, 15 min, 4°C to exclude the cell debris and intact cells. Supernatants that contain nuclei, were carefully transferred to a new tube and spun at 21,500 ×g, 30 min, 4°C. One batch of 250ml culture nuclei can be aliquoted equal to 5x10<sup>6</sup> nuclei/tube. Nuclei samples were resuspended with Micrococcal nuclease (Mnase) digestion buffer (50 mM Tris-HCl pH7.9, 5 mM CaCl<sub>2</sub>) and warmed at 37°C before start reaction 10 min. MNase (NEB-M0247S) was applied to the samples to determine the intact chromatin structure. We incubated 5x10<sup>6</sup> nuclei with the various Mnase concentration (0.001-10 U/μl) at 37°C for 15 min. For the latter experiment, we adjusted the lysis efficiency by adding 1% Triton X-100 in the reaction buffer. Thus, the MNase digestion condition was adjusted to 0.5 U/μl incubating at 37°C for 3 min with the 1.5x10<sup>7</sup> nuclei sample. The reaction was inhibited by adding 10mM EDTA. Afterward, genomic DNA was purified by phenol-chloroform

extraction method. After MNase reaction on chromatin, 1% SDS final concentration together with 50  $\mu\text{g/ml}$  proteinase K were added for protein denaturation and digestion respectively. Samples were incubated at 55°C overnight before PCI extraction. Samples with PCI solution were centrifuged at 20,000  $\times\text{g}$  for 10 min, then collect the aqueous phase. Samples were incubated with 100  $\mu\text{g/ml}$  RNase A for 30 min at 37°C and repeat the PCI extraction once. The aqueous phase was carefully transferred to a new tube and added 1/10 volume 3M sodium acetate and 2 volume of cold absolute ethanol, then mix and place in -20°C for 30 min. Samples were spun at 20,000  $\times\text{g}$ , 10 min, 4°C and washed once with 70% ethanol, then air dry. Pellets were resuspended in DNA loading buffer and resolved the bands in 1.5% agarose gel electrophoresis (100V., 75 min). The gel was stained with ethidium bromide and was observed by UV light.

### 5.2. In vitro CdtB activity on plasmid

pKS(-) bluescript plasmid, 3 kb circular DNA, was used as a substrate prepared by the standard plasmid extraction protocol. Various CdtB concentration was used to interact on circular plasmid in the CdtB activity buffer (20mM HEPES pH7.5, 150mM NaCl, 5mM  $\text{MgCl}_2$ , and 5mM  $\text{CaCl}_2$ ). The interaction was incubated at 37°C for 5h. The reaction was inhibited by adding 10mM EDTA to capture the divalent cation cofactor. Samples were mixed with DNA loading dye and resolved the bands in 1% agarose gel electrophoresis.

### 5.3. In vitro CdtB activity on chromatin

The chromatin of wild-type and *sir2 $\Delta$*  yeast were extracted by the method mentioned before. Reactions were set in the CdtB activity buffer (10mM HEPES pH7.5, 750 mM NaCl, 5 mM  $\text{MgCl}_2$ , and 5 mM  $\text{CaCl}_2$ ). Recombinant CdtB was added into the sample by 500 ng/ $\mu\text{l}$  and incubated at 5h and 24h in 37°C. Micrococcal nuclease (0.5 gel U/ $\mu\text{l}$ ) was applied to confirm the intact chromatin structure ( $1.5 \times 10^7$  nuclei) incubating at 37°C for 3 min. We stopped the reaction by adding 20 mM EDTA final concentration and place on ice. Phenol chloroform extraction was applied to isolate the digested chromatin. Chromatin samples were concentrated by ethanol precipitation (20,000  $\times\text{g}$ ; 10 min; 4°C). We used RNase A (0.2  $\mu\text{g}/\mu\text{l}$ ) to remove RNA in the samples



that resuspended in 150 mM NaCl/15 mM Na citrate buffer and incubated them for 30 min at 37°C. Phenol chloroform extraction and ethanol precipitation were repeated to remove RNase residue. Supernatants were removed and heated dry at 65°C for 5 min or until dry. Samples were resuspended with DW, mixed with loading dye and run on 2% agarose gel electrophoresis (100V., 75 min). The gel was stained with ethidium bromide and was observed by UV light.

## 6. The investigation of upregulated-DNA repair genes in the mutants

### 6.1. Data mining for DNA repair genes upregulation

Microarray data were received from ArrayExpress (EBI; (<https://www.ebi.ac.uk/arrayexpress/>) and Gene Expression Omnibus (NCBI; (<https://www.ncbi.nlm.nih.gov/geo/>) database. The query for searching experiments was set as words that involved in DNA damage or DNA damage agents that like DNA damage caused by CdtB. The DNA repair genes (GO:0006281) and their child term list were provided from the *Saccharomyces* Genome Database (SGD) which found 258 genes. The Affymetrix GeneChip Yeast Genome S98 (A-AFFY-27) and the Affymetrix GeneChip Yeast Genome 2.0 Array (A-AFFY-47) is the DNA microarray platform that we used. The A-AFFY-27 platform matched 214 out of 258 genes of the DNA repair and their children term which annotated by SGD, whereas another platform matched 255 out of 258 genes. The fold-expression of each experiment was evaluated as the ratio of treated compared with normal condition. The criteria for fold change expression is equal to or more than 1.5 folds. Moreover, we found 57 experiments of gene expression profiles in our CdtB resistant mutants. We search the upregulated DNA repair gene (criteria  $\geq 1.5$  folds) in the mutants compared to WT yeast in normal conditions. The upregulated genes in both lists were highlighted to use as gene candidates to determine the increase of the DNA repair process to fight against CdtB damage that may explain the CdtB resistant mechanism in our candidates.

## 6.2. RNA extraction

Yeast cells were grown in our standard method as mentioned before. The culture was washed with DEPC-treated water and resuspended in 350  $\mu$ l lysis buffer (500mM NaCl, 10mM EDTA, 1% SDS and 0.2 M Tris-Cl pH7.6). Glass beads were used to break the cells that contain 350  $\mu$ l phenol chloroform isoamyl alcohol (25:24:1) mixture. The maximum speed of vortex was applied for 1.5 min (2 times). We preferred a 2 ml microcentrifuge tube for the best result. The aqueous phase was separated by 16,000  $\times$ g; 15 min and concentrated by ethanol precipitation. Supernatants were removed and heated-dry at 65°C for 5 min or until dry. Afterward, we removed DNA by DNase (1 U per 5  $\mu$ g sample) and incubated in 37°C for 120 min. Phenol chloroform extraction and ethanol precipitation were repeated to remove DNase residue. We measured RNA concentration by Nanodrop and checked the RNA quality by 1.5% agarose gel electrophoresis (100V., 70 min). The gel was stained with ethidium bromide and was observed by UV light.

## 6.3. Quantitative real-time PCR (qPCR)

DNA-free mRNA samples were converted to cDNA using the ImProm-II kit (Promega®) with oligo dT primer. The reverse transcriptase worked in 42°C for 1 hour. cDNA samples were amplified with the qPCR master mix from NEB (Luna M3003S). The primers used were shown in Error! Reference source not found.. Gene expression level was calculated by the difference of cycle threshold comparing to WT and *ACT1* as a housekeeping gene.

Table 12 Primers and melting temperature of DNA repair gene expression

| No. | Name       | Sequences                     | Product (bp) | T <sub>m</sub> (°C) | Reference  |
|-----|------------|-------------------------------|--------------|---------------------|------------|
| 1   | ACT1-F75   | 5' -TGCCGAAAGAATGCAAAAGG-3'   | 75           | 57.56               | [208]      |
| 2   | ACT1-R75   | 5' -TCTGGAGGAGCAATGATCTTGA-3' | 75           | 58.89               | [208]      |
| 3   | ADA2-F138  | 5' -AGGAAAAGCATCGCCCTTA-3'    | 138          | 55.85               | This study |
| 4   | ADA2-R138  | 5' -TCCTGCCAATTACCGAGC-3'     | 138          | 57.05               | This study |
| 5   | DEF1-F144  | 5' -TCCTGCGCTAAAGTCCAA-3'     | 144          | 56.14               | This study |
| 6   | DEF1-R144  | 5' -TCCCATCTTGTCACTGCG-3'     | 144          | 56.98               | This study |
| 7   | EAF1-F132  | 5' -CTGACCGAACTATACTGCGT-3'   | 132          | 57.15               | This study |
| 8   | EAF1-R132  | 5' -CGCCTCGTCAAACCTTATAC-3'   | 132          | 56.35               | This study |
| 9   | EPL1-F148  | 5' -AAAGGCGATTTCAGGTGCT-3'    | 148          | 56.85               | This study |
| 10  | EPL1-R148  | 5' -CCACCTCTCTCTGTTGCA-3'     | 148          | 56.14               | This study |
| 11  | MRC1-F119  | 5' -TGAAAATGGGCCCAATGA-3'     | 119          | 56.43               | This study |
| 12  | MRC1-R119  | 5' -GTTTCGGGTGCTTTTCTTGC-3'   | 119          | 55.00               | This study |
| 13  | NHP6A-F169 | 5' -AAGAAGGACCCAAATGCCC-3'    | 169          | 57.62               | This study |
| 14  | NHP6A-R169 | 5' -CGTAAGGCTGCTTTTCCTC-3'    | 169          | 56.33               | This study |
| 15  | PDS5-F135  | 5' -CTACCTCCGATCAGCTGA-3'     | 135          | 55.04               | This study |
| 16  | PDS5-R135  | 5' -TGCTAACTAGTGCGTCCC-3'     | 135          | 56.36               | This study |
| 17  | SSL2-F131  | 5' -AGACCAACAGCAACAGCA-3'     | 131          | 57.02               | This study |
| 18  | SSL2-R131  | 5' -TCTCATCCTCCCAAGCGT-3'     | 131          | 57.54               | This study |

\*All primer sequences and specificities were designed by Primer3-py package

(<https://www.yeastgenome.org/primer3>) and checked by BLAST (<https://blast.ncbi.nlm.nih.gov/Blast.cgi>).

## 7. Screening molecular processes in CdtB resistant strains

### 7.1. Perspective of molecular processes that are required for CdtB cytotoxicity

The ORF names of CdtB resistant candidates from genome-wide screening (243 genes) were searched for enrichment functions in GO slim mapper and GO term finder programs. Gene ontology is the simple gene definition to describe the gene responsibility in the common language based on biological process, molecular function, and cellular components. GO slim mapper (<https://www.yeastgenome.org/cgi-bin/GO/goSlimMapper.pl>) was used to determine the overview of the molecular process. Many parameters were selected such as choosing a GO set as “Yeast GO-slim”, selecting all terms from Yeast GO-slim and selecting annotation methods as manually curated and high-throughput after the ORFs list was input. The database was searched on 15 Nov 2018. The GO-term list was shown as cluster frequency compared to genome frequency which revealed the frequency of the GO-term in the list compared to the genome. In addition, GO-term finder (<https://www.yeastgenome.org/goTermFinder>) was also used to search for the enriched GO-term that share among the list of genes. An ontology aspect was chosen as an appropriate category and p-value < 0.05. All GO-term names were arranged on the GO-term ancestor map by QuickGo software (<https://www.ebi.ac.uk/QuickGO/>).

## CHAPTER IV: RESULTS

In this study, *Saccharomyces cerevisiae* was used as a model for *Aggregatibacter actinomycetemcomitans* CdtB cytotoxicity as previously described [51]. The effect of CdtB to yeast growth was investigated in wild-type yeast (BY4741), a haploid Mat a strain. WT yeast was transformed with pYES2 empty vector or pYES2-CdtB plasmid. These plasmids contain the auxotrophic marker *URA3*, thus we can select the transformants using synthetic media lacking uracil (SC-Ura). The galactose inducible promoter controls CdtB expression by galactose supplemented media. The early log phase yeasts grown in the neutral sugar (2% sucrose) were switched to CdtB inducing media (2% galactose) and the optical density was measured every hour to monitor their growth rate (Figure 4). The growth rate of CdtB containing strain is the same as the control until 8h after induction. Afterwards, it was significantly reduced after 12h of induction

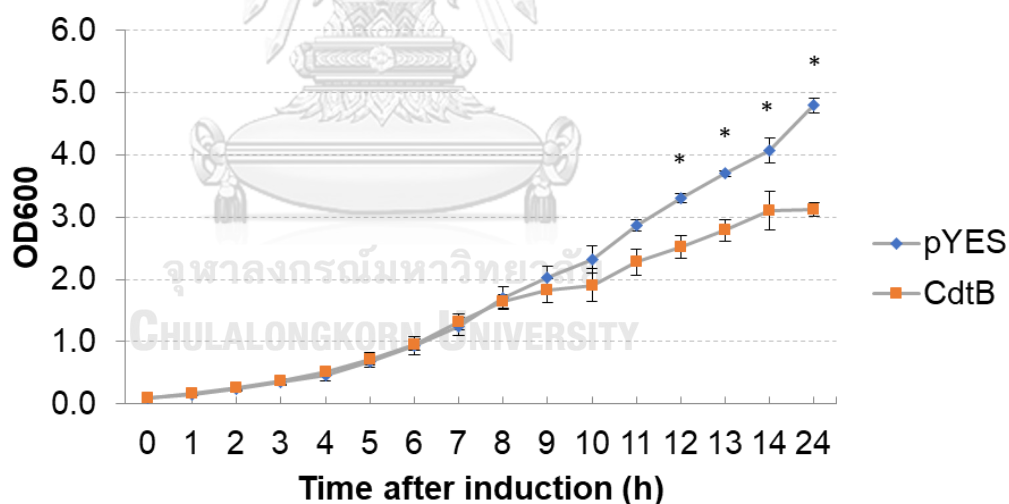


**Figure 4** Growth curve analysis of CdtB induction in yeast.

The growth of wild-type (BY4741) was determined using optical density (OD) at 600nm as a parameter. Cells started to grow from 0.1 OD<sub>600</sub> and OD measurement was done every hour. The growth rate of CdtB containing strain was significantly reduced after 12h of the induction (\*p < 0.05; t-test). The experiment was done in triplicates.

**Objective 1. To identify chromatin regulatory genes that are required for cytotoxicity of CdtB.**

Chromatin regulators keep the chromatin dynamic for the integrity of the genome. To explore the role of chromatin structure in response to CdtB, we first determined what chromatin regulatory genes are required. We examined CdtB susceptibility in the null mutants of various chromatin regulators which can be classified in 5 groups including (i) **Histones** (*hho1Δ* and *htz1Δ*), (ii) **SWR-complex** (*swr1Δ*, *swc2Δ*, *swc3Δ*, *swc5Δ*, *swc6Δ*, *swc7Δ*, and *arp6Δ*), (iii) **INO80-complex** (*nhp10Δ*, *arp5Δ*, and *arp8Δ*), (iv) **SIR-complex** (*sir2Δ*, *sir3Δ* and *sir4Δ*) and (v) **other histone modifying enzymes** including *gcn5Δ* (histone acetyltransferase), *ste20Δ* (histone kinase) and *dot1Δ* (histone methylase). These yeast strains were selected based on gene functions and focused on the unique subunits in these complexes. In general, these genes are responsible for regulation of the chromatin structure, thus controlling the DNA accessibility and gene transcription. We hypothesized that the gene deletions would make the mutant yeast strains resistant to CdtB if these chromatin regulatory genes are required for CdtB function.

To investigate the requirement of chromatin remodeling genes in CdtB function, CdtB susceptibility testing by spot tests and survival plating assays were performed. All null mutants were obtained from yeast deletion library of BY4741 background strain. (Invitrogen; Open Biosystems, USA). All yeast strains were transformed with pYES2 empty vector or pYES2-CdtB plasmid. The early log phase samples were prepared in sucrose media as the neutral sugar and spotted on the agar by 10-fold dilution method. The growth of the strains under CdtB expressing condition (galactose) was compared to that under repressive condition (glucose) and to the strains with pYES vector alone. In our result, CdtB susceptible phenotype in agreement with 41% survival rate was found in WT (Figures 5, 6). The relative growth rate of WT was set to compare with other mutants. The mutants are classified as CdtB resistant if the growth rate of the CdtB expressing strains is higher than WT, or CdtB non-resistant if the growth rate is less than or equal to WT. CdtB resistant phenotype was found in certain deletion strains of SWR-

complex, INO80-complex, SIR-complex and a histone variant *HTZ1* (Figure 5) suggesting that those genes are involved in CdtB function. On the other hand, other subunits of chromatin regulatory complexes and some histone modifying enzymes did not confer CdtB resistance (Figure 6), therefore they are not involved in CdtB function. The summary of phenotype and the function of each subunit are presented in Table 13.

In addition, we found that the level of CdtB protein of *htz1Δ* is slightly lower than WT (Figure 8A). This result suggests that the translational processes may also involve in CdtB function. We tested the strains for susceptibility to cycloheximide, a well-known protein synthesis inhibitor, and found that most of the mutants are more sensitive to cycloheximide than WT (Figure 9).

The function of each chromatin regulatory complex is connected. Since the deletion of *HTZ1* is resistant to CdtB, the histone variant exchange at transcription start site may involve in CdtB function. The replacement of Htz1 requires SWR-complex to deposit into nucleosome and INO80 complex to remove [122, 133]. SWR and INO80 complexes, thus, should also involve in CdtB function. Surprisingly, almost important subunits of chromatin regulators are resistant to CdtB (Figure 5 and Table 13) suggesting that the Htz1 exchange may facilitate CdtB to target yeast DNA. Deletion of *SIR2* or *SIR3* leads to resistance to CdtB toxicity. Sir proteins have a role in chromatin silencing which control the accessibility of DNA interacting proteins [162, 209, 210]. Moreover, the lack of other modifying enzymes that we examined showed non-resistant phenotype (Figure 6). Gcn5 functions as an acetyltransferase on Htz1 tail to keep it in the nucleosome and avoid the removal by INO80-complex [174]. Ste20 is a p21-activated kinase that phosphorylates H2B during apoptosis [211, 212]. Dot1 is a histone H3-K79 methylase and an inhibitor of Cdc25 and p53 activation resulting in cell cycle arrest [189]. However, these processes may not be involved in CdtB toxicity in yeast.

It is important that the null mutant genes and CdtB expression in our experiment are correct to reflect the phenotype of CdtB precisely. To verify the mutants, we confirmed the phenotypes by PCR. Genomic DNA of each mutants were extracted and amplified with their specific A and KanB primers at the deletion locus. Various PCR

conditions are performed depending on the melting temperature of the primers. The results are shown in **Figure 7**. We detected the expected PCR products in all samples suggesting that the deletion strains in our experiment are correct. Furthermore, it is possible that there are no CdtB expression in the mutants resulting the same phenotype as pYES control. To rule out this possibility, immunoblot assay was performed. The early log phase samples were induced the CdtB expression with 2% galactose for 6h [51]. Proteins from whole yeast lysate (30  $\mu$ g) was denatured to run on SDS-PAGE. Anti-CdtB antibody was used to detect the CdtB protein as illustrated in **Figures 8A and 8B**. These results confirmed that CdtB protein was expressed in all strains and the resistant phenotype was not due to the defect in CdtB expression.

In addition, plate sensitivity assay allows us to better observe the overall effect of CdtB, including the effect on colony size. Since CdtB-induced cell cycle arrest can lead to a small colony size, formation of larger colonies on galactose media also reflects resistance to the effect of CdtB. Our previous study showed that CdtB induced yeast cell cycle arrest at S, G2 phase [51]. Therefore, we examined cell cycle progression by DNA content analysis with propidium iodide (PI) staining and flow cytometry after 12h or 24h of CdtB expression (**Table 14 and Figures 10-12**). We selected three CdtB-resistant strains (*htz1 $\Delta$* , *sir2 $\Delta$* , and *arp5 $\Delta$* ) and other two are non-CdtB resistant strains (*swc7 $\Delta$*  and *sir4 $\Delta$* ). We did not observe the accumulation of S or G2/M phase in WT yeast both at 12h or 24h after CdtB induction. However, the accumulation of G2/M phase in certain mutants was more than WT, such as in *htz1 $\Delta$* , *arp5 $\Delta$* , and *sir4 $\Delta$* . The accumulation seems to be not associate to CdtB induction and CdtB resistant phenotype of the mutants. Therefore, cell cycle arrest of these mutants may not a factor which involve in CdtB function.

According to our finding, there are several processes that may involve in CdtB function. The process of Htz1 histone variant exchange may requires for CdtB function due to the CdtB resistant phenotype. It is undeniable that the accessibility of CdtB to DNA is necessary for DNA damage. The interruption of Htz1 deposition increases cell survival rate in CdtB exposed condition for example lack of Htz1 protein, dysfunction of



Htz1 deposition complex (SWR complex). Thus, Htz1 may be a factor to facilitate CdtB close to target DNA. Further experiment would investigate mechanisms how these mutants become CdtB resistance and what cellular processes involve in CdtB function.



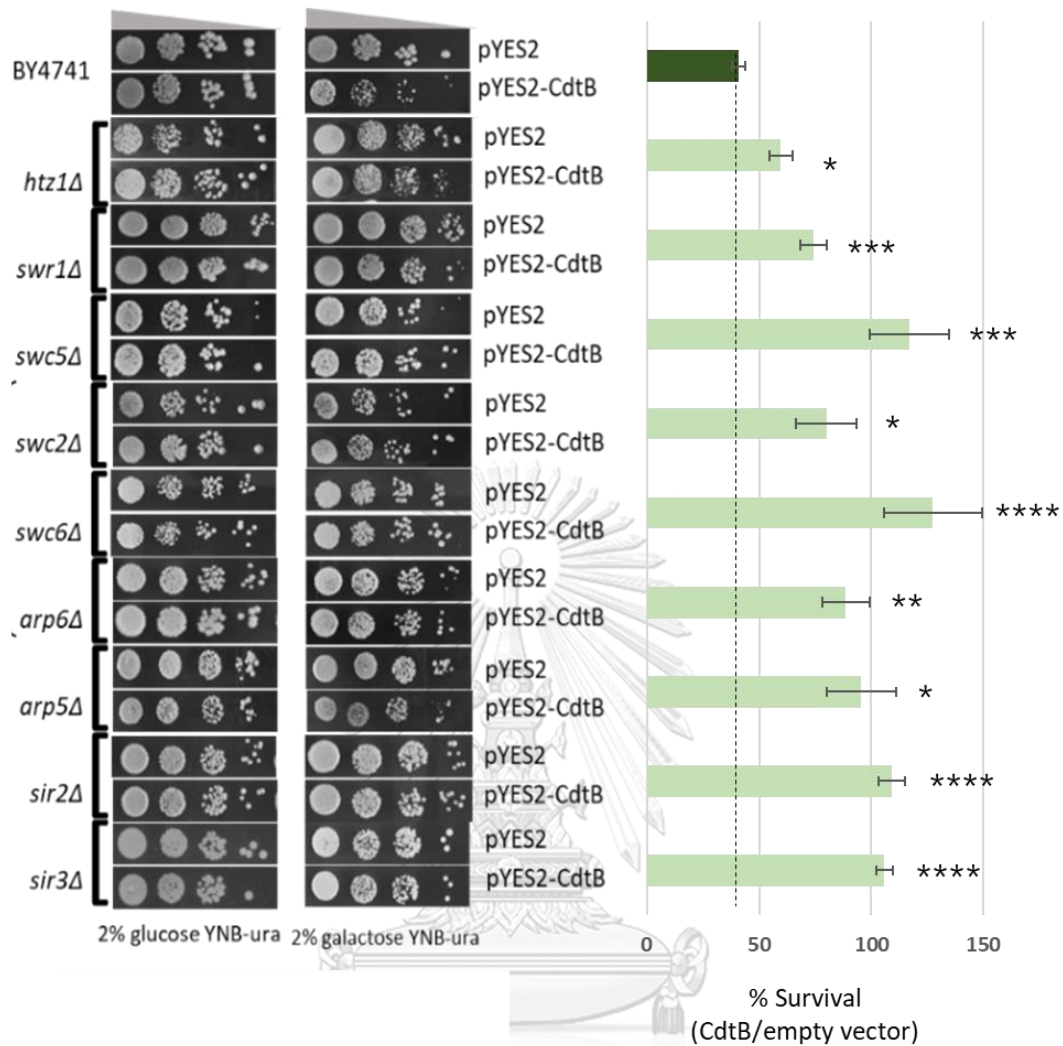


Figure 5 CdtB resistant profile of chromatin regulatory gene mutants.

A spot test of serial dilutions of wild-type and the deletion strain of chromatin regulators with pYES2-CdtB in comparison to pYES2 on glucose and galactose media. Photographs were taken after approximately 40 hours of incubation at 30°C. Samples were also plated on both media for survival assay. All colonies of CdtB containing strain were counted and compared to pYES2. The experiment was done in triplicates and three transformants. The results represent mean  $\pm$  SEM and p-value calculated by the Mann-Whitney U test.  $p \leq 0.05$  was considered the statistical significance. (\*, \*\*, \*\*\*, and \*\*\*\* respectively indicated  $p < 0.05$ ,  $p < 0.01$ ,  $p < 0.001$  and  $p < 0.0001$ )

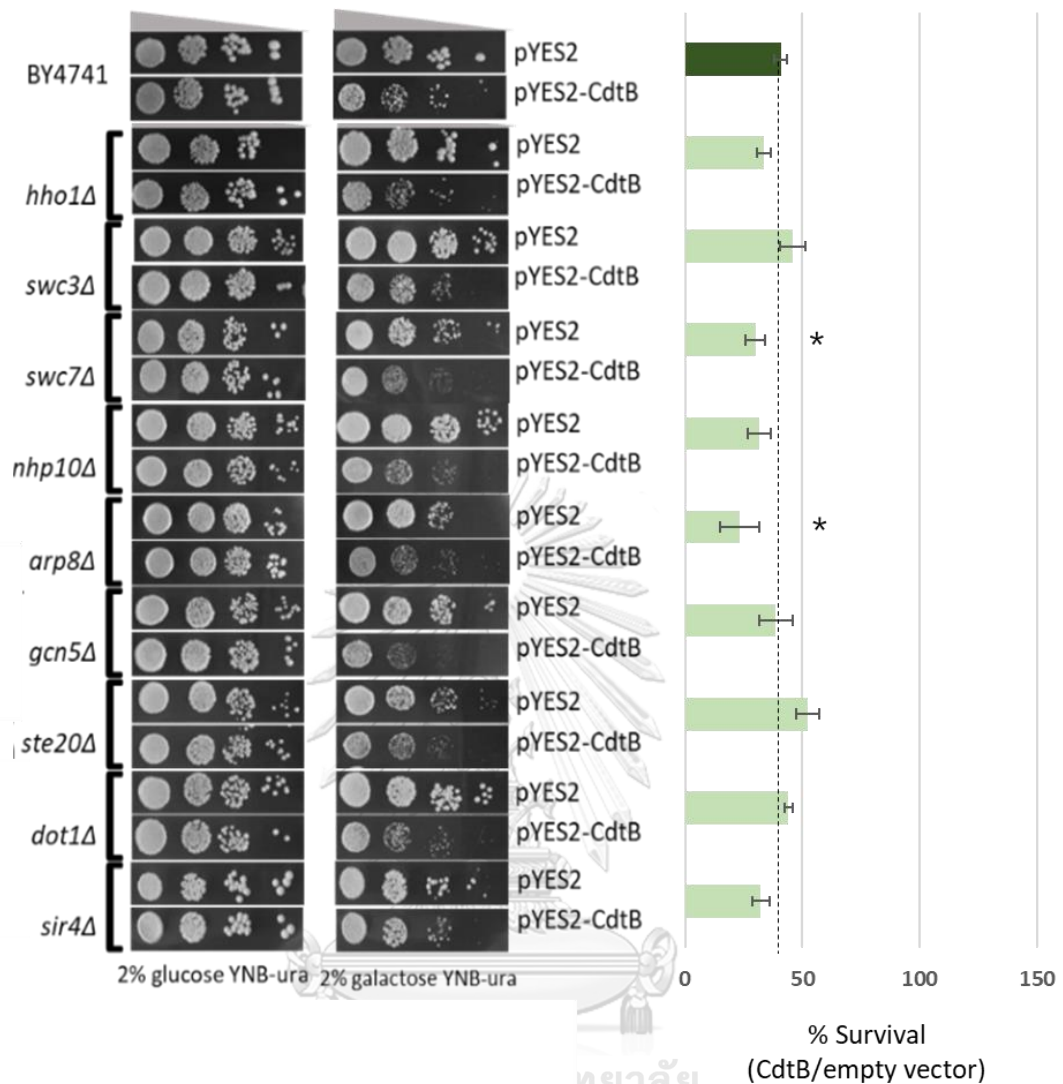


Figure 6 CdtB non-resistant profile of chromatin regulatory gene mutants.

A spot test of serial dilutions of wild-type and the deletion strain of chromatin regulators with pYES2-CdtB in comparison to pYES2 on glucose and galactose media. Photographs were taken after approximately 40 hours of incubation at 30°C. Samples were also plated on both media for survival assay. All colonies of CdtB containing strain were counted and compared to pYES2. The experiment was done in triplicates and three transformants. The results represent mean  $\pm$  SEM and p-value calculated by the Mann-Whitney U test.  $p \leq 0.05$  was considered the statistical significance. (\*, \*\*, \*\*\*, and \*\*\*\* respectively indicated  $p < 0.05$ ,  $p < 0.01$ ,  $p < 0.001$  and  $p < 0.0001$ )

Table 13 The summary of phenotype by CdtB susceptibility test and subunit functions

| Groups            | Gene          | Phenotype     | Function   | References          |
|-------------------|---------------|---------------|--|---------------------|
| Histone proteins  | <i>htz1Δ</i>  | Resistant     | Involved in the transcriptional regulation.<br>Prevention of the spread of silent heterochromatin.                         | [123, 130]          |
|                   | <i>hho1Δ</i>  | Non-resistant | A linker histone for chromatin structure.<br>Inhibits transcriptional silencing  | [213, 214]          |
| SWR-complex       | <i>swr1Δ</i>  | Resistant     | Histone exchange   | [120, 133, 135-137] |
|                   | <i>swc5Δ</i>  | Resistant     |  |                     |
|                   | <i>swc2Δ</i>  | Resistant     |  |                     |
|                   | <i>swc6Δ</i>  | Resistant     | Nucleosome binding and complex assembly  |                     |
|                   | <i>arp6Δ</i>  | Resistant     |  |                     |
|                   | <i>swc3Δ</i>  | Non-resistant | Subunit functions are unclear.   |                     |
|                   | <i>swc7Δ</i>  | Non-resistant | Subunit deletion does not affect to histone exchange activity, nucleosome binding and complex assembly.                    |                     |
| INO80-complex     | <i>arp5Δ</i>  | Resistant     | Htz1 exchange and nucleosome remodeling  | [122, 135, 215]     |
|                   | <i>arp8Δ</i>  | Non-resistant | Complex recruitment  |                     |
|                   | <i>nhp10Δ</i> | Non-resistant | Nucleosome binding   |                     |
| SIR-complex       | <i>sir2Δ</i>  | Resistant     | HDAC (H4K16), heterochromatin formation and rDNA silencer  | [162, 209, 210]     |
|                   | <i>sir3Δ</i>  | Resistant     | Heterochromatin formation and increase in silencing at the rDNA locus  |                     |
|                   | <i>sir4Δ</i>  | Non-resistant | Heterochromatin formation  |                     |
| Modifying enzymes | <i>gcn5Δ</i>  | Non-resistant | Gcn5 acetylates the Htz1 tail to keep it in the nucleosome avoiding the removal by INO80-C.                                | [174]               |
|                   | <i>ste20Δ</i> | Non-resistant | A kinase of p21-activated kinase (PAK).<br>PAK phosphorylates the apoptotic protein leading to the reduction of apoptosis. | [211, 212]          |
|                   | <i>dot1Δ</i>  | Non-resistant | A histone H3-K79 methylase.<br>Inhibit the activation of Cdc25 and p53 resulting in cell cycle arrest.                     | [189]               |

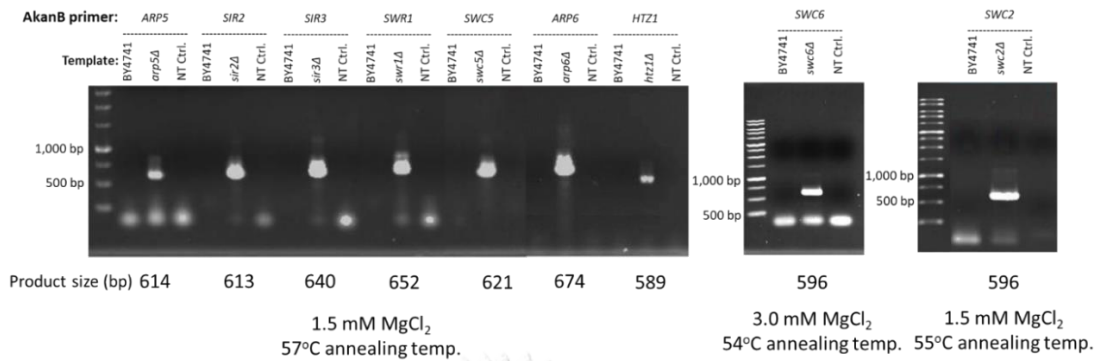


Figure 7 Strain confirmation by the PCR technique.

Positive PCR results were amplified by specific A and KanB primers with the various PCR conditions.

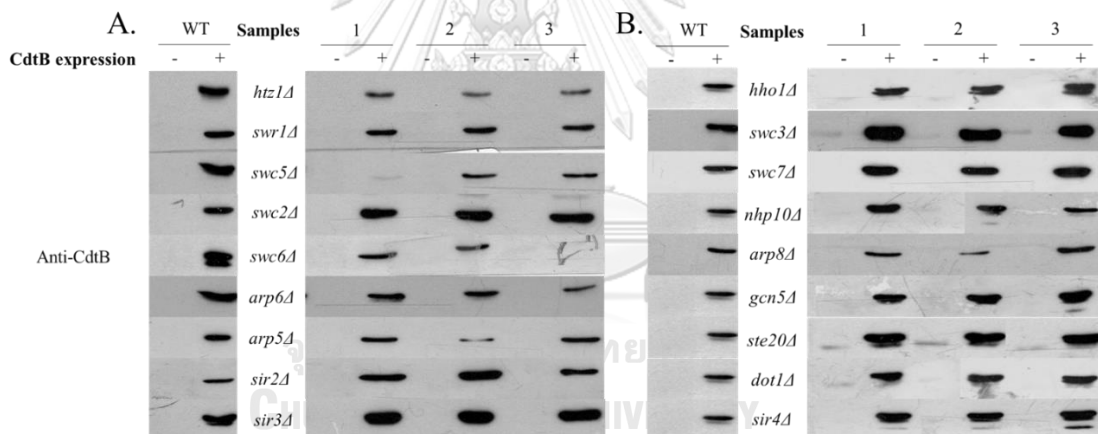


Figure 8 CdtB expression in CdtB resistant mutants

(A) and CdtB non-resistant mutants (B) by western blot assay. Proteins from whole yeast lysates were subjected after CdtB induction for 6h in 2% galactose media. Thirty micrograms of protein were loaded and size-separated by SDS-PAGE. Anti-CdtB antibody was used together with HRP conjugated secondary antibody to detect the target protein. The exposure time of each experimental set was various.

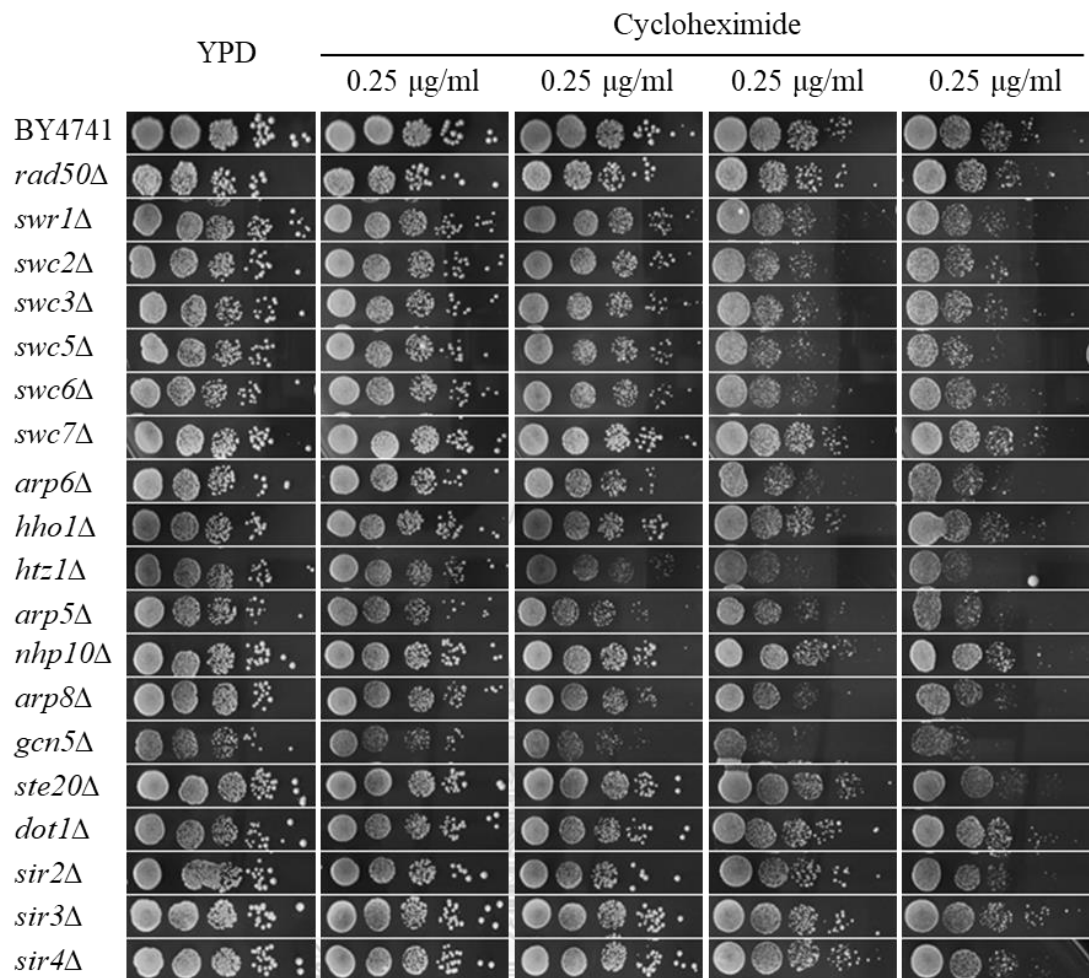


Figure 9 Cycloheximide sensitivity test.

Log phase culture of WT and mutants yeast were serially diluted and spotted on YPD or vary cycloheximide concentration YPD. Photographs were taken after approximately 3 days of incubation at 30 °C.

Table 14 DNA content analysis of CdtB-treated yeast

| Time after induction (h) | Strains      | % of yeast in cell cycle phase (pYES2) |          |          | % of yeast in cell cycle phase (CdtB) |          |          |
|--------------------------|--------------|--|----------|----------|---------------------------------------|----------|----------|
|                          |              | G1                                     | S        | G2/M     | G1                                    | S        | G2/M     |
| 0                        | BY4741       | 34.8±1.1                               | 15.4±0.1 | 49.8±1.2 | 32.2±1.0                              | 21.9±3.7 | 45.9±2.8 |
|                          | <i>htz1Δ</i> | 37.7±0.4                               | 11.4±0.1 | 50.9±0.4 | 40.1±2.0                              | 8.5±1.4  | 51.5±0.7 |
|                          | <i>sir2Δ</i> | 29.9±1.2                               | 21.0±3.3 | 49.2±2.8 | 31.0±0.3                              | 19.2±0.6 | 49.8±0.8 |
|                          | <i>arp5Δ</i> | 34.6±3.3                               | 11.4±0.8 | 54.0±2.6 | 34.4±0.7                              | 7.1±0.1  | 58.5±0.8 |
|                          | <i>swc7Δ</i> | 32.6±0.4                               | 18.0±1.3 | 49.4±1.4 | 34.5±0.5                              | 16.9±1.7 | 48.6±2.1 |
|                          | <i>sir4Δ</i> | 25.1±0.3                               | 29.3±0.1 | 45.6±0.4 | 24.1±0.6                              | 32.0±3.4 | 43.9±3.5 |
| 12                       | BY4741       | 34.8±2.2                               | 7.9±1.3  | 57.3±0.9 | 42.9±0.2                              | 13.8±0.3 | 43.3±0.1 |
|                          | <i>htz1Δ</i> | 35.5±0.2                               | 12.4±0.8 | 52.3±0.9 | 32.0±0.4                              | 11.9±0.4 | 56.1±0.5 |
|                          | <i>sir2Δ</i> | 45.3±0.4                               | 10.7±0.1 | 43.9±0.5 | 46.5±0.4                              | 17.5±0.4 | 36.0±0.7 |
|                          | <i>arp5Δ</i> | 27.7±0.4                               | 7.4±0.1  | 64.9±0.4 | 25.6±0.4                              | 14.5±1.1 | 64.9±0.4 |
|                          | <i>swc7Δ</i> | 40.8±0.7                               | 9.5±0.9  | 49.8±0.2 | 47.0±0.7                              | 22.8±1.0 | 30.2±1.6 |
|                          | <i>sir4Δ</i> | 28.3±0.8                               | 18.3±1.7 | 53.3±2.3 | 29.6±0.2                              | 25.3±0.9 | 45.1±0.9 |
| 24                       | BY4741       | 69.4±2.6                               | 9.2±3.4  | 21.3±0.8 | 65.9±1.8                              | 12.9±0.7 | 21.2±1.1 |
|                          | <i>htz1Δ</i> | 45.0±0.8                               | 8.5±0.7  | 46.5±0.7 | 35.0±0.2                              | 0.2±0.1  | 64.8±0.2 |
|                          | <i>sir2Δ</i> | 61.5±0.2                               | 5.4±0.3  | 33.1±0.1 | 58.7±0.4                              | 9.5±0.1  | 31.8±0.6 |
|                          | <i>arp5Δ</i> | 43.9±0.7                               | 6.9±0.9  | 49.2±0.5 | 46.8±0.3                              | 10.5±0.1 | 42.7±0.3 |
|                          | <i>swc7Δ</i> | 70.5±1.1                               | 8.4±1.4  | 21.0±0.4 | 69.0±0.6                              | 13.1±0.1 | 17.8±0.5 |
|                          | <i>sir4Δ</i> | 47.7±0.8                               | 12.7±0.7 | 39.6±0.6 | 44.9±0.3                              | 20.3±0.9 | 34.8±0.6 |

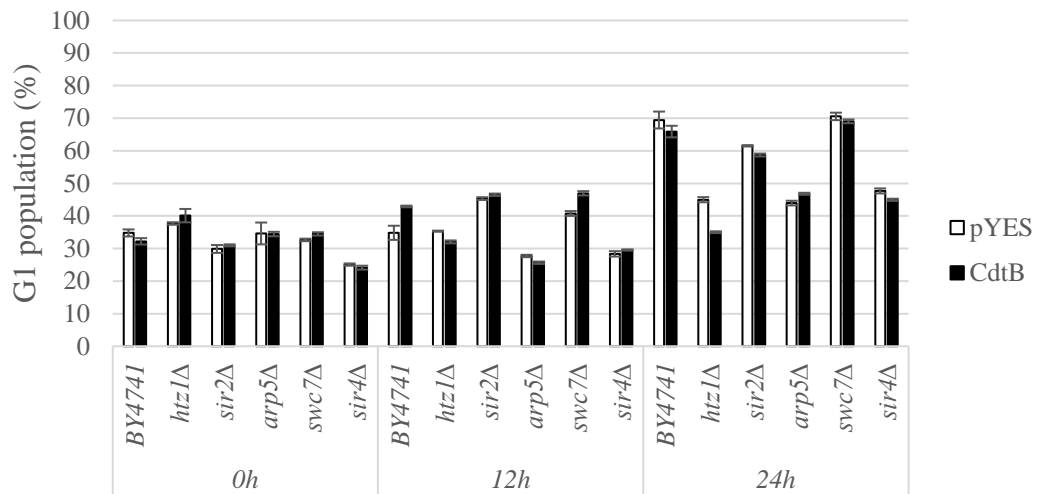


Figure 10 Effect of CdtB on the G1 cell cycle phase of the mutants.

Flow cytometric analysis of the DNA content of the G1 phase population in yeast with CdtB (white bar) or without CdtB (black bar) expression.

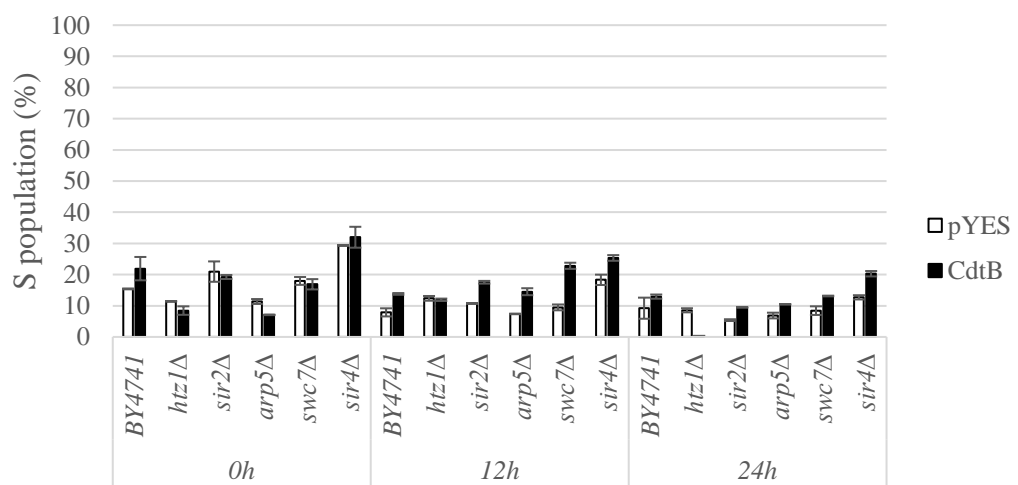


Figure 11 Effect of CdtB on the S cell cycle phase of the mutants.

Flow cytometric analysis of the DNA content of the S phase population in yeast with CdtB (white bar) or without CdtB (black bar) expression.



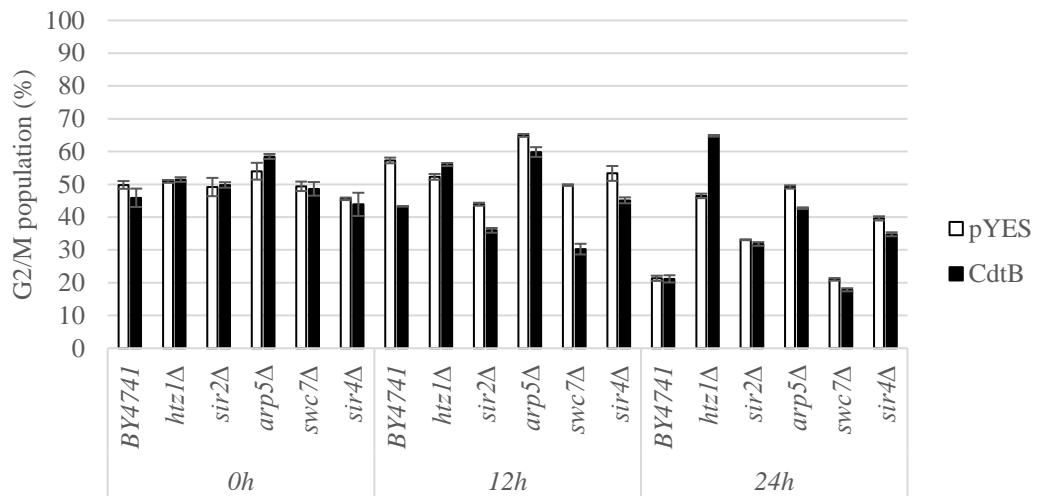


Figure 12 Effect of CdtB on the G2/M cell cycle phase of the mutants.

Flow cytometric analysis of the DNA content of the G2/M phase population in yeast with CdtB (white bar) or without CdtB (black bar) expression.

**Objective 2. To examine the mechanisms how chromatin regulatory genes, facilitate CdtB cytotoxicity.**

### **2.1. Testing the physical interaction between CdtB and Htz1 protein**

We hypothesized that CdtB may interact with certain components of the chromatin to target host DNA. Our preliminary results suggested that Htz1 and certain subunits of SWR complex are required for CdtB activity. The main function of the SWR complex is to exchange the histone variant Htz1 (Htz1-H2B) with H2A-H2B heterodimer into nucleosomes [123]. Thus, Htz1 may be involved in the chromatin targeting mechanism of CdtB. It may bind to CdtB and guide to the DNA. To test this hypothesis, physical interaction between Htz1 and CdtB was performed. Recombinant CdtB protein with 6-histidine tag was induced using *E. coli* as a host and was purified by immobilized metal affinity chromatography (IMAC) method. Moreover, the whole cell lysate of HA-tagged Htz1 was extracted and used for incubation with recombinant CdtB. Immunoprecipitation with antibody coated protein A beads was performed. Protein A has a potential to bind on Fc portion of immunoglobulin [216]. We prepared anti-CdtB antibody coated beads and added into the Htz1-CdtB interaction sample to precipitate these proteins. The precipitants were analyzed by SDS-PAGE and western blot technique using anti-CdtB and anti-HA antibodies. We could not observe co-precipitation of Htz1 when using anti-CdtB beads but Htz1 presented in the supernatant after immunoprecipitation (Figure 13). This suggested that CdtB do not have a stable interaction with Htz1.

To improved detection of transient interaction with chromatin, samples were cross-linked with formaldehyde before chromatin immunoprecipitation (ChIP) was performed. CdtB containing plasmid was transformed and induced the expression in Htz1:HA strains. Cross-linked samples were extracted and sheared to the small chromatin fragment by sonication. We used 2 kinds of precipitators for ChIP assay including anti-CdtB and anti-HA antibody coated beads. The precipitants were analyzed by SDS-PAGE and immunoblot assay using anti-CdtB and anti-HA antibodies. The result showed that CdtB and Htz1 do not co precipitate with each other (Figure 14). Thus,

CdtB do not have physical interaction with Htz1 and do not have the stable binding on chromatin to take the action.

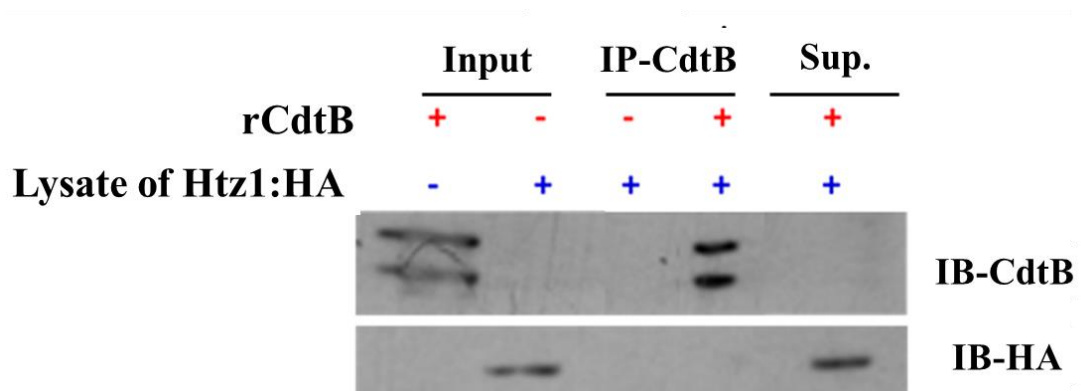


Figure 13 Physical interaction between recombinant CdtB and Htz1 protein in vitro.

6-histidine tagged recombinant CdtB incubating with Htz1:HA cell lysate was precipitated with anti-CdtB coated protein A beads. The precipitants were analyzed by immunoblot assay with anti-CdtB and anti-HA antibody. Sup. is the abbreviation of supernatant.

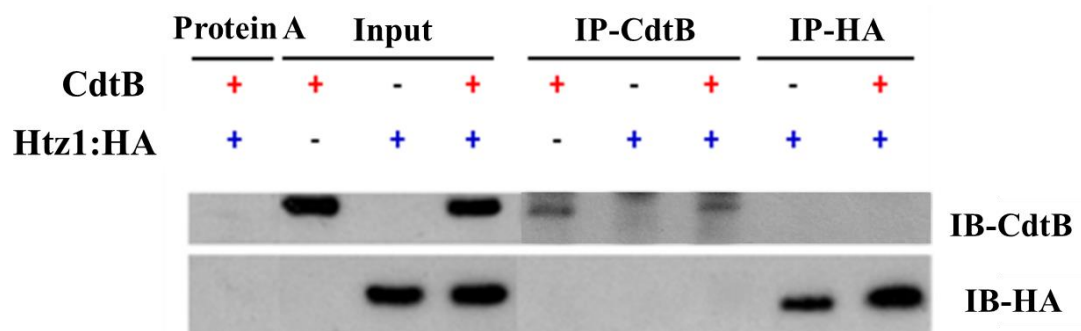


Figure 14 Chromatin immunoprecipitation result of CdtB and Htz1 interaction.

Cross-linked samples were extracted from Htz1:HA strains with or without CdtB expression. Chromatin was sheared into small fragments by sonication. Samples were precipitated by anti-CdtB and anti-HA coated beads. The precipitants were analyzed by immunoblot assay with anti-CdtB and anti-HA antibody.

Since Htz1 had no physical interaction with CdtB protein, the CdtB resistant mechanism might not be as easy as a direct interaction. We proposed several hypotheses that may explain how certain gene deletions could affect CdtB cytotoxicity. The first hypothesis was the reduction of nuclear localization of CdtB in the CdtB resistant strains. Due to the genotoxic property, it needs to localize to the nucleus to interact with host DNA. Second, we asked whether CdtB could induce DNA damage in the CdtB resistant strains. This could distinguish whether the gene deletion could prevent DNA damage, or it could enhance cellular processes after DNA damage to increase the survival rate. Next, the defect of the chromatin regulatory subunit may affect the chromatin structure. Mutant's chromatin may differ from wild-type which can prevent the DNA damage by CdtB more than wild-type. Furthermore, chromatin regulators play an important role in transcriptional control leading to better repair of CdtB damage.

## 2.2. Reduction of CdtB nuclear localization could be a CdtB-resistant mechanism

Nuclear localization is an important process of DNase activity of CdtB [51], CdtB resistance may result from any interference to the nuclear translocation process. We performed yeast cell fractionation to investigate CdtB localization after 8h of induction. The basic principle is to separate the cell components by the centrifugation speed which classify into two fractions including cytosol and nuclei. We compared CdtB localization between wild-type and nuclear localization signal lacking CdtB (CdtB $\Delta$ 11aa). For the fractionation markers, we used anti-phosphoglycerate kinase 1 (PGK1), a glycolytic enzyme that usually found in the cytosol, as a cytosolic marker and anti-histone H3 as a nuclear marker. We found that CdtB protein presented not only in the nucleus, but also in the cytosol (**Figure 15**). However, it is hard to quantitate the ratio of CdtB in nucleus compared to cytosol. Thus, we attempted to improve the quantitative technique using immunofluorescence. We prepared spheroplast, a cell wall digested yeast, by lyticase as a subject for intracellular immunostaining. We used anti-CdtB antibody and rhodamine-conjugated anti-rabbit IgG to determine CdtB localization. DAPI was used for nuclei staining.

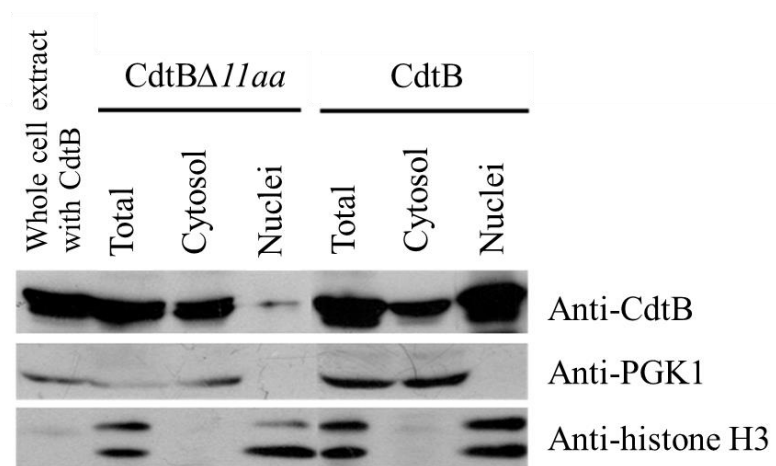


Figure 15 Cell fractionation and an immunoblotting assay of WT yeast.

WT and the nuclear localization defect of CdtB (*CdtBΔ11aa*) were used as subjects for localization study. An anti-phosphoglycerate kinase (PGK1) and anti-histone H3 antibody were used for the cytosolic and nuclear markers, respectively.

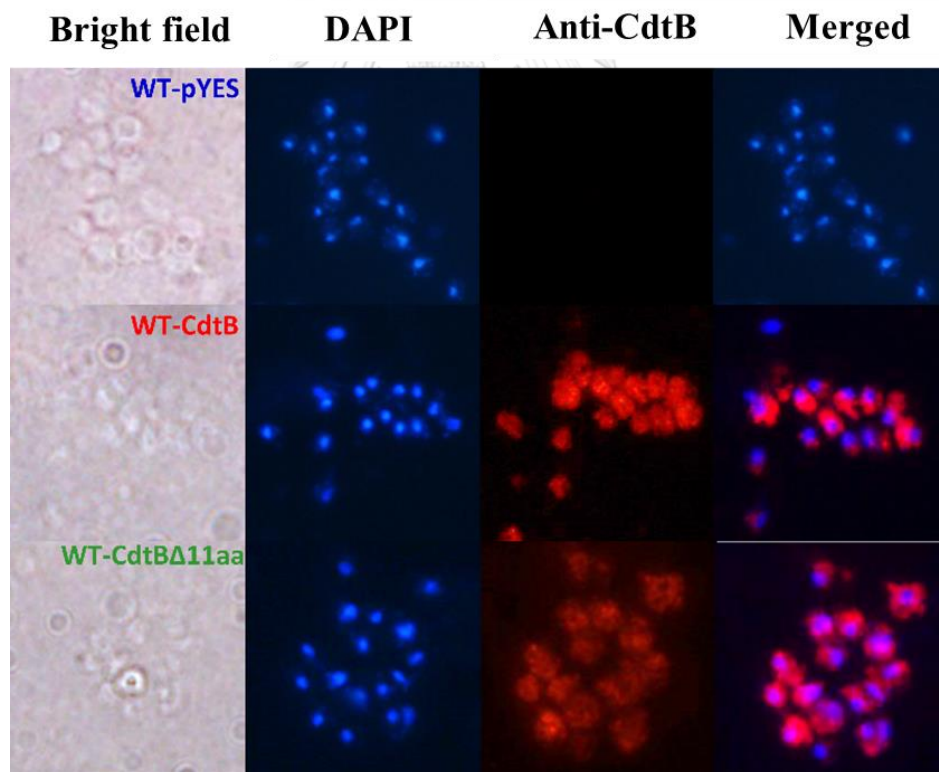


Figure 16 CdtB localization by the immunofluorescent method.

Spheroplasts were stained with anti-CdtB and rhodamine-conjugated antibody. Nuclei were stained by DAPI. CdtB localization of nuclear localization signal lacking CdtB (*CdtBΔ11aa*) were compared to wild-type CdtB.

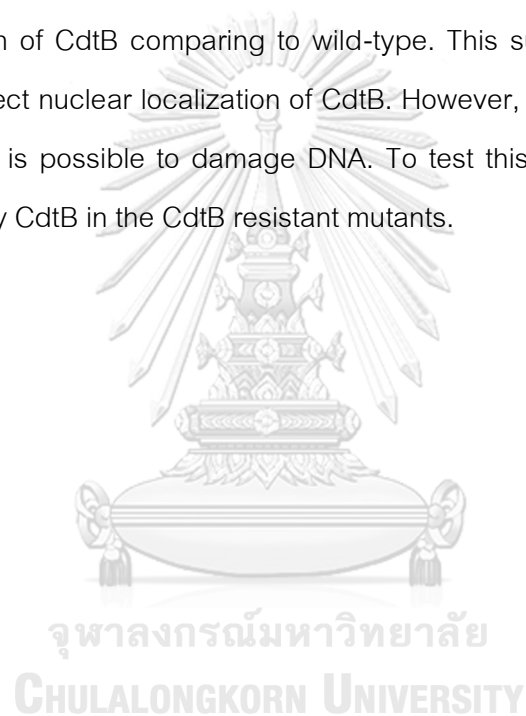
According to this method, the cell boundary images were not clear enough to determine the CdtB localization due to the disruption of cell wall integrity (Figure 16). This method is also not effective to investigate CdtB localization.

Another effective method for protein localization is to monitor the translocation of fluorescent proteins. We constructed the EGFP-tagged CdtB plasmid and transformed into yeast. We can control the protein expression by galactose inducible promoter. The successful CdtB-EGFP fusion protein was determined by western blot. Molecular weight of the fusion protein is quite double to CdtB (59 kD vs. 29 kD) which we can observe the band-shift of CdtB-EGFP protein (Figure 17A). The fusion protein expression level in CdtB resistant mutants were also compared to wild-type yeast (Figure 17B). Then, we investigated the toxicity of CdtB-EGFP in yeast by spot test because the fusion protein was considerably larger, and the size could interfere nuclear localization. CdtB-EGFP was less toxic than CdtB in wildtype yeast, but the cytotoxicity was clearly observed in CdtB-sensitive strain (*rad50Δ*), which has defective DNA repair, as shown in Figure 18. This suggested that the fusion protein is less toxic to yeast but, at least, it can translocate into the nucleus and causes DNA damage. Moreover, the EGFP was folded properly due to the illuminated fluorescence by colonies under the blue light chamber (Figure 18). Thus, we can use CdtB-EGFP fusion protein to determine nuclear localization in yeast.

Our backbone plasmid is pYES expression plasmid. It is possible that the high background of EGFP over expression may interfere the true signal. Therefore, the optimization of CdtB-EGFP localization study was performed. CdtB expression was induced by various sugar concentration including 1.9% galactose + 0.1% glucose, 0.1% galactose + 1.9% sucrose, and 2% galactose. Samples were stained with DAPI for nuclear territory and fixed on the slide. Fluorescent images were analyzed with Mander's coefficient to evaluate the percentage of localization from Just Another Co-localization Plug-in on imageJ software [217, 218]. The result revealed that 2% galactose is the best condition to identify the CdtB localization relative to EGFP background. (Figures 19 and

20). We can apply this condition to the investigation of CdtB localization in CdtB resistant mutants. Thus, the representative confocal fluorescent microscopic images of CdtB resistant mutants were shown in **Figure 21**. The relative CdtB nuclear localization was evaluated by Manders' coefficient in comparison to the signal of EGFP vector control (**Figure 22**). The result can be separated into 2 groups including CdtB nuclear localization is less than wild-type (*htz1Δ*, *swr1Δ*, *swc2Δ*, *swc6Δ*, *arp6Δ*, and *arp5Δ*) and the localization is quite the same as wild-type (*swc5Δ*, *sir2Δ* and *sir3Δ*).

According to the CdtB localization result, several mutants showed reduced nuclear localization of CdtB comparing to wild-type. This suggests that the chromatin regulators may affect nuclear localization of CdtB. However, CdtB could be observed in the nucleus which is possible to damage DNA. To test this, we investigated the DNA damage caused by CdtB in the CdtB resistant mutants.







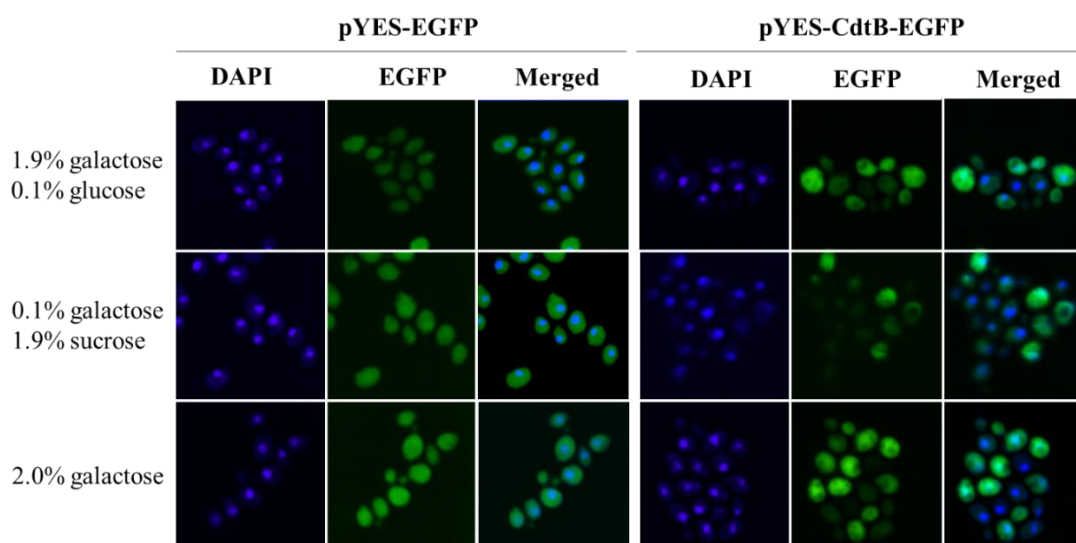


Figure 19 Representative fluorescent images (at 600x magnification) of localization of CdtB-EGFP and EGFP control in wild-type yeast at various concentrations of galactose (1.9% galactose + 0.1% glucose, 0.1% galactose + 1.9% sucrose, and 2.0% galactose, in order of the expression levels of CdtB-EGFP from the lowest to highest). DAPI was used to stain the yeast nuclei. Merged images of the DAPI and EGFP channels are also shown.

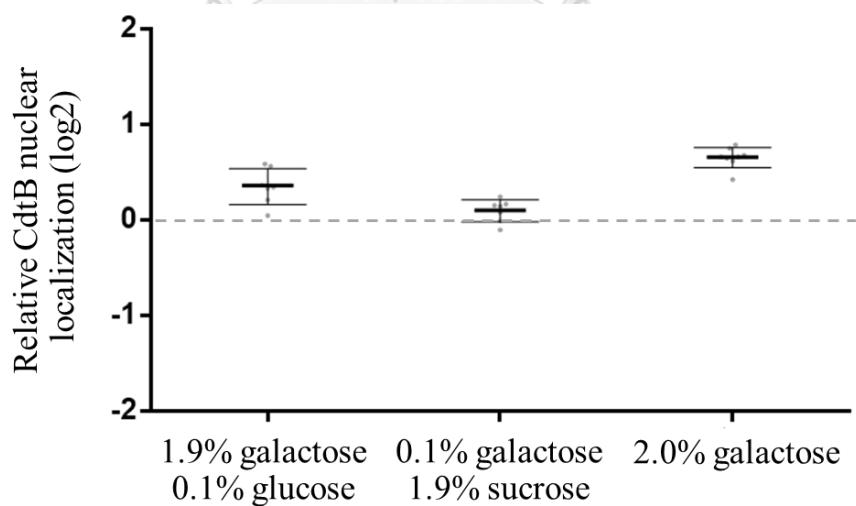


Figure 20 Quantification of nuclear localization of CdtB-EGFP relative to EGFP at the various galactose concentrations as in figure 19 is shown in log 2 scale.

The dotted line represents the background level.

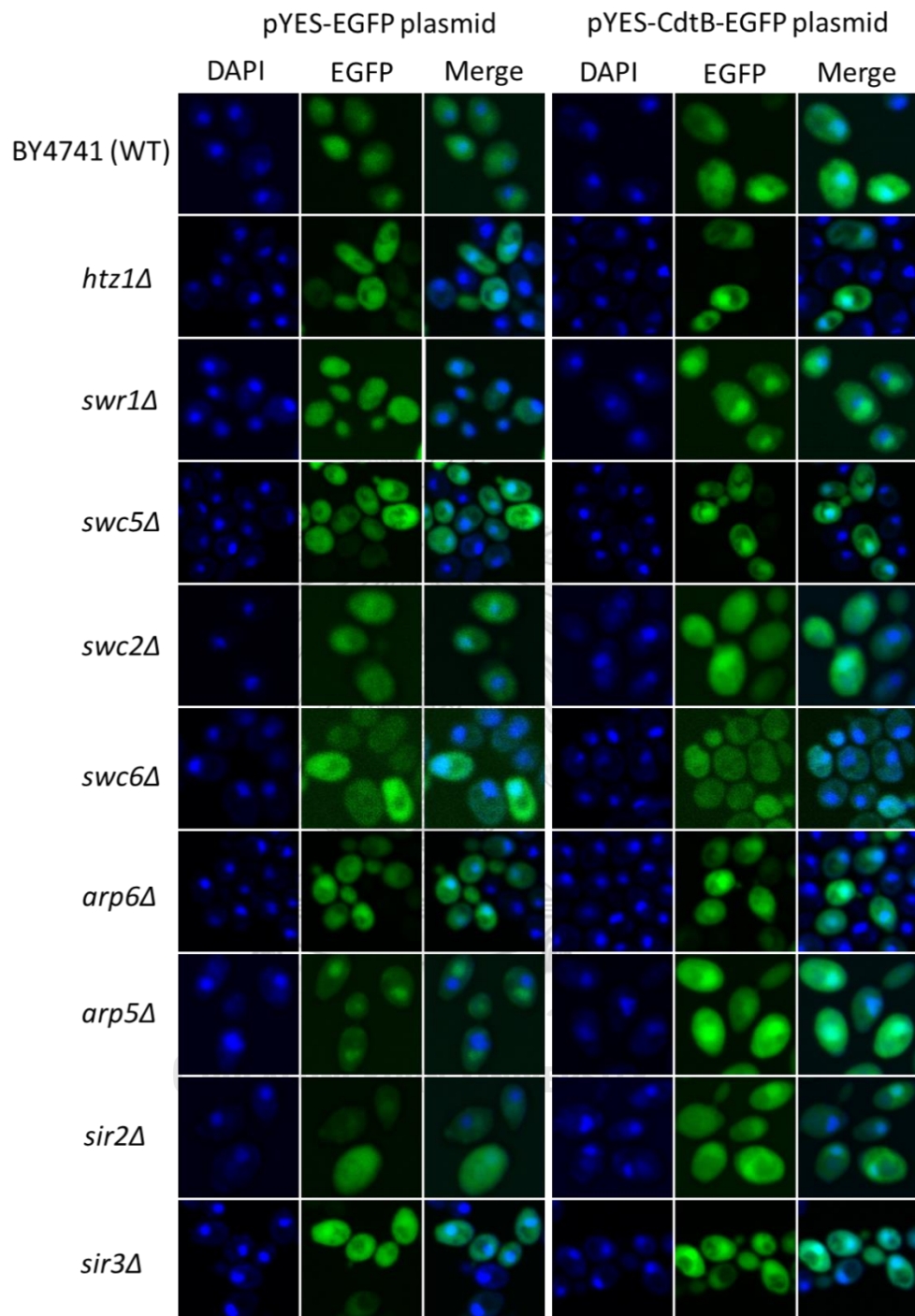


Figure 21 Localization of CdtB-EGFP and EGFP control were examined by confocal fluorescent microscopy.

Samples were induced CdtB expression by 2% galactose about 8 hours before the determination of nuclear localization. DAPI was used for nuclei staining. Samples were observed at 600x magnification.

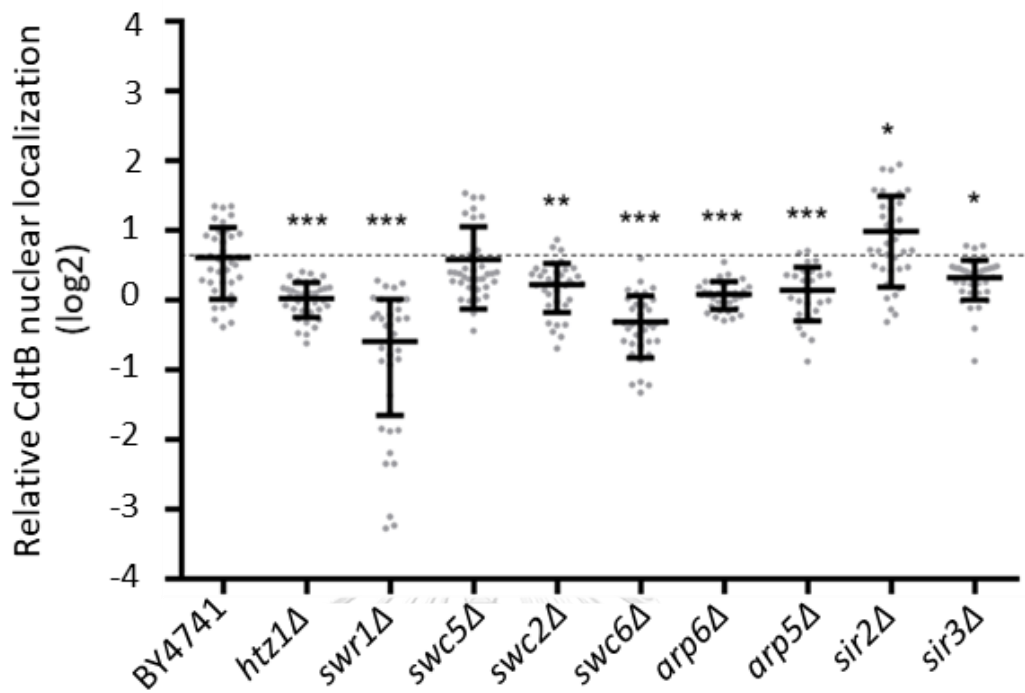


Figure 22 Mander's coefficient was used to calculate the relative CdtB nuclear localization ratio between CdtB-EGFP and EGFP control.

Nine cells of each samples were selected per an experiment randomly (N = 36 in total) and Mann-Whitney U test was used to analyze the data. \* $p < 0.050$ , \*\* $p < 0.010$ , and \*\*\* $p < 0.001$ .

### 2.3. Investigation of DNA damage caused by CdtB in CdtB resistant mutants

As CdtB protein was observed in the nuclei of CdtB resistant mutants, we asked if it could cause DNA breaks. Our previous study showed that yeast strains defective in homologous recombination (HR) were hypersensitive to CdtB, suggesting that HR is required to repair CdtB-induced DNA damages [51]. *RAD50* gene is one of the components of the MRX DNA break sensor complex that play an important role in HR repair pathway. Thus, *rad50Δ* can be applied as an indicator for DNA damage caused by CdtB using plate sensitivity assay. When we delete *RAD50* in the CdtB resistant mutant strains, we expect to see resistance if CdtB cannot induce DNA damage. On the other hand, if CdtB can induce DNA damage, we expect the strain to be hypersensitive. Thus, we deleted *RAD50* using PCR-based method in CdtB resistant strains (see details in materials and methods). The deletion of *RAD50* gene was confirmed by PCR (**Figure 23**). Unfortunately, we were unable to obtain *rad50Δ* in *arp5Δ* strain.

Double deletion strains were tested with plate sensitivity assay. *RAD50* deletion in each mutant was confirmed by the methyl methanesulfonate (MMS) sensitivity test. We observed the CdtB hypersensitivity phenotype of all mutants when combined with *rad50Δ*. The double deletion of *htz1Δ*, *swr1Δ*, *swc2Δ*, *swc6Δ* and *arp6Δ* strains, in which reduced CdtB translocation to nucleus was observed, became hypersensitive to CdtB (**Figure 24**). Moreover, we also found hypersensitive phenotype in *sir2Δ*, which showed the same CdtB localization as WT, when combined with *rad50Δ* (**Figure 24**). These suggest that CdtB could still induce DNA damage in these mutant strains, thus the resistant mechanism may occur after DNA damage. Interestingly, *swc5Δrad50Δ* and *sir3Δrad50Δ* seem to be more resistant to CdtB than *rad50Δ* strain (**Figure 24**). We reduced the galactose concentration to 0.1% to further test these 2 strains with lower level of CdtB expression and decreased fold-dilution from 10-fold to 5-fold. The result revealed that *swc5Δrad50Δ* is more resistant to CdtB than *rad50Δ*, whereas *sir3Δrad50Δ* is slightly resistant to CdtB, suggesting that *swc5Δ* may be able to reduce the level of CdtB-induced damages (**Figure 25**).

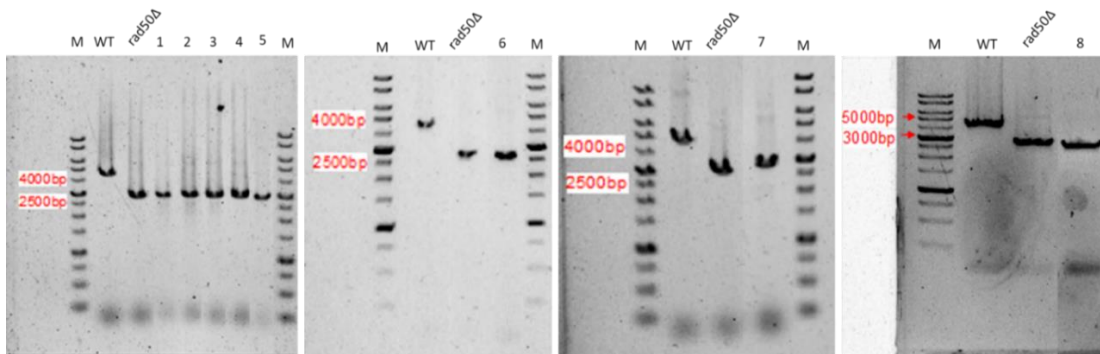


Figure 23 The deletions of RAD50 gene were confirmed by PCR with A and D specific primer.

PCR product size should be 2,728 bp if RAD50 was replaced by LEU2, if not, PCR product should be 4,548 bp. (M = 1kb DNA marker, lane 1 = *swr1Δ*, lane 2 = *swc2Δ*, lane 3 = *swc6Δ*, lane 4 = *arp6Δ*, lane 5 = *swc5Δ*, lane 6 = *htz1Δ*, lane 7 = *sir3Δ*, and lane 8 = *sir2Δ*)

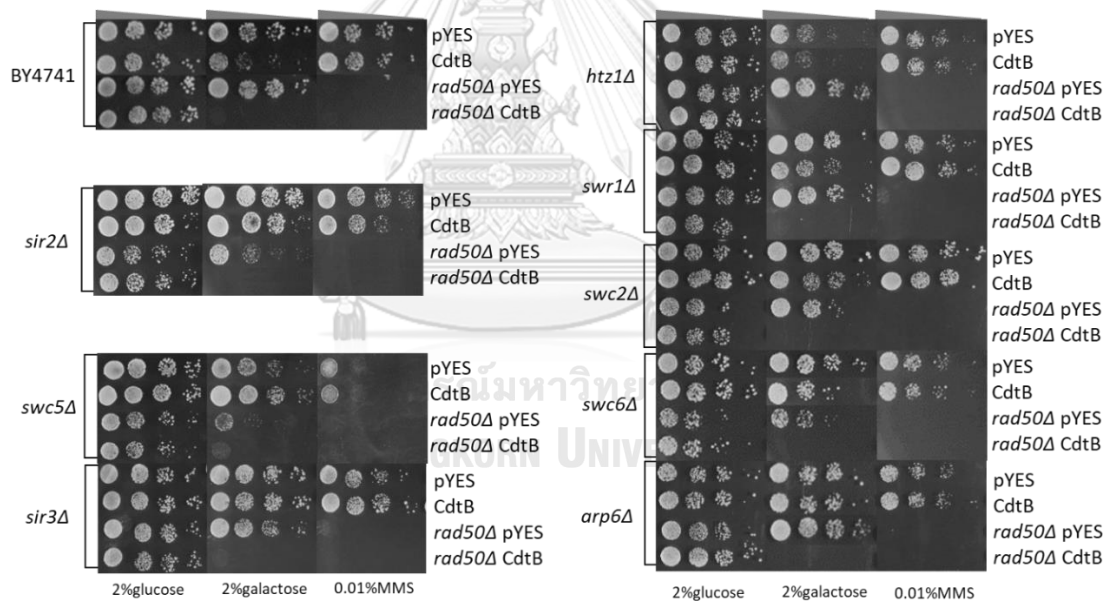


Figure 24 CdtB susceptibility test of CdtB resistant mutants which are defective in a DNA repair process.

Yeasts were induced CdtB expression by 2% galactose on the synthetic media. MMS, an alkylating agent, was applied to confirm the deletion of the RAD50 gene at 0.01% concentration.

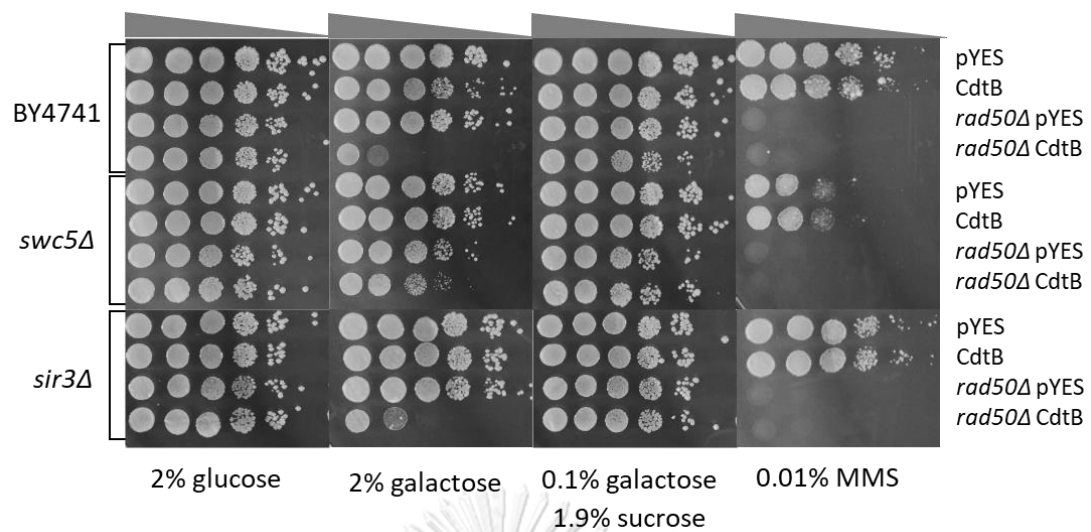


Figure 25 CdtB susceptibility test of *swc5Δrad50Δ* and *sir3Δrad50Δ* which are defective in a DNA repair process.

Yeasts were induced CdtB expression by 2% galactose and 0.1% galactose on the synthetic media. Fold-dilution in figure 17 was reduced from 10-fold to 5-fold MMS was used to confirm the deletion of RAD50 gene at 0.01% concentration.

#### 2.4. Investigating the CdtB on chromatin using *in vitro* DNase activity assay

*In vitro* DNase assay of CdtB on plasmid DNA has been tested in previous studies and found that the activity is very low comparing to *in vivo* DNase activity [38]. We hypothesized that CdtB may have a higher efficiency *in vitro* when use chromatin as a template if CdtB interact with the chromatin structure as a targeting mechanism. Moreover, we asked whether the changes in the chromatin structures of CdtB resistant mutants could affect CdtB accessibility to DNA. To test this hypothesis, *in vitro* DNase assay on chromatin substrate was performed which should prepare the intact chromatin structure and functional recombinant CdtB protein [207, 219]. Chromatin samples were digested with Micrococcal nuclease (MNase) to examine the extracted chromatin. MNase is an endo-exonuclease that cleave DNA at nucleosome free region used for chromatin study. Mnase should create a ladder-like pattern of DNA bands every about 150bp when applied it on the intact chromatin sample. We found that 1 U/ $\mu$ l MNase is optimal concentration for chromatin digestion. (Figure 26A). However, MNase

concentration was adjusted to 0.5 U/ $\mu$ l in the later experiment due to the improvement of nuclei lysis efficiency. Recombinant CdtB protein was expressed and purified by IMAC method (Figure 26B; see details on materials and methods). Besides, the recombinant protein was tested for DNase activity by using plasmid as a substrate (Figure 26C). The results showed that CdtB at 100 ng/ $\mu$ l can turn supercoiled plasmids into linearized form, suggesting that our recombinant CdtB has DNase activity.

Previously, we found that *sir2* $\Delta$  has a bit higher CdtB localization than WT and CdtB resistant mechanism should be after DNA damage. Thus, we hypothesized whether chromatin structure of *sir2* $\Delta$  is less facilitate than WT chromatin structure for CdtB damage. Chromatin of *sir2* $\Delta$  seems to be more sensitive than wildtype chromatin when digested by CdtB after 5h or 24h (Figure 27). It is possible that the absence of ladder-like bands is interpreted as the undigested intact chromatin. Therefore, we repeated the experiment and tested the *sir2* $\Delta$  intact chromatin structure by MNase. The positive control-like ladder bands would result if the chromatin was not digested. Unfortunately, the experiment was not reproducible. We cannot determine and summarize whether the difference of chromatin structure is a factor to facilitate CdtB function in yeast.



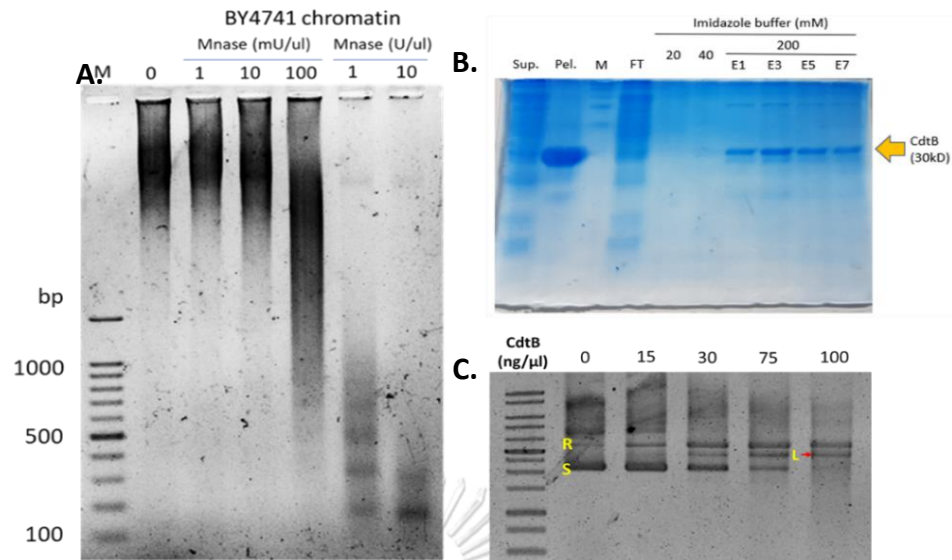


Figure 26 Preparation of in vitro DNase assay.

(A) Nuclei samples digested with various concentrations of micrococcal nuclease. (B) SDS-PAGE of recombinant CdtB protein purified by Ni-NTA beads. (C) In vitro DNase reaction of CdtB using plasmid as a substrate. R, S, and L are relaxed, supercoiled and linear form of the plasmid, respectively.

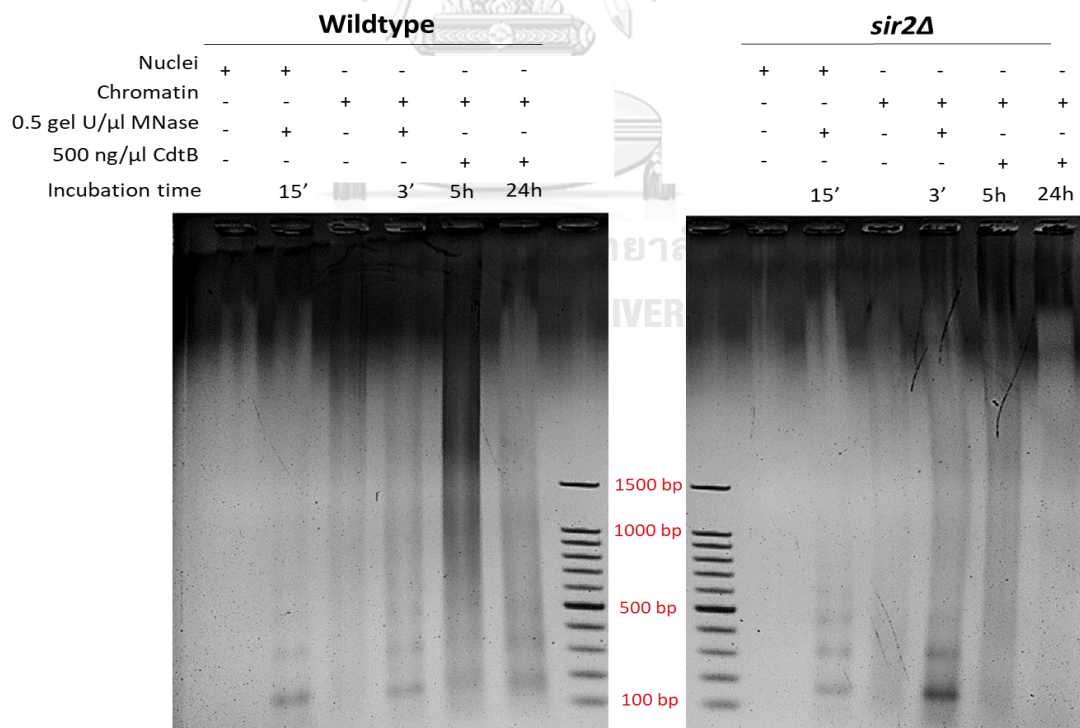


Figure 27 In vitro DNase I-like activity of CdtB in SIR2 deletion strain.

Wildtype and *sir2Δ* chromatin were extracted and digested with micrococcal nuclease or purified recombinant CdtB protein.



## 2.5. DNA repair gene expression in CdtB resistant candidates

Since we could observe DNA damage in certain CdtB resistant strains, this result suggests that CdtB resistant mechanism may occur after DNA damage. We hypothesized that DNA repair process in the mutant strains may be increased and this may overcome DNA damage from CdtB. As chromatin regulators play a role in the regulation of gene transcription, we wondered whether the expression of DNA repair genes may be upregulated. Therefore, we identified DNA repair genes that are upregulated upon DNA damaging conditions and in yeast strains with mutations of interest from publicly available datasets. We searched in microarray databases, ArrayExpress and Gene Expression Omnibus, for datasets related to DNA damaging conditions. These include ionizing radiation, such as gamma-radiation, and alkylating agents, such as methyl methanesulfonate (MMS) [220-224]. Additionally, we identified the DNA repair genes that are upregulated in CdtB resistant strains from available datasets [130, 225-228]. Eight genes that are upregulated in both lists were selected for further investigations (Table 15).

Although these DNA repair gene candidates were upregulated in various DNA damaging conditions, they may be not upregulated in CdtB expression condition. Therefore, we measured the expression levels of these 8 DNA repair genes upon CdtB expression in wild type strain. The levels of mRNA were measured at 0, 2, 4, 5, and 6h after CdtB induction by real-time PCR technique. ACT1 was used as housekeeping gene for normalization. The gene expression levels in the mutants were compared to those in WT yeast. The qPCR result revealed that all of the DNA repair gene candidates were upregulated by CdtB expression at about 2-4 h after CdtB induction (Figure 28) suggesting that all of these DNA repair genes responded to CdtB. We investigated the expression of these DNA repair genes in CdtB resistant mutants without CdtB expression. It appears that *ADA2*, *MRC1*, and *SSL2* were upregulated in most of our mutants. Furthermore, we found marked upregulation of *DEF1*, *EAF1* and *EPL1* in *swr1Δ* (Figure 29). The upregulation of certain DNA repair genes in CdtB resistant mutants may poise the cells to be able to readily repair the DNA damages induced by CdtB.

Table 15 List of upregulated genes in DNA damage conditions and upregulation in CdtB resistant candidates.

| DNA repair genes         | Description from SGD  | DNA damage condition induced gene upregulation   | Strains that upregulated gene  | References  |
|--------------------------|---|--|--|---|
| <i>ADA2</i><br>(YDR448W) | Transcription coactivator; component of the ADA and SAGA transcriptional adaptor/HAT (histone acetyltransferase) complexes.   | <ul style="list-style-type: none"> <li>● 10 Gy of gamma-ray; recovery time for 60 min<sup>a</sup></li> </ul>   | <ul style="list-style-type: none"> <li><i>htz1Δ</i><sup>b</sup></li> <li><i>swr1Δ</i><sup>b</sup></li> <li><i>swc2Δ</i><sup>b</sup></li> <li><i>swc5Δ</i><sup>b</sup></li> <li><i>arp6Δ</i><sup>c</sup></li> </ul> | <ul style="list-style-type: none"> <li>[224]<sup>a</sup></li> <li>[226]<sup>b</sup></li> <li>[227]<sup>c</sup></li> </ul> |
| <i>EPL1</i><br>(YFL024C) | Subunit of NuA4, an essential histone H4/H2A acetyltransferase complex; conserved region at N-terminus is essential for interaction with the NPC (nucleosome core particle); required for autophagy; homologous to Drosophila Enhancer of Polycomb; coding sequence contains length polymorphisms in different strains.           | <ul style="list-style-type: none"> <li>● 0.1% MMS; 60 min treatment; 30°C incubation<sup>d</sup></li> <li>● 0.001% MMS; 60 min treatment; 30°C incubation<sup>b</sup></li> </ul>     | <ul style="list-style-type: none"> <li><i>htz1Δ</i><sup>b</sup></li> <li><i>swr1Δ</i><sup>b</sup></li> <li><i>swc5Δ</i><sup>b</sup></li> </ul>   | <ul style="list-style-type: none"> <li>[226]<sup>b</sup></li> <li>[221]<sup>d</sup></li> </ul>                            |
| <i>PDS5</i><br>(YMR076C) | Cohesion maintenance factor; involved in sister chromatid condensation and cohesion; colocalizes with cohesin on chromosomes; performs its cohesin maintenance function in pre-anaphase cells by protecting the integrity of the cohesion complex; also required during meiosis; relocates to the cytosol in response to hypoxia. | <ul style="list-style-type: none"> <li>● 0.03% MMS; 30 min treatment; 30°C incubation<sup>e</sup></li> <li>● 0.02% MMS; 45, 90 min treatment; 30°C incubation<sup>f</sup></li> </ul> | <ul style="list-style-type: none"> <li><i>htz1Δ</i><sup>b</sup></li> <li><i>swc2Δ</i><sup>b</sup></li> <li><i>swc5Δ</i><sup>b</sup></li> </ul>   | <ul style="list-style-type: none"> <li>[226]<sup>b</sup></li> <li>[223]<sup>e</sup></li> <li>[222]<sup>f</sup></li> </ul> |
| <i>DEF1</i>              | RNAPII degradation factor; forms a complex with   | <ul style="list-style-type: none"> <li>● 0.12% MMS; 120 min treatment; 30°C</li> </ul>   | <ul style="list-style-type: none"> <li><i>htz1Δ</i><sup>b</sup></li> </ul>   | <ul style="list-style-type: none"> <li>[226]<sup>b</sup></li> </ul>   |

| DNA repair genes         | Description from SGD  | DNA damage condition induced gene upregulation   | Strains that upregulated gene                          | References   |
|--------------------------|---|--|--|--|
| (YKL054C)                | Rad2p in chromatin, enables ubiquitination and proteolysis of RNAPII present in an elongation complex;  | incubation <sup>g</sup>  | <i>arp6Δ</i> <sup>c</sup>                              | [227] <sup>c</sup><br>[220] <sup>g</sup>   |
| <i>EAF1</i><br>(YDR359C) | Component of the NuA4 histone acetyltransferase complex; acts as a platform for assembly of NuA4 subunits into the native complex; required for initiation of pre-meiotic DNA replication, likely due to its requirement for expression of IME1.  | <ul style="list-style-type: none"> <li>0.001% MMS; 60 min treatment; 30°C incubation<sup>a</sup></li> </ul>  | <i>htz1Δ</i> <sup>b</sup><br><i>swr1Δ</i> <sup>b</sup> | [224] <sup>a</sup><br>[226] <sup>b</sup>   |
| <i>MRC1</i><br>(YCL061C) | S-phase checkpoint protein required for DNA replication; couples DNA helicase and polymerase; interacts with and stabilizes Pol2p at stalled replication forks during stress, where it forms a pausing complex with Tof1p and is phosphorylated by Mec1p; defines a novel S-phase checkpoint with Hog1p that coordinates DNA replication and transcription upon osmstress; protects uncapped telomeres; Dia2p-dependent degradation mediates checkpoint recovery; mammalian claspin homolog | <ul style="list-style-type: none"> <li>0.03% MMS; 30 min treatment; 30°C incubation<sup>e</sup></li> <li>0.1% MMS; 60 min treatment; 30°C incubation<sup>d</sup></li> </ul>  | <i>htz1Δ</i> <sup>b</sup><br><i>swc2Δ</i> <sup>b</sup> | [226] <sup>b</sup><br>[221] <sup>d</sup><br>[223] <sup>e</sup>                       |
| <i>SSL2</i><br>(YIL143C) | Subunit of the core form of RNA polymerase transcription factor TFIIF; has both protein kinase and DNA-dependent ATPase/helicase activities; essential for transcription and nucleotide excision repair; interacts with Tfb4p.  | <ul style="list-style-type: none"> <li>0.1% MMS; 60 min treatment; 30°C incubation<sup>d</sup></li> <li>0.12% MMS; 120 min treatment; 30°C incubation<sup>f</sup></li> </ul> | <i>htz1Δ</i> <sup>b</sup><br><i>swc2Δ</i> <sup>b</sup> | [226] <sup>b</sup><br>[221] <sup>d</sup><br>[222] <sup>f</sup><br>[220] <sup>g</sup> |

| DNA repair genes                  | Description from SGD   | DNA damage condition induced gene upregulation   | Strains that upregulated gene                                | References   |
|-----------------------------------|--|--|--|--|
| <p><i>NHP6A</i><br/>(YPR052C)</p> | <p>High-mobility group (HMG) protein; binds to and remodels nucleosomes; involved in recruiting FACT and other chromatin remodeling complexes to chromosomes; functionally redundant with Nhp6Bp; required for transcriptional initiation fidelity of some tRNA genes; homologous to mammalian HMGB1 and HMGB2; NHP6A has a paralog, NHP6B, that arose from the whole genome duplication; protein abundance increases in response to DNA replication stress.</p> | <ul style="list-style-type: none"> <li>● 0.02% MMS; 90, 120 min treatment; 30°C incubation<sup>9</sup></li> <li>● 170 Gy of gamma-ray; recovery time for 60 min<sup>9</sup></li> </ul> | <p><i>swr1Δ<sup>h</sup></i><br/><i>sir2Δ<sup>i</sup></i></p> | <p>[220]<sup>9</sup><br/>[130]<sup>h</sup><br/>[225]<sup>i</sup></p> |

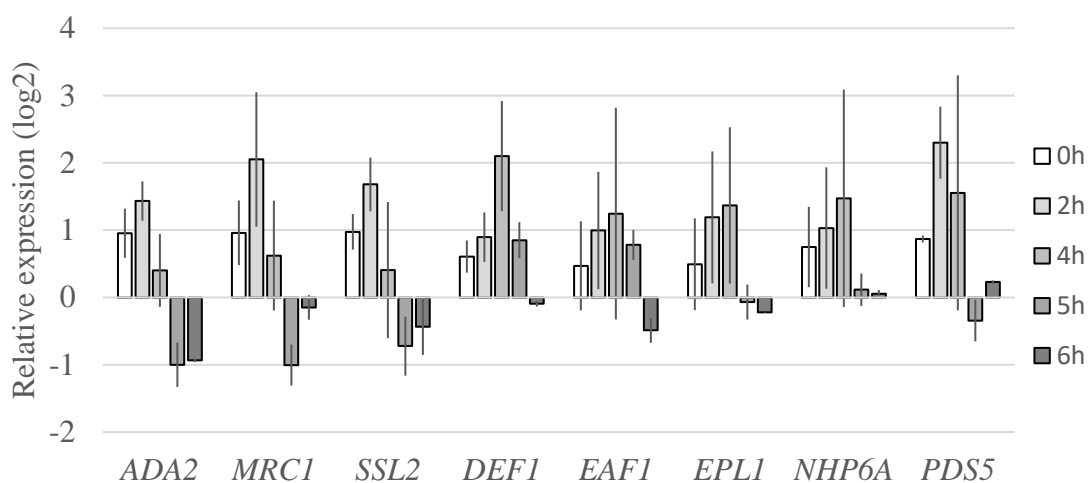


Figure 28 The responsiveness of DNA repair gene expression to DNA damage caused by CdtB. The expression of the DNA repair genes was determined at various time points after CdtB induction.

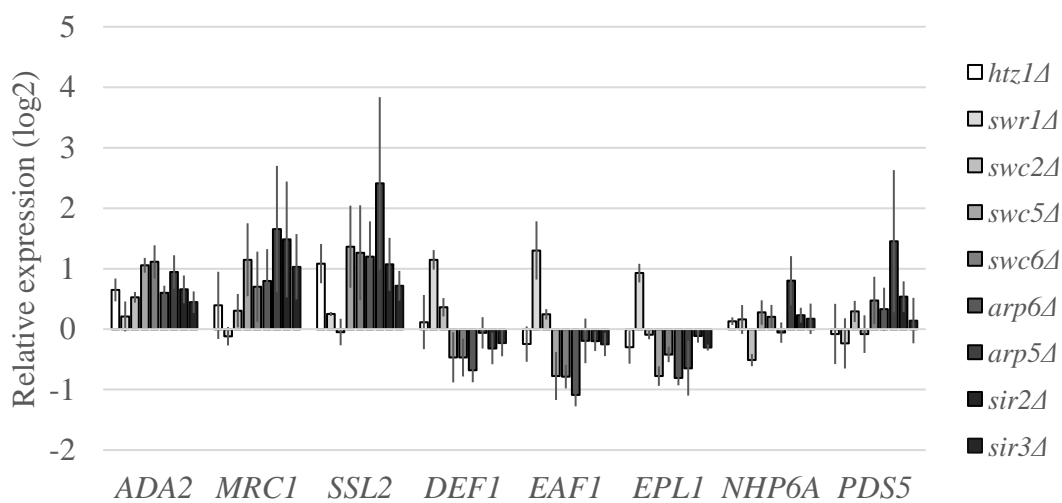


Figure 29 The upregulation of DNA repair gene in CdtB resistant candidates. The expression of the DNA repair gene was determined at the log phase of yeast strains without CdtB expression.

### **Objective 3. To globally identify genes that are required for CdtB cytotoxicity.**

To identify host genes that are required for CdtB cytotoxicity in a genome-wide manner, we performed a screen for mutations that result in CdtB resistance in the yeast deletion library.

#### **3.1 Genome-wide screening of CdtB resistant yeast deletion strains**

Approximately 5,000 strains, each carrying a single deletion of a non-essential open reading frame (ORF), in the yeast deletion library (Invitrogen; Open Biosystems, USA) were used to investigate the gene requirement for CdtB cytotoxicity. In primary screening, we identified 513 deletion strains showing comparable growth to wild type on 2% galactose (inducing media) in the dilutions where most mutants did not grow. These were compiled in 96-well plates and dilutions were spotted on solid media with 2% galactose and with 2% glucose (repressing media). Mutants that revealed growth on galactose plate, at the dilution that wild-type did not grow, were selected for further confirmation. The CdtB resistant phenotype was confirmed by spot test of serial dilutions of CdtB resistant strains. When comparing the growth on galactose with that on glucose, CdtB expression leads to the reduction of both the number of colonies and colony size in WT yeast. We confirmed the CdtB resistant phenotype in 281 mutants. The confirmatory screening was performed at least 4 times and mutants that consistently showed resistance was classified as CdtB resistant mutants. CdtB expression was checked by immunoblot assay to rule out the possibility of any defect in CdtB induction by galactose. Mutants that showed no or weak expressions of CdtB were omitted from further analysis. Finally, 243 null mutants were classified as CdtB resistant (shown in the appendix).

#### **3.2 Gene Ontology analysis of genes required for CdtB cytotoxicity**

Gene Ontology (GO) is used to describe gene functions and relationships related to the biological process, molecular function, and cellular component. The list of genes whose deletion confers CdtB resistant (243 genes) was analyzed by the GO Slim Mapper tool on SGD. These genes have been annotated to localize to a variety of cellular components including the nucleus (28%), mitochondrion (19%), endoplasmic

reticulum (11%) vacuole (9%), plasma membrane (9%), Golgi apparatus (2%), and unknown (22%). The top 10 broad GO terms identified according to the 3 categories: biological processes, molecular functions, and cellular components are summarized in **Figures 30 - 32** **Figure 31**.

Furthermore, analysis on GO-term finder, an online search tool for the enriched GO-term that shared among in the list of genes, revealed that “organic anion transport (OAT)” (GO:0015711) to be significantly enriched in the gene list, as compared to the genome frequency in the biological process category (p-value = 0.03846; searched on 15 Nov 2018). The enriched genes have 16 genes in the list of 243 CdtB resistant genes (6.6%) with this GO term annotation, while the genome frequency was 135 in 7165 genes (1.9%). These 16 genes are listed in **Table 16**. We searched for GO terms associated with these 16 genes concerning cellular components and found that most genes are localized in the membrane part (15 genes), vacuole (8 genes) and vacuolar membrane (6 genes). When we searched for GO terms related to molecular functions, most genes show transporter activity (14 genes) and terms related to transmembrane transporter activity (9 genes). These results suggest that these 16 genes, that localize to membrane/vacuolar and function as transporters, may play an important role in CdtB cytotoxicity.

Since a significant gap in our knowledge on intracellular translocation of CdtB is with regards to how CdtB moves from ER to the nucleus, we identified genes in the CdtB resistant list that localized to the ER. From our search, 25 genes showed ER localization (**Table 17**) and 16 genes showed transcriptional regulation (**Table 18**). Among these, 12 genes localize to the ER membrane. Interestingly, *HRD3*, which encodes an ER membrane protein that plays a central role in ER-associated protein degradation (ERAD), was also included in this list. Furthermore, 16 genes identified as transcriptional regulation has *PAF1*, and RNA polymerase II associated factor, which is related to transcriptional elongation process.

### 3.3 CdtB localization in CdtB resistant candidates which involved in organic anion transport

Since certain organic anion transport genes are required for CdtB cytotoxicity, we hypothesized that CdtB translocation may be defective in the deletion strains. We used CdtB-EGFP fusion protein as a tool to examine CdtB localization in these 16 OAT mutants. Representative confocal fluorescent microscopic images are shown in **Figure 33**. Fluorescent intensity was quantified and CdtB nuclear localization was analyzed using Mander's coefficient from just another co-localization plug-in on the ImageJ program in comparison to the EGFP vector control. The results revealed that all mutant strains showed less CdtB nuclear localization than wildtype (**Figure 34**).

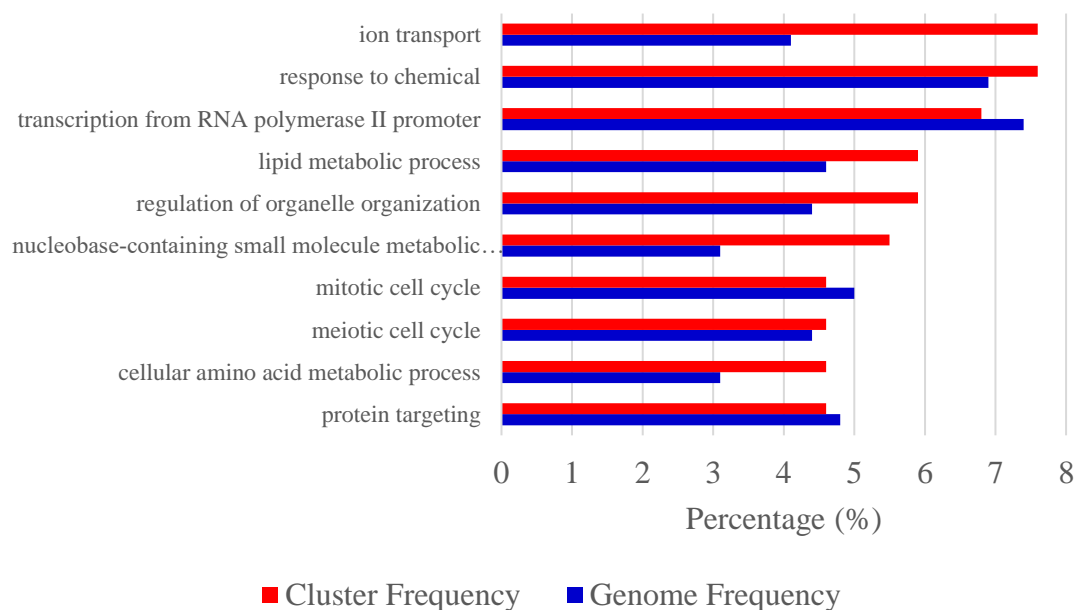


**Figure 30** Biological processes of 243 candidates from yeast genome-wide screening analyzed by GO slim mapper.

Data of top 10-sorted by cluster frequency was shown.



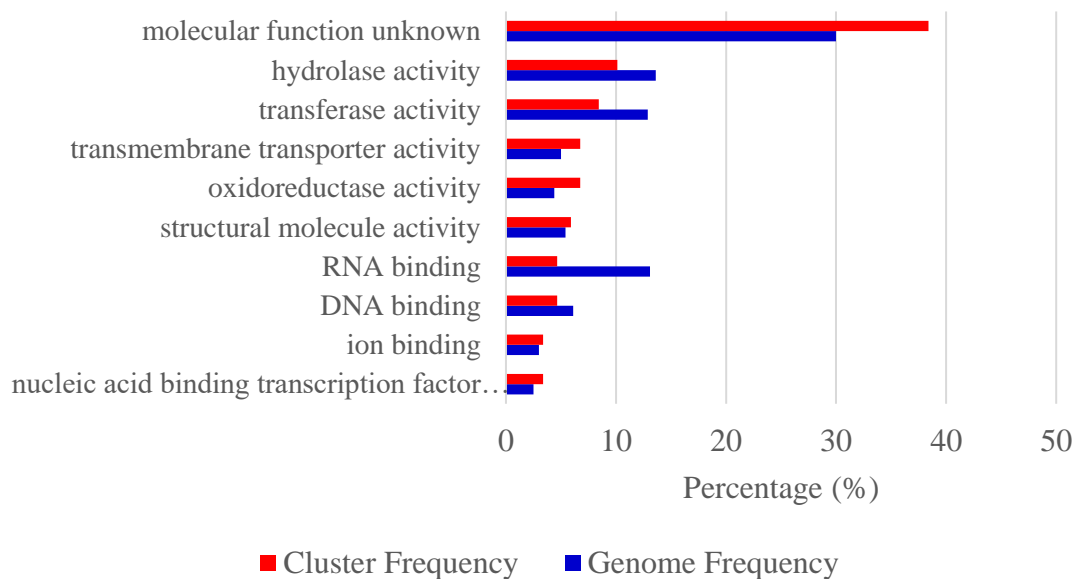


Figure 31 Molecular function of 243 candidates from yeast genome-wide screening analyzed by GO slim mapper.

Data of top-10 sorted by cluster frequency was shown.

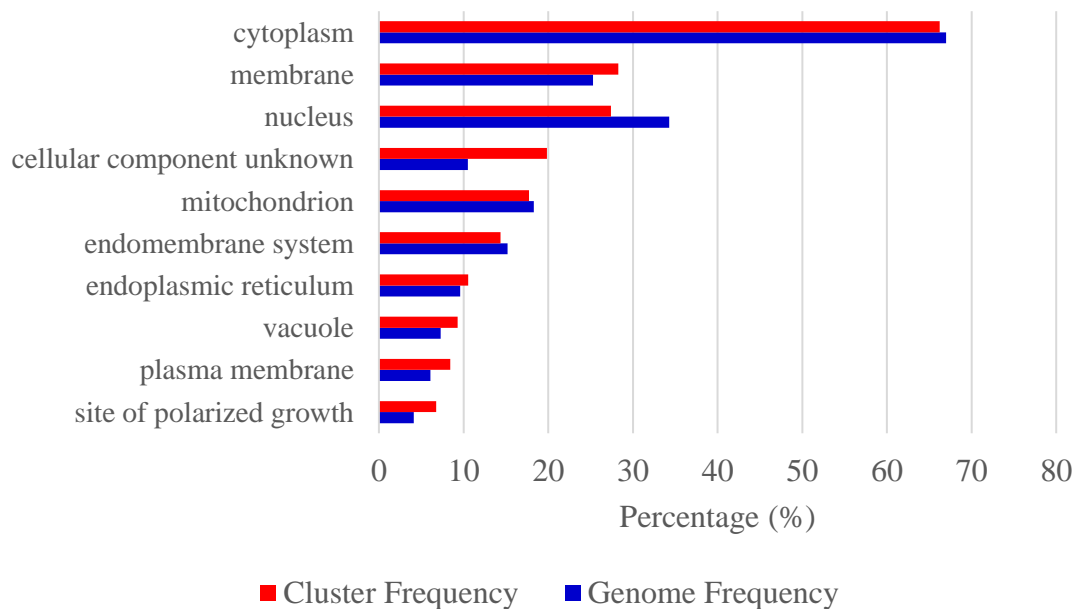


Figure 32 Cellular components of 243 candidates from yeast genome-wide screening analyzed by GO slim mapper.

Data of top-10 sorted by cluster frequency was shown.

Table 16 List of 16 organic anion transport genes that showed CdtB resistant phenotype

| Classification       | Systematic name | Standard name | Description from SGD   |
|----------------------|-----------------|---------------|--|
| Fatty acid transport | <i>YBR041W</i>  | <i>FAT1</i>   | Very long chain fatty acyl-CoA synthetase and fatty acid transporter; activates imported fatty acids with a preference for very long lengths (C20-C26); has a separate function in the transport of long chain fatty acids   |
|                      | <i>YOR049C</i>  | <i>RSB1</i>   | Putative sphingoid long-chain base (LCB) efflux transporter; integral membrane transporter that localizes to the plasma membrane and may transport long chain bases (LCBs) from the cytoplasmic side toward the extracytoplasmic side of the membrane; role in glycerophospholipid translocation; suppressor of the sphingoid LCB sensitivity of an LCB-lyase mutation |
|                      | <i>YLR193C</i>  | <i>UPS1</i>   | Phosphatidic acid transfer protein; plays a role in phospholipid metabolism by transporting phosphatidic acid from the outer to the inner mitochondrial membrane; localizes to the mitochondrial intermembrane space; null mutant has altered cardiolipin and phosphatidic acid levels; ortholog of human PRELI  |
|                      | <i>YNL264C</i>  | <i>PDR17</i>  | Phosphatidylinositol transfer protein (PITP); downregulates Plb1p-mediated turnover of phosphatidylcholine; forms a complex with Psd2p which appears essential for maintenance of vacuolar PE levels; found in the cytosol and microsomes; homologous to Pdr16p; deletion affects phospholipid composition   |
|                      | <i>YJL145W</i>  | <i>SFH5</i>   | Non-classical phosphatidylinositol transfer protein (PITP); exhibits PI- but not PC-transfer activity; localizes to the peripheral endoplasmic reticulum,  |

| Classification                   | Systematic name | Standard name | Description from SGD  |
|----------------------------------|-----------------|---------------|---|
|                                  |                 |               | cytosol and microsomes; similar to Sec14p; partially relocalizes to the plasma membrane upon DNA replication stress   |
| Amino acid and protein transport | <i>YMR088C</i>  | <i>VBA1</i>   | Permease of basic amino acids in the vacuolar membrane  |
|                                  | <i>YCL069W</i>  | <i>VBA3</i>   | Permease of basic amino acids in the vacuolar membrane; <i>VBA3</i> has a paralog, <i>VBA5</i> , that arose from a segmental duplication  |
|                                  | <i>YGR206W</i>  | <i>MVB12</i>  | ESCRT-I subunit required to stabilize ESCRT-I core complex oligomers; the ESCRT-I core complex (Stp22p, Vps28p, Srn2p) is involved in ubiquitin-dependent sorting of proteins into the endosome; deletion mutant is sensitive to rapamycin and nystatin   |
|                                  | <i>YPR058W</i>  | <i>YMC1</i>   | Secondary mitochondrial inner membrane glycine transporter; required with <i>HEM25</i> for the transport of glycine into mitochondria for the initiation of heme biosynthesis; proposed role in oleate metabolism and glutamate biosynthesis; member of the mitochondrial carrier (MCF) family; localizes to the vacuole in response to H <sub>2</sub> O <sub>2</sub> ; <i>YMC1</i> has a paralog, <i>YMC2</i> , that arose from the whole genome duplication |
|                                  | <i>YPR149W</i>  | <i>NCE102</i> | Protein of unknown function; contains transmembrane domains; involved in secretion of proteins that lack classical secretory signal sequences; component of the detergent-insoluble glycolipid-enriched complexes (DIGs); <i>NCE102</i> has a paralog, <i>FHN1</i> , that arose from the whole genome duplication   |
|                                  | <i>YOR130C</i>  | <i>ORT1</i>   | Ornithine transporter of the mitochondrial inner membrane; exports ornithine from mitochondria as part of arginine biosynthesis; functionally complemented by human ortholog, <i>SLC25A15</i> , which is associated with hyperammonaemia-   |



| Classification         | Systematic name | Standard name | Description from SGD   |
|------------------------|-----------------|---------------|--|
|                        |                 |               | hyperornithinaemia-homocitrullinuria (HHH) syndrome, but HHH-associated variants fail to complement  |
|                        | <i>YER119C</i>  | <i>AVT6</i>   | Vacuolar aspartate and glutamate exporter; member of a family of seven genes ( <i>AVT1-7</i> ) related to vesicular GABA-glycine transporters; involved in compartmentalizing acidic amino acids in response to nitrogen starvation; <i>AVT6</i> has a paralog, <i>AVT5</i> , that arose from the whole genome duplication   |
| Carbohydrate transport | <i>YKL217W</i>  | <i>JEN1</i>   | Monocarboxylate/proton symporter of the plasma membrane; transport activity is dependent on the pH gradient across the membrane; mediates high-affinity uptake of carbon sources lactate, pyruvate, and acetate, and also of the micronutrient selenite, whose structure mimics that of monocarboxylates; expression and localization are tightly regulated, with transcription repression, mRNA degradation, and protein endocytosis and degradation all occurring in the presence of glucose |
| Pyruvate transport     | <i>YHR162W</i>  | <i>MPC2</i>   | Highly conserved subunit of the mitochondrial pyruvate carrier (MPC); expressed during growth on fermentable carbon sources, and heterodimerizes with Mpc1p to form the fermentative isoform of MPC; MPC localizes to the mitochondrial inner membrane and mediates pyruvate uptake; <i>MPC2</i> paralog, <i>MPC3</i> , heterodimerizes with Mpc1p to form the respiratory MPC isoform   |
| FAD transport          | <i>YGL139W</i>  | <i>FLC3</i>   | Putative FAD transporter, similar to Flc1p and Flc2p; localized to the ER; <i>FLC3</i> has a paralog, <i>FLC1</i> , that arose from the whole genome duplication   |
| Ion transport          | <i>YNR013C</i>  | <i>PHO91</i>  | Low-affinity vacuolar phosphate transporter; exports phosphate from the vacuolar lumen to the cytosol;   |

| Classification | Systematic name | Standard name | Description from SGD   |
|----------------|-----------------|---------------|--|
|                |                 |               | <p>regulates phosphate and polyphosphate metabolism; acts upstream of Pho81p in regulation of the PHO pathway; localizes to sites of contact between the vacuole and mitochondria (vCLAMPs); deletion of pho84, pho87, pho89, pho90, and pho91 causes synthetic lethality; transcription independent of Pi and Pho4p activity; overexpression results in vigorous growth</p> |



Table 17 CdtB resistant genes that associate with endoplasmic reticulum

| Systematic name | Standard name | Description from SGD   |
|-----------------|---------------|--|
| <i>YBL082C</i>  | <i>ALG3</i>   | Dolichol-P-Man dependent alpha(1-3) mannosyltransferase; involved in synthesis of dolichol-linked oligosaccharide donor for N-linked glycosylation of proteins; G353A missense mutation in human ortholog <i>ALG3</i> implicated in carbohydrate deficient glycoprotein syndrome type IV, which is characterized by microcephaly, severe epilepsy, minimal psychomotor development, partial deficiency of sialic acids in serum glycoproteins; wild-type human <i>ALG3</i> can complement yeast <i>alg3</i> mutant |
| <i>YBR041W</i>  | <i>FAT1</i>   | Very long chain fatty acyl-CoA synthetase and fatty acid transporter; activates imported fatty acids with a preference for very long lengths (C20-C26); has a separate function in the transport of long chain fatty acids   |
| <i>YBR130C</i>  | <i>SHE3</i>   | Protein adaptor between Myo4p and the She2p-mRNA complex; part of the mRNA localization machinery that restricts accumulation of certain proteins to the bud; also required for cortical ER inheritance  |
| <i>YCL069W</i>  | <i>VBA3</i>   | Permease of basic amino acids in the vacuolar membrane; <i>VBA3</i> has a paralog, <i>VBA5</i> , that arose from a segmental duplication   |
| <i>YDL122W</i>  | <i>UBP1</i>   | Ubiquitin-specific protease; removes ubiquitin from ubiquitinated proteins; cleaves at the C terminus of ubiquitin fusions irrespective of their size; capable of cleaving polyubiquitin chains  |
| <i>YDL204W</i>  | <i>RTN2</i>   | Reticulon protein; involved in nuclear pore assembly and maintenance of tubular ER morphology; promotes membrane curvature; regulates the ER asymmetry-induced inheritance block during ER stress; role in ER-derived peroxisomal biogenesis; interacts with Sec6p, Yip3p, and Sbh1p; less abundant than <i>RTN1</i> ; member of RTNLA (reticulon-like A) subfamily; protein increases in abundance and relocalizes to plasma membrane upon DNA replication stress   |
| <i>YDR504C</i>  | <i>SPG3</i>   | Protein required for high temperature survival during stationary phase; not required for growth on nonfermentable carbon sources; SWAT-GFP and mCherry fusion proteins localize to the endoplasmic reticulum   |
| <i>YEL016C</i>  | <i>NPP2</i>   | Nucleotide pyrophosphatase/phosphodiesterase; mediates extracellular   |

| Systematic name  | Standard name | Description from SGD   |
|------------------|---------------|--|
|                  |               | nucleotide phosphate hydrolysis along with Npp1p and Pho5p; activity and expression enhanced during conditions of phosphate starvation; involved in spore wall assembly; SWAT-GFP and mCherry fusion proteins localize to the endoplasmic reticulum; <i>NPP2</i> has a paralog, <i>NPP1</i> , that arose from the whole genome duplication; <i>npp1 npp2</i> double mutant exhibits reduced dityrosine fluorescence relative to single mutants |
| <i>YGL032C</i>   | <i>AGA2</i>   | Adhesion subunit of a-agglutinin of a-cells; C-terminal sequence acts as a ligand for alpha-agglutinin (Sag1p) during agglutination, modified with O-linked oligomannosyl chains, linked to anchorage subunit Aga1p via two disulfide bonds   |
| <i>YGL139W</i>   | <i>FLC3</i>   | Putative FAD transporter, similar to Flc1p and Flc2p; localized to the ER; <i>FLC3</i> has a paralog, <i>FLC1</i> , that arose from the whole genome duplication   |
| <i>YGR263C</i>   | <i>SAY1</i>   | Sterol deacetylase; component of the sterol acetylation/deacetylation cycle along with Atf2p; active both in the endoplasmic reticulum (ER) and in lipid droplets; integral membrane protein with active site in the ER lumen; green fluorescent protein (GFP)-fusion protein localizes to the ER  |
| <i>YHL044W</i>   | -             | Putative integral membrane protein; member of <i>DUP240</i> gene family; green fluorescent protein (GFP)-fusion protein localizes to the plasma membrane in a punctate pattern    |
| <i>YIL023C</i>   | <i>YKE4</i>   | Zinc transporter; localizes to the ER; null mutant is sensitive to calcofluor white, leads to zinc accumulation in cytosol; ortholog of the mouse KE4 and member of the ZIP (ZRT, IRT-like Protein) family   |
| <i>YJL134W</i>   | <i>LCB3</i>   | Long-chain base-1-phosphate phosphatase; specific for dihydrosphingosine-1-phosphate, regulates ceramide and long-chain base phosphates levels, involved in incorporation of exogenous long chain bases in sphingolipids; <i>LCB3</i> has a paralog, <i>YSR3</i> , that arose from the whole genome duplication  |
| <i>YJL145W</i>   | <i>SFH5</i>   | Non-classical phosphatidylinositol transfer protein (PITP); exhibits PI- but not PC-transfer activity; localizes to the peripheral endoplasmic reticulum, cytosol and microsomes; similar to Sec14p; partially relocalizes to the plasma membrane upon DNA replication stress  |
| <i>YJR010C-A</i> | <i>SPC1</i>   | Subunit of the signal peptidase complex (SPC); SPC cleaves the signal  |

| Systematic name | Standard name | Description from SGD   |
|-----------------|---------------|--|
|                 |               | sequence from proteins targeted to the endoplasmic reticulum (ER); homolog of the <i>SPC12</i> subunit of mammalian signal peptidase complex; protein abundance increases in response to DNA replication stress  |
| <i>YLR207W</i>  | <i>HRD3</i>   | ER membrane protein that plays a central role in ERAD; forms HRD complex with Hrd1p and ER-associated protein degradation (ERAD) determinants that engages in lumen to cytosol communication and coordination of ERAD events   |
| <i>YML128C</i>  | <i>MSC1</i>   | Protein of unknown function; mutant is defective in directing meiotic recombination events to homologous chromatids; the authentic, non-tagged protein is detected in highly purified mitochondria and is phosphorylated   |
| <i>YNL012W</i>  | <i>SPO1</i>   | Meiosis-specific prospore protein; required for meiotic spindle pole body duplication and separation; required to produce bending force necessary for proper prospore membrane assembly during sporulation; has similarity to phospholipase B  |
| <i>YNR075W</i>  | <i>COS10</i>  | Endosomal protein involved in turnover of plasma membrane proteins; member of the DUP380 subfamily of conserved, often subtelomeric COS genes; required for the multivesicular vesicle body sorting pathway that internalizes plasma membrane proteins for degradation; Cos proteins provide ubiquitin in trans for nonubiquitinated cargo proteins                    |
| <i>YOR049C</i>  | <i>RSB1</i>   | Putative sphingoid long-chain base (LCB) efflux transporter; integral membrane transporter that localizes to the plasma membrane and may transport long chain bases (LCBs) from the cytoplasmic side toward the extracytoplasmic side of the membrane; role in glycerophospholipid translocation; suppressor of the sphingoid LCB sensitivity of an LCB-lyase mutation |
| <i>YPL154C</i>  | <i>PEP4</i>   | Vacuolar aspartyl protease (proteinase A); required for posttranslational precursor maturation of vacuolar proteinases; important for protein turnover after oxidative damage; plays a protective role in acetic acid induced apoptosis; synthesized as a zymogen, self-activates  |
| <i>YPR063C</i>  | -             | ER-localized protein of unknown function   |
| <i>YPR109W</i>  | <i>GLD1</i>   | Predicted membrane protein; SWAT-GFP and mCherry fusion proteins   |



| Systematic name | Standard name | Description from SGD  |
|-----------------|---------------|---|
|                 |               | localize to the endoplasmic reticulum; diploid deletion strain has high budding index   |
| <i>YPR149W</i>  | <i>NCE102</i> | Protein of unknown function; contains transmembrane domains; involved in secretion of proteins that lack classical secretory signal sequences; component of the detergent-insoluble glycolipid-enriched complexes (DIGs); <i>NCE102</i> has a paralog, <i>FHN1</i> , that arose from the whole genome duplication |



Table 18 CdtB resistant genes that associate with transcriptional regulation

| Systematic name | Standard name | Description from SGD   |
|-----------------|---------------|--|
| YBL066C         | SEF1          | Putative transcription factor; has homolog in <i>Kluyveromyces lactis</i>  |
| YBR033W         | EDS1          | Putative zinc cluster protein, predicted to be a transcription factor; not an essential gene; <i>EDS1</i> has a paralog, <i>RGT1</i> , that arose from the whole genome duplication  |
| YBR133C         | HSL7          | Protein arginine N-methyltransferase; exhibits septin and Hsl1p-dependent localization to the bud neck in budded cells and periodic Hsl1p-dependent phosphorylation; required with Hsl1p, and Elm1p for the mother-bud neck recruitment, phosphorylation, and degradation of Swe1p; interacts directly with Swe1p; relocates away from bud neck upon DNA replication stress; human homolog <i>PRMT5</i> can complement yeast <i>hsl7</i> mutant  |
| YBR279W         | PAF1          | Component of the Paf1p complex involved in transcription elongation; binds to and modulates the activity of RNA polymerases I and II; required for expression of a subset of genes, including cell cycle-regulated genes; involved in <i>SER3</i> repression by helping to maintain SRG1 transcription-dependent nucleosome occupancy; homolog of human <i>PD2/hPAF1</i>   |
| YCR033W         | SNT1          | Subunit of the Set3C deacetylase complex; interacts directly with the Set3C subunit, Sif2p; putative DNA-binding protein; mutant has increased aneuploidy tolerance; relocates to the cytosol in response to hypoxia   |
| YIL131C         | FKH1          | Forkhead family transcription factor; rate-limiting replication origin activator; evolutionarily conserved lifespan regulator; binds multiple chromosomal elements with distinct specificities, cell cycle dynamics; regulates transcription elongation, chromatin silencing at mating loci, expression of G2/M phase genes; facilitates clustering, activation of early-firing replication origins; binds HML recombination enhancer, regulates donor preference during mating-type switching |
| YKL015W         | PUT3          | Transcriptional activator; binds specific gene recruitment sequences and is required for DNA zip code-mediated targeting of genes to nuclear periphery; regulates proline utilization genes, constitutively binds <i>PUT1</i> and <i>PUT2</i> promoters as a dimer, undergoes conformational change to form active state; binds other promoters only under activating conditions;  |

| Systematic name | Standard name | Description from SGD   |
|-----------------|---------------|--|
|                 |               | differentially phosphorylated in presence of different nitrogen sources; has a Zn(2)-Cys(6) binuclear cluster domain   |
| <i>YKR064W</i>  | <i>OAF3</i>   | Putative transcriptional repressor with Zn(2)-Cys(6) finger; negatively regulates transcription in response to oleate levels, based on mutant phenotype and localization to oleate-responsive promoters; the authentic, non-tagged protein is detected in highly purified mitochondria in high-throughput studies; forms nuclear foci upon DNA replication stress  |
| <i>YFR034C</i>  | <i>PHO4</i>   | Basic helix-loop-helix (bHLH) transcription factor of the myc-family; activates transcription cooperatively with Pho2p in response to phosphate limitation; binding to 'CACGTG' motif is regulated by chromatin restriction, competitive binding of Cbf1p to the same DNA binding motif and cooperation with Pho2p; function is regulated by phosphorylation at multiple sites and by phosphate availability   |
| <i>YDL233W</i>  | <i>MFG1</i>   | Regulator of filamentous growth; interacts with <i>FLO11</i> promoter and regulates <i>FLO11</i> expression; binds to transcription factors Flo8p and Mss11p; green fluorescent protein (GFP)-fusion protein localizes to the nucleus; <i>YDL233W</i> is not an essential gene   |
| <i>YGL166W</i>  | <i>CUP2</i>   | Copper-binding transcription factor; activates transcription of the metallothionein genes <i>CUP1-1</i> and <i>CUP1-2</i> in response to elevated copper concentrations; required for regulation of copper genes in response to DNA-damaging reagents; <i>CUP2</i> has a paralog, <i>HAA1</i> , that arose from the whole genome duplication   |
| <i>YGL181W</i>  | <i>GTS1</i>   | Protein involved in Arf3p regulation and in transcription regulation; localizes to the nucleus and to endocytic patches; contains an N-terminal Zn-finger and ArfGAP homology domain, a C-terminal glutamine-rich region, and a UBA (ubiquitin associated) domain; <i>gts1</i> mutations affect budding, cell size, heat tolerance, sporulation, life span, ultradian rhythms, endocytosis; expression oscillates in a pattern similar to metabolic oscillations |
| <i>YLR442C</i>  | <i>SIR3</i>   | Silencing protein; interacts with Sir2p, Sir4p, and histone H3/H4 tails to establish transcriptionally silent chromatin; required for spreading of silenced chromatin; recruited to chromatin through interaction with Rap1p;  |

| Systematic name | Standard name | Description from SGD   |
|-----------------|---------------|--|
|                 |               | C-terminus assumes variant winged helix-turn-helix (wH) fold that mediates homodimerization, which is critical for holo-SIR complex loading; required for telomere hypercluster formation in quiescent yeast cells; has paralog <i>ORC1</i> from whole genome duplication  |
| <i>YML062C</i>  | <i>MFT1</i>   | Subunit of the THO complex; THO is a nuclear complex comprised of Hpr1p, Mft1p, Rlr1p, and Thp2p, that is involved in transcription elongation and mitotic recombination; involved in telomere maintenance   |
| <i>YOL089C</i>  | <i>HAL9</i>   | Putative transcription factor containing a zinc finger; overexpression increases salt tolerance through increased expression of the <i>ENA1</i> (Na <sup>+</sup> /Li <sup>+</sup> extrusion pump) gene while gene disruption decreases both salt tolerance and <i>ENA1</i> expression; <i>HAL9</i> has a paralog, <i>TBS1</i> , that arose from the whole genome duplication |
| <i>YOR172W</i>  | <i>YRM1</i>   | Zinc finger transcription factor involved in multidrug resistance; Zn(2)-Cys(6) zinc finger transcription factor; activates genes involved in multidrug resistance; paralog of Yrr1p, acting on an overlapping set of target genes   |



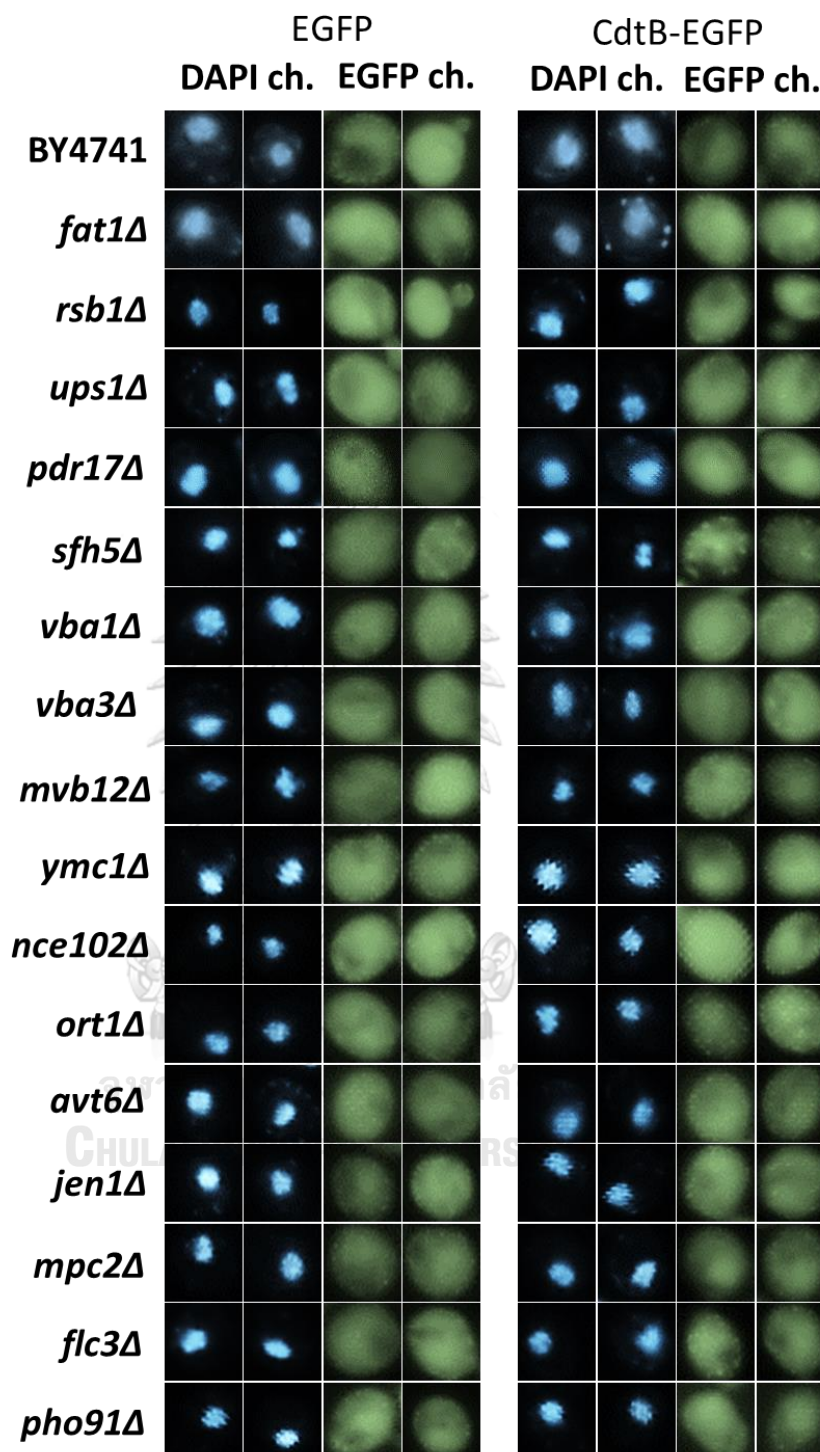


Figure 33 CdtB nuclear localization was reduced in mutants associated with organic anion transport. Representative fluorescent images (at 600x magnification) of localization of CdtB-EGFP and EGFP control in WT and mutants associated with the GO term organic anion transport are shown. DAPI was used to stain the yeast nuclei. Two examples of each sample are shown.

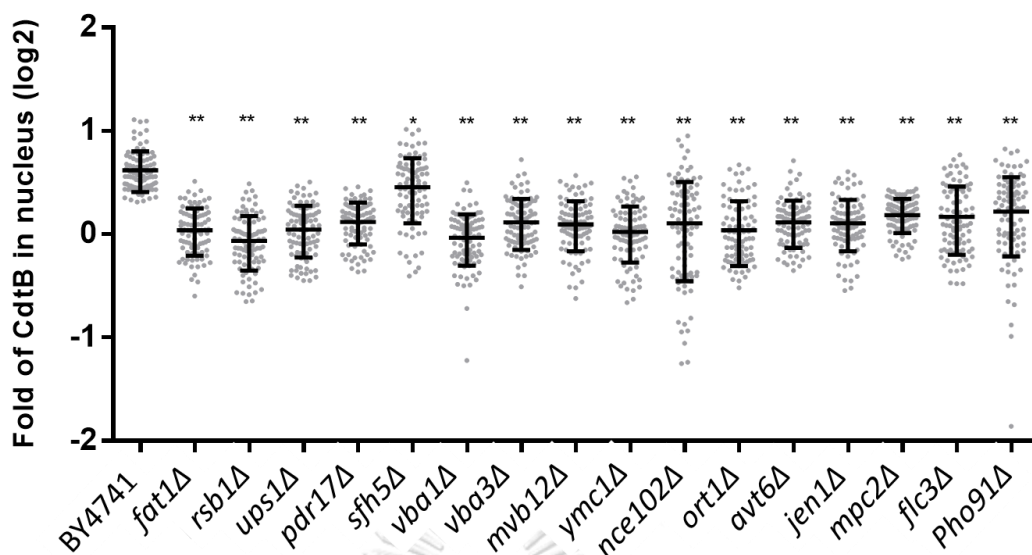


Figure 34 The ratio of nuclear localization of CdtB-EGFP relative to EGFP control was calculated using Manders' coefficient.

Thirty cells were randomly selected for each sample in each experiment (total N = 90) and the Mann-Whitney U test was used to analyze the data. (\*p < 0.001, \*\* p < 0.0001)

## CHAPTER V: DISCUSSION

In this study, we examined the role of chromatin regulators and performed a genome-wide analysis to identify host genes that facilitate AaCdtB cytotoxicity using yeast model. Our results showed that certain chromatin regulators, especially SWR-complex and SIR-complex components, play an important role in AaCdtB toxicity. We investigated the mechanisms by which mutations in these genes could lead to resistance to AaCdtB, and proposed that several pathways may lead to CdtB resistance, including effects on nuclear localization and DNA repair gene expression. In addition, our genome-wide screen showed that many genes and cellular processes may influence the function of CdtB in host cells, particularly those that may affect CdtB transport.

In the first part, our studies on chromatin regulators showed that the lack of Htz1 and certain SWR-complex components led to CdtB resistance. SWR and INO80 complexes play a role in Htz1 histone replacement on nucleosome to control gene transcription and heterochromatin spreading [130]. Thus, it appears that Htz1 deposition in the chromatin may be required for CdtB cytotoxicity. We examined several potential mechanisms underlying the phenotype.

In the second part, our genome-wide screening for CdtB resistant phenotype showed an enrichment of genes related to Gene Ontology term 'organic anion transport'. These genes play an important role in nutrient transport to maintain cellular homeostasis and in cargo transport to suitable locations. We discuss the possible cellular mechanisms that may be involved in CdtB function in host cells.

### 1. Chromatin regulators and CdtB cytotoxicity

We examined CdtB susceptibility of yeast cells lacking one of 18 non-essential chromatin regulatory genes. We observed CdtB resistance in several yeast mutants, including i.) SWR complex components (*swr1Δ*, *swc2Δ*, *swc5Δ*, *swc6Δ*, and *arp6Δ*), ii.) *htz1Δ*, iii.) INO80 complex component (*arp5Δ*), and iv.) SIR complex components (*sir2Δ* and *sir3Δ*).

Interestingly, mutations of SWR1 complex components that confer CdtB resistance correlate with their requirements for complex integrity and enzymatic activity (Figures 5 and 6). Specifically, only SWR-C subunits that are involved in Htz1 deposition are required for CdtB function. Swr1p is a ATPase catalytic subunit [123] and serves as a scaffold protein for the binding of N-module, C-module and RvB1/2 [136, 229]. Swc2 directly binds to H2A.Z, prevents H2A.Z eviction [136, 230] and targets SWR-C to nucleosome free regions [229]. Swc6 and Arp6 are important for H2A.Z deposition *in vivo* [231]. On the other hand, *swc3Δ* and *swc7Δ* are not resistant to CdtB. Swc3 is not involved in Htz1 incorporation *in vitro* [136], but the level is reduced *in vivo* [231], while Swc7 does not contribute to nucleosome or H2A.Z binding [136]. Thus, Htz1 deposition and Htz1 may be involved in the chromatin targeting mechanism of CdtB.

On the other hand, the related chromatin remodeler INO80-complex, which plays a reciprocal role to SWR complex in Htz1 exchange, did not appear to affect CdtB activity. This complex contains 4 modules including RvB1/2 head module, Arp5 neck module, Nhp10 body module and Arp8 foot module. The deletion of *ARP8* or *NHP10* did not lead to CdtB resistance, but deletion of *ARP5* did (Figures 5 and 6). Interestingly, INO80 complex is involved in several processes including transcription regulation, DNA replication and also DNA damage repair (reviewed in [232]). Previous studies found that Arp8 helps to recruit INO80-C to DNA damage in mammalian cells [233] and Nhp10 is involved in stable  $\gamma$ H2A.X binding of INO80-C [145]. We previously showed that cells with defect in DNA break repair, particularly homologous recombination repair, are hypersensitive to CdtB. Thus, the role of INO80 in DNA repair may mask the effect of the deletions of *ARP8* or *NHP10* on CdtB activity. Arp5 was shown to localized to the +1 nucleosome [234] suggesting that it may be involved in gene transcription process. Thus, it may affect CdtB activity through changes in gene expression.

Here, we investigated several potential mechanisms that may explain how mutations in these chromatin remodelers and *HTZ1* could lead to CdtB resistance.



### 1.1. Interaction with Htz1

A possible explanation for the role of chromatin regulators in CdtB activity could be a direct physical interaction. Our results suggested that certain SWR-complex components and Htz1 are required for CdtB activity. We asked whether Htz1 could facilitate the interaction between CdtB and DNA through physical interaction. We performed co-immunoprecipitation assay; however, we could not detect physical interaction between Htz1 and CdtB (Figure 13). Moreover, chromatin immunoprecipitation also could not detect CdtB interaction with chromatin (Figure 14).

It is possible that we could not detect the physical interaction because of low IP efficiency. In addition, the use of whole cell extract in the immunoprecipitation assay may not allow detection of weak or transient interactions in the nucleus. Thus, further optimization of the assay or the use of more sensitive methods for the detection of protein-protein interaction should be performed.

To further examine the interaction between CdtB and chromatin, we tested the *in vitro* DNase activity of CdtB on chromatin substrates. Unfortunately, we were not able to consistently obtain intact chromatin preparation and purified CdtB activity for the experiment.

### 1.2. CdtB nuclear localization

As a genotoxin, CdtB needs to be translocated to the nucleus to target host DNA. AaCdtB contains a nuclear localization signal [54], which is required for cytotoxicity in both mammalian and yeast cells [51]. This suggests that CdtB uses similar mechanism for nuclear translocation in yeast and that yeast could be a good model to study this process. One possible explanation for CdtB resistance could be the reduction in nuclear localization. We investigated intracellular localization of CdtB using several approaches, including cell fractionation, intracellular immunofluorescence and CdtB-EGFP fusion protein. We could observe the best result with CdtB-EGFP. However, since EGFP alone could also enter the yeast nuclei [235], we calculated the ratio of nuclear localization of CdtB-EGFP in comparison to EGFP alone. Our results showed

that nuclear localization was reduced in most CdtB resistant mutants (Figures 21 and 22) suggesting that the reduction of CdtB translocation into the nucleus is a factor that interrupt CdtB cytotoxicity in yeast.

It is unclear how deletions of chromatin regulators could disrupt nuclear localization of CdtB. Interestingly, several units of SWR complex play a role in vacuolar protein sorting (VPS). This is related to the Carboxypeptidase Y (CPY) pathway, a major transport pathway of newly synthesized proteins from the trans-Golgi network to the pre-vacuolar compartment (PVC) [236]. Among CdtB resistant mutants, several mutants showed reduced nuclear localization of CdtB, including *htz1Δ*, *swr1Δ*, *swc2Δ*, *swc6Δ*, *arp6Δ*, and *arp5Δ* (Figures 21 and 22). Interestingly, aberrant secretion of ER proteins has also been observed in several of these mutants, including *htz1Δ*, *swr1Δ*, *swc2Δ/vps72Δ*, *swc6Δ/vps71Δ*, *arp6Δ*, and *arp5Δ* [237]. This implies that the defect in protein sorting of these mutants may explain the reduced CdtB nuclear localization. Moreover, *htz1Δ* showed defect in retrograde protein transport from Golgi to ER [238]. In addition, Htz1-K14 acetylation also affects ER homeostasis [238]. Moreover, *swr1Δ*, *swc2Δ*, *swc3Δ*, *swc6Δ*, *arp6Δ*, and *sir4Δ* led to secretion of ER resident proteins [202, 237]. These studies suggest that Htz1 and SWR complex may regulate protein trafficking, which could affect CdtB translocation to the nucleus.

### 1.3. DNA damage

Although CdtB nuclear localization was reduced in CdtB resistant mutants, CdtB was still observed in the nuclei of these mutants. Thus, we asked if it could cause DNA breaks. We previously showed that yeast strains defective in homologous recombination (HR), for example, *rad50Δ*, a subunit of DNA damage sensor, is hypersensitive to CdtB [51]. Thus, we could use *rad50Δ* as a DNA damage indicator to determine if CdtB causes DNA damage in CdtB resistant strains. Interestingly, when combining *rad50Δ* with various deletions that showed CdtB resistance, only *swc5Δrad50Δ* showed more CdtB resistance than *rad50Δ*. (Figure 25). This result suggests that CdtB can still cause DNA damage in most mutant strains, but there seems

to be less DNA damage in *swc5Δ*. A previous study showed that Swc5 is not restricted to +1 nucleosome [135], but distributes together with Swc4. Swc5 contains two domains; acidic domain and the BCNT domain. The acidic domain is identified as a binding domain for H2A-H2B dimer, whereas BCNT domain is required for Htz1 deposition [137]. The mechanism how the lack of Swc5 leads to CdtB resistance is unclear, but it appears to be distinct from that of SWR complex.

#### 1.4. DNA repair

Another hypothesis that could explain CdtB resistance in chromatin regulator mutants is their effects on gene expression that could indirectly lead to enhance DNA repair. The upregulation of DNA repair genes may rescue the cytotoxicity caused by CdtB. Through data mining, we found several DNA repair genes that respond to several kinds of DNA damaging agents [220-224]. Moreover, we searched for the DNA repair genes that are upregulated in CdtB resistant strains in the existing database [130, 225-228]. The genes in show upregulation in both conditions were further examined. Interestingly, we found that 3 DNA repair genes, *ADA2*, *MRC1*, and *SSL2*, are upregulated in most CdtB resistant mutants (Figure 29). This may promote cell survival.

Upregulation of *ADA2*, *MRC1*, and *SSL2* may lead to increased resistance to CdtB. In particular, *Mrc1* is an activator of Rad53, a DNA damage checkpoint kinase, upon DNA replication stress [239, 240]. Our previous study showed that Rad53 plays a more important role than Chk1 to promote yeast survival from CdtB-induced damage [51]. Therefore, the upregulation of *MRC1* may help activate Rad53 and increase resistance to CdtB. *Ssl2* is involved in the initiation of transcription and DNA repair [241-243]. Interestingly, overexpression of *SSL2* led to increased resistance to Adriamycin and Actinomycin D, but not Aclarubicin [244]. Adriamycin and Aclarubicin inhibit topoisomerase II [245-247], while Actinomycin D is an inhibitor of RNA synthesis [248]. Adriamycin intercalates into the DNA, inhibits the progression of topoisomerase II [249] and causes DNA damage [250]. Moreover, a previous study reported that Etoposide, a topoisomerase II inhibitor, induces nucleoplasmic reticulum (NR) formation, a network of

nuclear envelope invagination associated with DNA damage induced by ionizing radiation [251-253]. Recently, Azzi-Martin and colleagues demonstrated that *Helicobacter hepaticus* CDT (HhCDT) induces NR formation to promote the survival of hepatocytic and intestinal cell lines [254]. This evidence suggests that NR may be important for survival from DNA damage. Besides, the helicase function of Ssl2 has been shown to protect yeast from Adriamycin toxicity [255]. Thus, the deletion of certain chromatin regulatory genes may upregulate DNA repair genes and increase resistance to DNA break inducing agents.

### 1.5. Other mechanisms

The recruitment of DNA-DSBs to the nuclear periphery is required to prevent illegitimate recombination of DNA breaks. Swr1 and Htz1 are required for DSB localization to the nuclear periphery, but not Arp5 or Arp8 [146]. The lack of Swr1 or Htz1 may increase cell death in DNA damage conditions [146, 256]. In addition, a previous study demonstrated that Htz1 acetylation, which required Swr1 to deposit Htz1 into nucleosome, enhanced sister chromatid cohesion and promote HR repair [257].

Moreover, INO80 complex also plays a role in homologous recombination repair. INO80 is required for the dynamic histone exchange from Htz1 to H2A, which is a substrate for Mec1/Tel1 to become phosphorylated H2A ( $\gamma$ -H2A) [258].  $\gamma$ -H2A plays a fundamental role in homologous repair because it is required for sister chromatin cohesion which stabilizes the homologous sequence at the break site [259, 260]. It has been reported that Arp5 was recruited the DSB site caused by HO-endonuclease in a  $\gamma$ -H2A-independent manner [261]. However, how Arp5-facilitate CdtB function is unclear. Interestingly, despite their roles in DSB repair, mutations of SWR and INO80 subunits could still lead to CdtB resistance.

Chromatin structure controls DNA accessibility and heterochromatin could limit DNA-protein interaction. Silence Information Regulator or SIR regulates heterochromatin formation at three major loci in the genome, including telomeric region, yeast mating type loci, and ribosomal DNA (rDNA) region. Htz1 is a key player to prevent

heterochromatin spreading [130, 231]. Lack of Htz1 leads to heterochromatin spreading that may limit access of DNA-binding proteins, including CdtB. According to the phenotypic testing, deletion of *SIR2* and *SIR3*, but not *SIR4*, subunits are resistant to CdtB (Figures 5 and 6). Sir4 plays a role in the key initial step in heterochromatin formation at telomere or mating type loci, but not rDNA locus [162]. Furthermore, rDNA silencing is required to prevent homologous recombination and maintain rDNA integrity [262]. Thus, heterochromatin formation at rDNA loci may be a process that involves in CdtB function.

Because Sir2 is involved in many important cellular processes, there could be several mechanisms how *sir2Δ* confers CdtB resistance. Examples include the effect on yeast lifespan and rDNA silencing. In the laboratory, yeast replicative lifespan is approximately 20 – 30 cycles [263]. *SIR2* deletion leads to reduced replicative lifespan in yeast [149]. The accumulation of Extrachromosomal rDNA circles (ERC) and increased homologous recombination of the rDNA loci contribute to cellular aging [168].

Smith and colleagues proposed a model of Sir2-dependent rDNA silencing regulation [171]. The magnitude of rDNA silencing depends on the amount of Sir2 in the nucleolus. Since Sir4 can bind to Sir2 and may prevent it from entering the nucleolus, *sir4Δ* may lead to increased nucleolar Sir2 concentration [264] and increased rDNA silencing. Thus, *sir4Δ* may have an opposite effect to *sir2Δ* as we observed for CdtB resistance. The reduction of rDNA silencing in *sir2Δ* and *sir3Δ* may contribute to CdtB resistance.

Beside chromatin silencing function, Sir2 is also involved in DNA damage repair. The deletion of *SIR2* leads to hypersensitivity to methyl methanesulfonate (MMS), a DNA alkylating agent [265]. However, SIR complex is shown to promote non-homologous end joining (NHEJ) at S-phase [266]. We previously showed that homologous recombination is more important than NHEJ for the repair of CdtB-induced damages [51]. Therefore, the defect in NHEJ of *SIR* deletion may not affect cell survival upon CdtB expression.

Altogether our study on chromatin regulators suggests that their effects on CdtB activity appear to be indirect, through their roles in the regulation of protein translocation

and gene expression. However, further investigations are still required to identify the gene expression changes that lead to CdtB resistance.

## 2. Genome-wide identification of host genes required for CdtB cytotoxicity.

To further explore the effects of host factors on CdtB activity, we took advantage of the yeast deletion library and performed a genome-wide screen for deletions that confer resistance to CdtB intoxication. Similar genome-wide screening has been done to identify mutations that are hypersensitive to CdtB, but none for CdtB resistance [50]. The yeast deletion library has been very useful to study the effects of chemicals, toxins or drugs [267]. The limitation of this screen is that we are unable to investigate the role of essential genes on CdtB function [268]. Moreover, as the primary screening was based on growth on galactose media, mutants that do not grow well on galactose or have a slow growth phenotype would not be detected. It also cannot be ascertained here what compensatory mechanisms or indirect effects occur in the mutant strains while they survive from CdtB.

We identified 243 genes with diverse roles and localized in different cellular compartments that may be required for CdtB toxicity. As in the cases of other toxins, the interaction with host proteins is often required by effector molecules to exert their effect on target molecules. [269] We hypothesized that these genes may be required for CdtB to translocate into the nucleus or to act on its DNA substrates. We observed an enrichment of genes related to the biological process GO term “organic anion transport” (16 genes) (**Figure 31 and Table 16**). Most of these genes are responsible for fatty acid, amino acid and protein transport, and the gene products are found on the membranes and vacuoles, and function as transmembrane transporters.

Previous studies suggest that CdtB subunit is transported to the nucleus by retrograde pathway via golgi complex and ER [63]. A previous report using insertional mutagenesis in haploid human cells identified mutations in 12 genes that are differentially required for the toxicity of CDTs from 4 different bacterial species [270]. CDT was shown to require sphingomyelin synthase 1 (SGMS1), synaptogyrin 2

(SYNGR2), Golgi glycoprotein 1 (GLG1) and the vacuolar ATPase subunit 2 (ATP6V0A2), which are membrane proteins involved in membrane binding and internalization. Unlike in natural intoxication when CdtA and CdtC bind to the host cell surface [60], CdtB was heterologously expressed in our yeast model [51]. Thus, we could not study the pathway from the cell membrane to the ER, but we could focus on the translocation from the ER to the nucleus. Interestingly, several ER-associated genes were identified in our screen, including *HRD3*, a component of the ER-associated protein degradation (ERAD) pathway. ERAD pathway has previously been implicated in host cell entry and toxicity of several bacterial toxins, including AaCDT and HdCDT, but not CjCDT [271]. We speculate that the deletions of ERAD component genes would have a similar effect on HdCDT, but this requires further tests. Together, our results added to the current knowledge and further suggest that the functions of the organic anion transport process and endomembrane system play important roles in facilitating CdtB translocation and cytotoxicity.

We examined the translocation using EGFP-tagged CdtB using confocal fluorescence microscopy (Figures 33 and 34). Our results showed that all of the 16 mutants associated with the GO term organic anion transport showed less CdtB nuclear localization than the wildtype strain. Therefore, the reduction of CdtB nuclear transport could be a factor that lead to CdtB resistant phenotype.

Among these 16 genes, 5 genes are involved in fatty acid and phospholipid transport. *PDR17* and *SFH5* belong to SFH family, whose function is the regulation of phosphoinositides transfer [272]. Deletion of *PDR17* leads to abnormal phospholipid composition of the cell membrane by increasing phosphatidylcholine (PC) and decreasing phosphatidylethanolamine (PE) [273]. Phosphatidylethanolamine is an important component for the structure and function of mitochondria and other intracellular organelles [274]. In addition, *ups1Δ* also shows CdtB resistance. Ups1 controls PE production by maintaining the level of Psd1, a phosphatidylserine decarboxylase. The loss of Ups1 leads to a decrease in Psd1 level and, subsequently, PE production [275]. Since autophagosome formation requires PE [276], *pdr17Δ* and

*ups1Δ* may decrease autophagy. Moreover, *ups1Δ* also has decreased level of Cardiolipin (CL) [275], which plays a role in the regulation of cytochrome-c release from mitochondria [277-279]. Cytochrome c release is an important step that initiates intrinsic apoptosis. PE and CL are both important for mitochondrial function. The mitochondrial membrane potential requires PE and CL for the import of pre-proteins into and across the inner membrane. The roles of these genes suggest that autophagy, apoptosis and mitochondrial function may be important for CdtB-induced cell death. However, the underlying mechanisms require further investigations.

Furthermore, 65 genes localized to the nucleus were identified in this screen. These genes are of particular interest since it is unknown if CdtB requires interactions with any host proteins or cofactors to damage the DNA. Genes with functions related to DNA metabolism and chromatin may be involved in the interaction of CdtB with DNA. In contrast to the phenotype of selected chromatin regulator mutants we examined in the first part, we identified only *sir3Δ* from the genome-wide screen. This may be due to the reduced growth rate of other mutants on galactose media. Moreover, the level of resistance may not be high enough to be detected in the screen. The genes identified in this study have diverse cellular functions. How these different processes in the nucleus could affect CdtB toxicity requires further investigations.

Taken together, this study has shed light on the complex interplay of multiple host factors with CdtB that were previously unknown. Moreover, there have been very few genome-wide studies on mutations that confer resistance to genotoxins or other DNA damaging agents. Thus, our results add to the current knowledge on host-toxin interactions. Although our screen was performed in yeast, several of the genes identified have orthologs in humans. Thus, this study provides additional candidates to be further tested in human cells. The information will be useful for further investigation into strategies to combat these genotoxins and/or to employ them in other applications, such as in cancer therapy.



## CHAPTER VI: CONCLUSION

- 1) The absence of certain important subunits of chromatin remodelers namely Htz1, Swr1, Swc2, Swc5, Swc6, Arp6, Arp5, Sir2, and Sir3 reduced CdtB cytotoxicity.
- 2) Nuclear localization of CdtB was reduced in several chromatin regulatory mutants, such as *htz1Δ*, *swr1Δ*, *swc2Δ*, *swc6Δ*, *arp6Δ*, and *arp5Δ*, consistent with their defect in ER protein homeostasis. However, CdtB nuclear translocation did not appear to be completely blocked in these mutants.
- 3) CdtB could still induce DNA damage in several CdtB resistant mutants, such as the strains lacking *HTZ1*, *SWR1*, *SWC2*, *SWC6*, *ARP6*, *SIR2*, or *SIR3*, suggesting that resistant mechanism may occur after CdtB damage.
- 4) Three DNA repair genes, *ADA2*, *MRC1* and *SSL2*, were upregulated in CdtB resistant mutants, except for *swr1Δ* and *swc2Δ*.
- 5) CdtB resistant mechanisms of chromatin regulatory mutants may involve multiple cellular processes, such as reduced nuclear localization of CdtB and upregulation of DNA repair genes.
- 6) The genome-wide screen for gene deletions that confer CdtB resistance suggests that several cellular processes may be required for CdtB toxicity. These include organic anion transport, ER-associated protein degradation pathway, and phospholipid transport.
- 7) The reduction of nuclear localization may be a factor that leads to CdtB resistance in the mutants lacking organic anion transport genes.

## REFERENCES



จุฬาลงกรณ์มหาวิทยาลัย  
**CHULALONGKORN UNIVERSITY**

1. Johnson, W.M. and H. Lior, *A new heat-labile cytolethal distending toxin (CLDT) produced by Campylobacter spp.* Microb Pathog, 1988. 4(2): p. 115-26.
2. Johnson, W.M. and H. Lior, *A new heat-labile cytolethal distending toxin (CLDT) produced by Escherichia coli isolates from clinical material.* Microb Pathog, 1988. 4(2): p. 103-13.
3. Jinadasa, R.N., et al., *Cytolethal distending toxin: a conserved bacterial genotoxin that blocks cell cycle progression, leading to apoptosis of a broad range of mammalian cell lineages.* Microbiology, 2011. 157(Pt 7): p. 1851-75.
4. Smith, J.L. and D.O. Bayles, *The contribution of cytolethal distending toxin to bacterial pathogenesis.* Crit Rev Microbiol, 2006. 32(4): p. 227-48.
5. DiRienzo, J.M., *Uptake and processing of the cytolethal distending toxin by mammalian cells.* Toxins (Basel), 2014. 6(11): p. 3098-116.
6. Ahmed, H.J., et al., *Prevalence of cdtABC genes encoding cytolethal distending toxin among Haemophilus ducreyi and Actinobacillus actinomycetemcomitans strains.* Journal of Medical Microbiology, 2001. 50(10): p. 860-864.
7. Belibasakis, G., et al., *Inhibited proliferation of human periodontal ligament cells and gingival fibroblasts by Actinobacillus actinomycetemcomitans: involvement of the cytolethal distending toxin.* Eur J Oral Sci, 2002. 110(5): p. 366-73.
8. Tan, K.S., K.P. Song, and G. Ong, *Cytolethal distending toxin of Actinobacillus actinomycetemcomitans - Occurrence and association with periodontal disease.* Journal of Periodontal Research, 2002. 37(4): p. 268-272.
9. Wang, X.Q., et al., *Prevalence and distribution of Aggregatibacter actinomycetemcomitans and its cdtB gene in subgingival plaque of Chinese periodontitis patients.* BMC Oral Health, 2014. 14.
10. Fox, J.G., et al., *Gastroenteritis in NF-kappaB-deficient mice is produced with wild-type Campylobacter jejuni but not with C. jejuni lacking cytolethal distending toxin despite persistent colonization with both strains.* Infect Immun, 2004. 72(2): p. 1116-25.

11. Hickey, T.E., et al., *Campylobacter jejuni* cytolethal distending toxin mediates release of interleukin-8 from intestinal epithelial cells. *Infect Immun*, 2000. **68**(12): p. 6535-41.
12. Kaakoush, N.O., et al., *Global Epidemiology of Campylobacter Infection*. *Clin Microbiol Rev*, 2015. **28**(3): p. 687-720.
13. Buc, E., et al., *High Prevalence of Mucosa-Associated E-coli Producing Cyclomodulin and Genotoxin in Colon Cancer*. *Plos One*, 2013. **8**(2).
14. Svensson, L.A., P. Henning, and T. Lagergard, *The cytolethal distending toxin of Haemophilus ducreyi inhibits endothelial cell proliferation*. *Infection and Immunity*, 2002. **70**(5): p. 2665-2669.
15. Wising, C., et al., *The cytolethal distending toxin of Haemophilus ducreyi aggravates dermal lesions in a rabbit model of chancroid*. *Microbes and Infection*, 2005. **7**(5-6): p. 867-874.
16. Ge, Z.M., et al., *Bacterial cytolethal distending toxin promotes the development of dysplasia in a model of microbially induced hepatocarcinogenesis*. *Cellular Microbiology*, 2007. **9**(8): p. 2070-2080.
17. Liyanage, N.P.M., et al., *Contribution of Helicobacter hepaticus Cytolethal Distending Toxin Subunits to Human Epithelial Cell Cycle Arrest and Apoptotic Death in vitro*. *Helicobacter*, 2013. **18**(6): p. 433-443.
18. Haghjoo, E. and J.E. Galan, *Salmonella typhi* encodes a functional cytolethal distending toxin that is delivered into host cells by a bacterial-internalization pathway. *Proc Natl Acad Sci U S A*, 2004. **101**(13): p. 4614-9.
19. Miller, R. and M. Wiedmann, *Dynamic Duo-The Salmonella Cytolethal Distending Toxin Combines ADP-Ribosyltransferase and Nuclease Activities in a Novel Form of the Cytolethal Distending Toxin*. *Toxins (Basel)*, 2016. **8**(5).
20. Hyma, K.E., et al., *Evolutionary genetics of a new pathogenic Escherichia species: Escherichia albertii and related Shigella boydii strains*. *J Bacteriol*, 2005. **187**(2): p. 619-28.

21. Okuda, J., et al., *Examination of diarrheogenicity of cytolethal distending toxin: suckling mouse response to the products of the cdtABC genes of Shigella dysenteriae*. *Infect Immun*, 1997. **65**(2): p. 428-33.
22. Fais, T., et al., *Impact of CDT Toxin on Human Diseases*. *Toxins* (Basel), 2016. **8**(7).
23. Scott, D.A. and J.B. Kaper, *Cloning and sequencing of the genes encoding Escherichia coli cytolethal distending toxin*. *Infect Immun*, 1994. **62**(1): p. 244-51.
24. Pickett, C.L., et al., *Cloning, sequencing, and expression of the Escherichia coli cytolethal distending toxin genes*. *Infect Immun*, 1994. **62**(3): p. 1046-51.
25. Gargi, A., M. Reno, and S.R. Blanke, *Bacterial toxin modulation of the eukaryotic cell cycle: are all cytolethal distending toxins created equally?* *Front Cell Infect Microbiol*, 2012. **2**: p. 124.
26. Haubek, D., *The highly leukotoxic JP2 clone of Aggregatibacter actinomycetemcomitans: evolutionary aspects, epidemiology and etiological role in aggressive periodontitis*. *APMIS Suppl*, 2010(130): p. 1-53.
27. Black, R.E., et al., *Experimental Campylobacter jejuni infection in humans*. *J Infect Dis*, 1988. **157**(3): p. 472-9.
28. Cope, L.D., et al., *A diffusible cytotoxin of Haemophilus ducreyi*. *Proc Natl Acad Sci U S A*, 1997. **94**(8): p. 4056-61.
29. Stevens, M.K., et al., *A hemoglobin-binding outer membrane protein is involved in virulence expression by Haemophilus ducreyi in an animal model*. *Infect Immun*, 1996. **64**(5): p. 1724-35.
30. Toth, I., et al., *Production of cytolethal distending toxins by pathogenic Escherichia coli strains isolated from human and animal sources: establishment of the existence of a new cdt variant (Type IV)*. *J Clin Microbiol*, 2003. **41**(9): p. 4285-91.
31. Pickett, C.L. and C.A. Whitehouse, *The cytolethal distending toxin family*. *Trends Microbiol*, 1999. **7**(7): p. 292-7.

32. Sugai, M., et al., *The cell cycle-specific growth-inhibitory factor produced by Actinobacillus actinomycetemcomitans is a cytolethal distending toxin*. Infect Immun, 1998. **66**(10): p. 5008-19.
33. Yamada, T., et al., *Variation of loop sequence alters stability of cytolethal distending toxin (CDT): crystal structure of CDT from Actinobacillus actinomycetemcomitans*. Protein Sci, 2006. **15**(2): p. 362-72.
34. Nestic, D., Y. Hsu, and C.E. Stebbins, *Assembly and function of a bacterial genotoxin*. Nature, 2004. **429**(6990): p. 429-33.
35. Hontz, J.S., et al., *Differences in crystal and solution structures of the cytolethal distending toxin B subunit: Relevance to nuclear translocation and functional activation*. J Biol Chem, 2006. **281**(35): p. 25365-72.
36. Peres, S.Y., et al., *A new cytolethal distending toxin (CDT) from Escherichia coli producing CNF2 blocks HeLa cell division in G2/M phase*. Mol Microbiol, 1997. **24**(5): p. 1095-107.
37. Comayras, C., et al., *Escherichia coli cytolethal distending toxin blocks the HeLa cell cycle at the G2/M transition by preventing cdc2 protein kinase dephosphorylation and activation*. Infect Immun, 1997. **65**(12): p. 5088-95.
38. Fahrner, J., et al., *Cytolethal distending toxin (CDT) is a radiomimetic agent and induces persistent levels of DNA double-strand breaks in human fibroblasts*. DNA Repair (Amst), 2014. **18**: p. 31-43.
39. Sert, V., et al., *The bacterial cytolethal distending toxin (CDT) triggers a G2 cell cycle checkpoint in mammalian cells without preliminary induction of DNA strand breaks*. Oncogene, 1999. **18**(46): p. 6296-304.
40. Elwell, C.A. and L.A. Dreyfus, *DNase I homologous residues in CdtB are critical for cytolethal distending toxin-mediated cell cycle arrest*. Mol Microbiol, 2000. **37**(4): p. 952-63.
41. Shenker, B.J., et al., *A novel mode of action for a microbial-derived immunotoxin: the cytolethal distending toxin subunit B exhibits*

- phosphatidylinositol 3,4,5-triphosphate phosphatase activity*. J Immunol, 2007. **178**(8): p. 5099-108.
42. Lara-Tejero, M. and J.E. Galan, *A bacterial toxin that controls cell cycle progression as a deoxyribonuclease I-like protein*. Science, 2000. **290**(5490): p. 354-7.
  43. Tribble, D.R., et al., *Assessment of the duration of protection in Campylobacter jejuni experimental infection in humans*. Infect Immun, 2010. **78**(4): p. 1750-9.
  44. DiRienzo, J.M., et al., *Functional and structural characterization of chimeras of a bacterial genotoxin and human type I DNase*. FEMS Microbiol Lett, 2009. **291**(2): p. 222-31.
  45. Dlakic, M., *Functionally unrelated signalling proteins contain a fold similar to Mg<sup>2+</sup>-dependent endonucleases*. Trends Biochem Sci, 2000. **25**(6): p. 272-3.
  46. Damek-Poprawa, M., et al., *Localization of Aggregatibacter actinomycetemcomitans cytolethal distending toxin subunits during intoxication of live cells*. Infect Immun, 2012. **80**(8): p. 2761-70.
  47. Dlakic, M., *Is CdtB a nuclease or a phosphatase?* Science, 2001. **291**(5504): p. 547.
  48. Shenker, B.J., et al., *The toxicity of the Aggregatibacter actinomycetemcomitans cytolethal distending toxin correlates with its phosphatidylinositol-3,4,5-triphosphate phosphatase activity*. Cell Microbiol, 2016. **18**(2): p. 223-43.
  49. Boesze-Battaglia, K., et al., *The Aggregatibacter actinomycetemcomitans Cytolethal Distending Toxin Active Subunit CdtB Contains a Cholesterol Recognition Sequence Required for Toxin Binding and Subunit Internalization*. Infect Immun, 2015. **83**(10): p. 4042-55.
  50. Kitagawa, T., H. Hoshida, and R. Akada, *Genome-wide analysis of cellular response to bacterial genotoxin CdtB in yeast*. Infect Immun, 2007. **75**(3): p. 1393-402.
  51. Matangkasombut, O., et al., *Cytolethal distending toxin from Aggregatibacter actinomycetemcomitans induces DNA damage, S/G2 cell cycle arrest, and*

- caspase- independent death in a Saccharomyces cerevisiae model. Infect Immun*, 2010. **78**(2): p. 783-92.
52. Heymont, J., et al., *TEP1, the yeast homolog of the human tumor suppressor gene PTEN/MMAC1/TEP1, is linked to the phosphatidylinositol pathway and plays a role in the developmental process of sporulation. Proc Natl Acad Sci U S A*, 2000. **97**(23): p. 12672-7.
53. McSweeney, L.A. and L.A. Dreyfus, *Nuclear localization of the Escherichia coli cytolethal distending toxin CdtB subunit. Cell Microbiol*, 2004. **6**(5): p. 447-58.
54. Nishikubo, S., et al., *An N-terminal segment of the active component of the bacterial genotoxin cytolethal distending toxin B (CDTB) directs CDTB into the nucleus. J Biol Chem*, 2003. **278**(50): p. 50671-81.
55. Shenker, B.J., et al., *Blockade of the PI-3K signalling pathway by the Aggregatibacter actinomycetemcomitans cytolethal distending toxin induces macrophages to synthesize and secrete pro-inflammatory cytokines. Cell Microbiol*, 2014. **16**(9): p. 1391-404.
56. Tsuruda, K., et al., *CdtC-Induced Processing of Membrane-Bound CdtA Is a Crucial Step in Aggregatibacter actinomycetemcomitans Cytolethal Distending Toxin Holotoxin Formation. Infect Immun*, 2018. **86**(3).
57. Ueno, Y., et al., *Biogenesis of the Actinobacillus actinomycetemcomitans cytolethal distending toxin holotoxin. Infect Immun*, 2006. **74**(6): p. 3480-7.
58. Frisan, T., *Bacterial genotoxins: The long journey to the nucleus of mammalian cells. Biochim Biophys Acta*, 2016. **1858**(3): p. 567-75.
59. Lindmark, B., et al., *Outer membrane vesicle-mediated release of cytolethal distending toxin (CDT) from Campylobacter jejuni. BMC Microbiol*, 2009. **9**: p. 220.
60. Hu, X., D. Nestic, and C.E. Stebbins, *Comparative structure-function analysis of cytolethal distending toxins. Proteins*, 2006. **62**(2): p. 421-34.
61. Hu, X. and C.E. Stebbins, *Dynamics and assembly of the cytolethal distending toxin. Proteins*, 2006. **65**(4): p. 843-55.



62. Mise, K., et al., *Involvement of ganglioside GM3 in G(2)/M cell cycle arrest of human monocytic cells induced by Actinobacillus actinomycetemcomitans cytolethal distending toxin*. Infect Immun, 2005. **73**(8): p. 4846-52.
63. Guerra, L., et al., *Cellular internalization of cytolethal distending toxin: a new end to a known pathway*. Cell Microbiol, 2005. **7**(7): p. 921-34.
64. Carette, J.E., et al., *Haploid genetic screens in human cells identify host factors used by pathogens*. Science, 2009. **326**(5957): p. 1231-5.
65. Prokazova, N.V., et al., *Ganglioside GM3 and its biological functions*. Biochemistry (Mosc), 2009. **74**(3): p. 235-49.
66. Bainbridge, P., *Wound healing and the role of fibroblasts*. J Wound Care, 2013. **22**(8): p. 407-8, 410-12.
67. Belibasakis, G.N., et al., *Cell cycle arrest of human gingival fibroblasts and periodontal ligament cells by Actinobacillus actinomycetemcomitans: involvement of the cytolethal distending toxin*. APMIS, 2004. **112**(10): p. 674-85.
68. Cortes-Bratti, X., et al., *The Haemophilus ducreyi cytolethal distending toxin induces cell cycle arrest and apoptosis via the DNA damage checkpoint pathways*. J Biol Chem, 2001. **276**(7): p. 5296-302.
69. Hassane, D.C., R.B. Lee, and C.L. Pickett, *Campylobacter jejuni cytolethal distending toxin promotes DNA repair responses in normal human cells*. Infection and Immunity, 2003. **71**(1): p. 541-545.
70. Jain, D., et al., *Cell cycle arrest & apoptosis of epithelial cell line by cytolethal distending toxin positive Campylobacter jejuni*. Indian J Med Res, 2009. **129**(4): p. 418-23.
71. Liyanage, N.P., et al., *Helicobacter hepaticus cytolethal distending toxin causes cell death in intestinal epithelial cells via mitochondrial apoptotic pathway*. Helicobacter, 2010. **15**(2): p. 98-107.
72. Sato, T., et al., *p53-independent expression of p21(CIP1/WAF1) in plasmacytic cells during G(2) cell cycle arrest induced by Actinobacillus*

- actinomycetemcomitans* cytolethal distending toxin. Infection and Immunity, 2002. **70**(2): p. 528-534.
73. Shenker, B.J., et al., *Actinobacillus actinomycetemcomitans* immunosuppressive protein is a member of the family of cytolethal distending toxins capable of causing a G2 arrest in human T cells. J Immunol, 1999. **162**(8): p. 4773-80.
  74. Whitehouse, C.A., et al., *Campylobacter jejuni* cytolethal distending toxin causes a G2-phase cell cycle block. Infect Immun, 1998. **66**(5): p. 1934-40.
  75. Cortes-Bratti, X., T. Frisan, and M. Thelestam, *The cytolethal distending toxins induce DNA damage and cell cycle arrest*. Toxicon, 2001. **39**(11): p. 1729-36.
  76. Li, L., et al., *The Haemophilus ducreyi cytolethal distending toxin activates sensors of DNA damage and repair complexes in proliferating and non-proliferating cells*. Cell Microbiol, 2002. **4**(2): p. 87-99.
  77. Lock, R.B., et al., *Concentration-dependent differences in the mechanisms by which caffeine potentiates etoposide cytotoxicity in HeLa cells*. Cancer Res, 1994. **54**(18): p. 4933-9.
  78. Rabin, S.D., J.G. Flitton, and D.R. Demuth, *Aggregatibacter actinomycetemcomitans cytolethal distending toxin induces apoptosis in nonproliferating macrophages by a phosphatase-independent mechanism*. Infect Immun, 2009. **77**(8): p. 3161-9.
  79. Shenker, B.J., et al., *Expression of the cytolethal distending toxin (Cdt) operon in Actinobacillus actinomycetemcomitans: evidence that the CdtB protein is responsible for G2 arrest of the cell cycle in human T cells*. J Immunol, 2000. **165**(5): p. 2612-8.
  80. Shenker, B.J., et al., *Induction of apoptosis in human T cells by Actinobacillus actinomycetemcomitans cytolethal distending toxin is a consequence of G2 arrest of the cell cycle*. J Immunol, 2001. **167**(1): p. 435-41.
  81. Ohara, M., et al., *Cytolethal distending toxin induces caspase-dependent and -independent cell death in MOLT-4 cells*. Infect Immun, 2008. **76**(10): p. 4783-91.

82. Ohara, M., et al., *Caspase-2 and caspase-7 are involved in cytolethal distending toxin-induced apoptosis in Jurkat and MOLT-4 T-cell lines*. *Infect Immun*, 2004. **72**(2): p. 871-9.
83. Kassebaum, N.J., et al., *Global burden of severe periodontitis in 1990-2010: a systematic review and meta-regression*. *J Dent Res*, 2014. **93**(11): p. 1045-53.
84. Henderson, B., et al., *Molecular pathogenicity of the oral opportunistic pathogen Actinobacillus actinomycetemcomitans*. *Annu Rev Microbiol*, 2003. **57**: p. 29-55.
85. Fine, D.H., et al., *Aggregatibacter actinomycetemcomitans and its relationship to initiation of localized aggressive periodontitis: longitudinal cohort study of initially healthy adolescents*. *J Clin Microbiol*, 2007. **45**(12): p. 3859-69.
86. Mayer, M.P., et al., *Identification of a cytolethal distending toxin gene locus and features of a virulence-associated region in Actinobacillus actinomycetemcomitans*. *Infect Immun*, 1999. **67**(3): p. 1227-37.
87. van Winkelhoff, A.J. and J. Slots, *Actinobacillus actinomycetemcomitans and Porphyromonas gingivalis in nonoral infections*. *Periodontol 2000*, 1999. **20**: p. 122-35.
88. Belibasakis, G.N., et al., *The cytolethal distending toxin induces receptor activator of NF-kappaB ligand expression in human gingival fibroblasts and periodontal ligament cells*. *Infect Immun*, 2005. **73**(1): p. 342-51.
89. Belibasakis, G.N., et al., *Cytokine responses of human gingival fibroblasts to Actinobacillus actinomycetemcomitans cytolethal distending toxin*. *Cytokine*, 2005. **30**(2): p. 56-63.
90. Ishihara, K. and T. Hirano, *IL-6 in autoimmune disease and chronic inflammatory proliferative disease*. *Cytokine Growth Factor Rev*, 2002. **13**(4-5): p. 357-68.
91. Ohara, M., et al., *Topical application of Aggregatibacter actinomycetemcomitans cytolethal distending toxin induces cell cycle arrest in the rat gingival epithelium in vivo*. *J Periodontal Res*, 2011. **46**(3): p. 389-95.

92. Hassane, D.C., R.B. Lee, and C.L. Pickett, *Campylobacter jejuni* cytolethal distending toxin promotes DNA repair responses in normal human cells. *Infect Immun*, 2003. **71**(1): p. 541-5.
93. Aragon, V., K. Chao, and L.A. Dreyfus, *Effect of cytolethal distending toxin on F-actin assembly and cell division in Chinese hamster ovary cells*. *Infect Immun*, 1997. **65**(9): p. 3774-80.
94. Gelfanova, V., E.J. Hansen, and S.M. Spinola, *Cytolethal distending toxin of Haemophilus ducreyi induces apoptotic death of Jurkat T cells*. *Infect Immun*, 1999. **67**(12): p. 6394-402.
95. Lee, M.G. and P. Nurse, *Complementation used to clone a human homologue of the fission yeast cell cycle control gene cdc2*. *Nature*, 1987. **327**(6117): p. 31-5.
96. Tsai, L.H., E. Harlow, and M. Meyerson, *Isolation of the human cdk2 gene that encodes the cyclin A- and adenovirus E1A-associated p33 kinase*. *Nature*, 1991. **353**(6340): p. 174-7.
97. Fattaey, A. and R.N. Booher, *Myt1: a Wee1-type kinase that phosphorylates Cdc2 on residue Thr14*. *Prog Cell Cycle Res*, 1997. **3**: p. 233-40.
98. Ferguson, A.M., et al., *Normal cell cycle and checkpoint responses in mice and cells lacking Cdc25B and Cdc25C protein phosphatases*. *Mol Cell Biol*, 2005. **25**(7): p. 2853-60.
99. Smith, J., et al., *The ATM-Chk2 and ATR-Chk1 Pathways in DNA Damage Signaling and Cancer*. *Advances in Cancer Research*, Vol 108, 2010. **108**: p. 73-112.
100. Pfeiffer, P., W. Goedecke, and G. Obe, *Mechanisms of DNA double-strand break repair and their potential to induce chromosomal aberrations*. *Mutagenesis*, 2000. **15**(4): p. 289-302.
101. Chapman, J.R., M.R. Taylor, and S.J. Boulton, *Playing the end game: DNA double-strand break repair pathway choice*. *Mol Cell*, 2012. **47**(4): p. 497-510.

102. Lavin, M.F., *ATM and the Mre11 complex combine to recognize and signal DNA double-strand breaks*. *Oncogene*, 2007. **26**(56): p. 7749-58.
103. Harada, K. and G.R. Ogden, *An overview of the cell cycle arrest protein, p21(WAF1)*. *Oral Oncol*, 2000. **36**(1): p. 3-7.
104. Shiloh, Y., *ATM and related protein kinases: safeguarding genome integrity*. *Nat Rev Cancer*, 2003. **3**(3): p. 155-68.
105. Fedor, Y., et al., *From single-strand breaks to double-strand breaks during S-phase: a new mode of action of the Escherichia coli Cytotoxic Distending Toxin*. *Cell Microbiol*, 2013. **15**(1): p. 1-15.
106. Toczyski, D.P., D.J. Galgoczy, and L.H. Hartwell, *CDC5 and CKII control adaptation to the yeast DNA damage checkpoint*. *Cell*, 1997. **90**(6): p. 1097-106.
107. Oza, P., et al., *Mechanisms that regulate localization of a DNA double-strand break to the nuclear periphery*. *Genes Dev*, 2009. **23**(8): p. 912-27.
108. Schober, H., et al., *Yeast telomerase and the SUN domain protein Mps3 anchor telomeres and repress subtelomeric recombination*. *Genes Dev*, 2009. **23**(8): p. 928-38.
109. Luger, K., M.L. Dechassa, and D.J. Tremethick, *New insights into nucleosome and chromatin structure: an ordered state or a disordered affair?* *Nature Reviews Molecular Cell Biology*, 2012. **13**(7): p. 436-447.
110. Luger, K., et al., *Crystal structure of the nucleosome core particle at 2.8 angstrom resolution*. *Nature*, 1997. **389**(6648): p. 251-260.
111. Smith, S. and B. Stillman, *Stepwise assembly of chromatin during DNA replication in vitro*. *EMBO J*, 1991. **10**(4): p. 971-80.
112. Berezney, R., et al., *The nuclear matrix: A structural milieu for genomic function*. *International Review of Cytology*, Vol 162a, 1995. **162a**: p. 1-65.
113. English, C.M., et al., *Structural basis for the histone chaperone activity of Asf1*. *Cell*, 2006. **127**(3): p. 495-508.

114. Henikoff, S., *Nucleosome destabilization in the epigenetic regulation of gene expression*. Nature Reviews Genetics, 2008. **9**(1): p. 15-26.
115. Kulaeva, O.I., F.K. Hsieh, and V.M. Studitsky, *RNA polymerase complexes cooperate to relieve the nucleosomal barrier and evict histones*. Proceedings of the National Academy of Sciences of the United States of America, 2010. **107**(25): p. 11325-11330.
116. Weber, C.M. and S. Henikoff, *Histone variants: dynamic punctuation in transcription*. Genes & Development, 2014. **28**(7): p. 672-682.
117. Tagami, H., et al., *Histone H3.1 and H3.3 complexes mediate nucleosome assembly pathways dependent or independent of DNA synthesis*. Cell, 2004. **116**(1): p. 51-61.
118. Stoler, S., et al., *A Mutation in Cse4, an Essential Gene Encoding a Novel Chromatin-Associated Protein in Yeast, Causes Chromosome Nondisjunction and Cell-Cycle Arrest at Mitosis*. Genes & Development, 1995. **9**(5): p. 573-586.
119. Venkatesh, S. and J.L. Workman, *Histone exchange, chromatin structure and the regulation of transcription*. Nat Rev Mol Cell Biol, 2015. **16**(3): p. 178-89.
120. Gerhold, C.B. and S.M. Gasser, *INO80 and SWR complexes: relating structure to function in chromatin remodeling*. Trends Cell Biol, 2014. **24**(11): p. 619-31.
121. Yen, K.Y., V. Vinayachandran, and B.F. Pugh, *SWR-C and INO80 Chromatin Remodelers Recognize Nucleosome-free Regions Near+1 Nucleosomes*. Cell, 2013. **154**(6): p. 1246-1256.
122. Papamichos-Chronakis, M., et al., *Global Regulation of H2A.Z Localization by the INO80 Chromatin-Remodeling Enzyme Is Essential for Genome Integrity*. Cell, 2011. **144**(2): p. 200-213.
123. Mizuguchi, G., et al., *ATP-driven exchange of histone H2AZ variant catalyzed by SWR1 chromatin remodeling complex*. Science, 2004. **303**(5656): p. 343-8.
124. Sterner, D.E. and S.L. Berger, *Acetylation of histones and transcription-related factors*. Microbiology and Molecular Biology Reviews, 2000. **64**(2): p. 435-+.

125. Palladino, F., et al., *Sir3 and Sir4 Proteins Are Required for the Positioning and Integrity of Yeast Telomeres*. Cell, 1993. **75**(3): p. 543-555.
126. Smith, J.S. and J.D. Boeke, *An unusual form of transcriptional silencing in yeast ribosomal DNA*. Genes & Development, 1997. **11**(2): p. 241-254.
127. Rine, J., et al., *A suppressor of mating-type locus mutations in Saccharomyces cerevisiae: evidence for and identification of cryptic mating-type loci*. Genetics, 1979. **93**(4): p. 877-901.
128. Talbert, P.B. and S. Henikoff, *Histone variants - ancient wrap artists of the epigenome*. Nature Reviews Molecular Cell Biology, 2010. **11**(4): p. 264-275.
129. Suto, R.K., et al., *Crystal structure of a nucleosome core particle containing the variant histone H2A.Z*. Nature Structural Biology, 2000. **7**(12): p. 1121-1124.
130. Meneghini, M.D., M. Wu, and H.D. Madhani, *Conserved histone variant H2A.Z protects euchromatin from the ectopic spread of silent heterochromatin*. Cell, 2003. **112**(5): p. 725-36.
131. Kobor, M.S., et al., *A protein complex containing the conserved Swi2/Snf2-related ATPase Swr1p deposits histone variant H2A.Z into euchromatin*. Plos Biology, 2004. **2**(5): p. 587-599.
132. Watanabe, S. and C.L. Peterson, *The INO80 family of chromatin-remodeling enzymes: regulators of histone variant dynamics*. Cold Spring Harb Symp Quant Biol, 2010. **75**: p. 35-42.
133. Luk, E., et al., *Stepwise Histone Replacement by SWR1 Requires Dual Activation with Histone H2A.Z and Canonical Nucleosome*. Cell, 2010. **143**(5): p. 725-736.
134. Wu, W.H., et al., *Swc2 is a widely conserved H2AZ-binding module essential for ATP-dependent histone exchange*. Nature Structural & Molecular Biology, 2005. **12**(12): p. 1064-1071.
135. Yen, K., V. Vinayachandran, and B.F. Pugh, *SWR-C and INO80 chromatin remodelers recognize nucleosome-free regions near +1 nucleosomes*. Cell, 2013. **154**(6): p. 1246-56.

136. Wu, W.H., et al., *Swc2 is a widely conserved H2AZ-binding module essential for ATP-dependent histone exchange*. *Nat Struct Mol Biol*, 2005. **12**(12): p. 1064-71.
137. Sun, L. and E. Luk, *Dual function of Swc5 in SWR remodeling ATPase activation and histone H2A eviction*. *Nucleic Acids Res*, 2017. **45**(17): p. 9931-9946.
138. Wu, W.H., et al., *N terminus of Swr1 binds to histone H2AZ and provides a platform for subunit assembly in the chromatin remodeling complex*. *J Biol Chem*, 2009. **284**(10): p. 6200-7.
139. Udugama, M., A. Sabri, and B. Bartholomew, *The INO80 ATP-Dependent Chromatin Remodeling Complex Is a Nucleosome Spacing Factor*. *Molecular and Cellular Biology*, 2011. **31**(4): p. 662-673.
140. Santisteban, M.S., M. Hang, and M.M. Smith, *Histone variant H2A.Z and RNA polymerase II transcription elongation*. *Mol Cell Biol*, 2011. **31**(9): p. 1848-60.
141. Yu, E.Y., et al., *Regulation of telomere structure and functions by subunits of the INO80 chromatin remodeling complex*. *Mol Cell Biol*, 2007. **27**(16): p. 5639-49.
142. Zhang, H., et al., *The Yaf9 component of the SWR1 and NuA4 complexes is required for proper gene expression, histone H4 acetylation, and Htz1 replacement near telomeres*. *Mol Cell Biol*, 2004. **24**(21): p. 9424-36.
143. Papamichos-Chronakis, M., J.E. Krebs, and C.L. Peterson, *Interplay between Ino80 and Swr1 chromatin remodeling enzymes regulates cell cycle checkpoint adaptation in response to DNA damage*. *Genes Dev*, 2006. **20**(17): p. 2437-49.
144. van Attikum, H., et al., *Recruitment of the INO80 complex by H2A phosphorylation links ATP-dependent chromatin remodeling with DNA double-strand break repair*. *Cell*, 2004. **119**(6): p. 777-88.
145. Morrison, A.J., et al., *INO80 and gamma-H2AX interaction links ATP-dependent chromatin remodeling to DNA damage repair*. *Cell*, 2004. **119**(6): p. 767-75.
146. Horigome, C., et al., *SWR1 and INO80 chromatin remodelers contribute to DNA double-strand break perinuclear anchorage site choice*. *Mol Cell*, 2014. **55**(4): p. 626-39.



147. van Attikum, H., O. Fritsch, and S.M. Gasser, *Distinct roles for SWR1 and INO80 chromatin remodeling complexes at chromosomal double-strand breaks*. EMBO J, 2007. **26**(18): p. 4113-25.
148. Holmes, S.G., et al., *Hyperactivation of the silencing proteins, Sir2p and Sir3p, causes chromosome loss*. Genetics, 1997. **145**(3): p. 605-14.
149. Kaeberlein, M., M. McVey, and L. Guarente, *The SIR2/3/4 complex and SIR2 alone promote longevity in Saccharomyces cerevisiae by two different mechanisms*. Genes Dev, 1999. **13**(19): p. 2570-80.
150. Imai, S., et al., *Transcriptional silencing and longevity protein Sir2 is an NAD-dependent histone deacetylase*. Nature, 2000. **403**(6771): p. 795-800.
151. Moazed, D., et al., *Silent information regulator protein complexes in Saccharomyces cerevisiae: a SIR2/SIR4 complex and evidence for a regulatory domain in SIR4 that inhibits its interaction with SIR3*. Proc Natl Acad Sci U S A, 1997. **94**(6): p. 2186-91.
152. Aparicio, O.M., B.L. Billington, and D.E. Gottschling, *Modifiers of position effect are shared between telomeric and silent mating-type loci in S. cerevisiae*. Cell, 1991. **66**(6): p. 1279-87.
153. Klar, A.J., S. Fogel, and K. Macleod, *MAR1-a Regulator of the HMa and HMalpha Loci in SACCHAROMYCES CEREVISIAE*. Genetics, 1979. **93**(1): p. 37-50.
154. Rine, J. and I. Herskowitz, *Four genes responsible for a position effect on expression from HML and HMR in Saccharomyces cerevisiae*. Genetics, 1987. **116**(1): p. 9-22.
155. Gottlieb, S. and R.E. Esposito, *A new role for a yeast transcriptional silencer gene, SIR2, in regulation of recombination in ribosomal DNA*. Cell, 1989. **56**(5): p. 771-6.
156. Ivy, J.M., A.J. Klar, and J.B. Hicks, *Cloning and characterization of four SIR genes of Saccharomyces cerevisiae*. Mol Cell Biol, 1986. **6**(2): p. 688-702.

157. Bitterman, K.J., et al., *Inhibition of silencing and accelerated aging by nicotinamide, a putative negative regulator of yeast sir2 and human SIRT1*. J Biol Chem, 2002. **277**(47): p. 45099-107.
158. Lin, S.J., P.A. Defossez, and L. Guarente, *Requirement of NAD and SIR2 for life-span extension by calorie restriction in Saccharomyces cerevisiae*. Science, 2000. **289**(5487): p. 2126-8.
159. Gardner, K.A., J. Rine, and C.A. Fox, *A region of the Sir1 protein dedicated to recognition of a silencer and required for interaction with the Orc1 protein in saccharomyces cerevisiae*. Genetics, 1999. **151**(1): p. 31-44.
160. Kimmerly, W., et al., *Roles of two DNA-binding factors in replication, segregation and transcriptional repression mediated by a yeast silencer*. EMBO J, 1988. **7**(7): p. 2241-53.
161. Triolo, T. and R. Sternglanz, *Role of interactions between the origin recognition complex and SIR1 in transcriptional silencing*. Nature, 1996. **381**(6579): p. 251-3.
162. Kueng, S., M. Oppikofer, and S.M. Gasser, *SIR proteins and the assembly of silent chromatin in budding yeast*. Annu Rev Genet, 2013. **47**: p. 275-306.
163. Smith, J.S. and J.D. Boeke, *An unusual form of transcriptional silencing in yeast ribosomal DNA*. Genes Dev, 1997. **11**(2): p. 241-54.
164. Shou, W., et al., *Exit from mitosis is triggered by Tem1-dependent release of the protein phosphatase Cdc14 from nucleolar RENT complex*. Cell, 1999. **97**(2): p. 233-44.
165. Straight, A.F., et al., *Net1, a Sir2-associated nucleolar protein required for rDNA silencing and nucleolar integrity*. Cell, 1999. **97**(2): p. 245-56.
166. Huang, J. and D. Moazed, *Association of the RENT complex with nontranscribed and coding regions of rDNA and a regional requirement for the replication fork block protein Fob1 in rDNA silencing*. Genes Dev, 2003. **17**(17): p. 2162-76.

167. Ha, C.W., et al., *The beta-1,3-glucanoyltransferase Gas1 regulates Sir2-mediated rDNA stability in Saccharomyces cerevisiae*. *Nucleic Acids Res*, 2014. **42**(13): p. 8486-99.
168. Park, P.U., P.A. Defossez, and L. Guarente, *Effects of mutations in DNA repair genes on formation of ribosomal DNA circles and life span in Saccharomyces cerevisiae*. *Mol Cell Biol*, 1999. **19**(5): p. 3848-56.
169. Kennedy, B.K., et al., *Redistribution of silencing proteins from telomeres to the nucleolus is associated with extension of life span in S. cerevisiae*. *Cell*, 1997. **89**(3): p. 381-91.
170. Sinclair, D.A., K. Mills, and L. Guarente, *Accelerated aging and nucleolar fragmentation in yeast sgs1 mutants*. *Science*, 1997. **277**(5330): p. 1313-6.
171. Smith, J.S., et al., *Distribution of a limited Sir2 protein pool regulates the strength of yeast rDNA silencing and is modulated by Sir4p*. *Genetics*, 1998. **149**(3): p. 1205-19.
172. Tropberger, P., et al., *Regulation of Transcription through Acetylation of H3K122 on the Lateral Surface of the Histone Octamer*. *Cell*, 2013. **152**(4): p. 859-872.
173. Williams, S.K., D. Truong, and J.K. Tyler, *Acetylation in the globular core of histone H3 on lysine-56 promotes chromatin disassembly during transcriptional activation*. *Proc Natl Acad Sci U S A*, 2008. **105**(26): p. 9000-5.
174. Halley, J.E., et al., *Roles for H2A.Z and its acetylation in GAL1 transcription and gene induction, but not GAL1-transcriptional memory*. *PLoS Biol*, 2010. **8**(6): p. e1000401.
175. Jacobson, S.J., P.M. Laurenson, and L. Pillus, *Functional analyses of chromatin modifications in yeast*. *Methods Enzymol*, 2004. **377**: p. 3-55.
176. Lee, T.I. and R.A. Young, *Transcription of eukaryotic protein-coding genes*. *Annu Rev Genet*, 2000. **34**: p. 77-137.
177. Drogen, F., et al., *Phosphorylation of the MEKK Ste11p by the PAK-like kinase Ste20p is required for MAP kinase signaling in vivo*. *Curr Biol*, 2000. **10**(11): p. 630-9.

178. Wu, C., et al., *Molecular characterization of Ste20p, a potential mitogen-activated protein or extracellular signal-regulated kinase kinase (MEK) kinase kinase from Saccharomyces cerevisiae*. J Biol Chem, 1995. **270**(27): p. 15984-92.
179. Raitt, D.C., F. Posas, and H. Saito, *Yeast Cdc42 GTPase and Ste20 PAK-like kinase regulate Sho1-dependent activation of the Hog1 MAPK pathway*. EMBO J, 2000. **19**(17): p. 4623-31.
180. Gancedo, J.M., *Control of pseudohyphae formation in Saccharomyces cerevisiae*. FEMS Microbiol Rev, 2001. **25**(1): p. 107-23.
181. Sheu, Y.J., Y. Barral, and M. Snyder, *Polarized growth controls cell shape and bipolar bud site selection in Saccharomyces cerevisiae*. Mol Cell Biol, 2000. **20**(14): p. 5235-47.
182. Goehring, A.S., et al., *Synthetic lethal analysis implicates Ste20p, a p21-activated protein kinase, in polarisome activation*. Mol Biol Cell, 2003. **14**(4): p. 1501-16.
183. Holly, S.P. and K.J. Blumer, *PAK-family kinases regulate cell and actin polarization throughout the cell cycle of Saccharomyces cerevisiae*. J Cell Biol, 1999. **147**(4): p. 845-56.
184. Wu, C., et al., *The phosphorylation site for Ste20p-like protein kinases is essential for the function of myosin-I in yeast*. J Biol Chem, 1997. **272**(49): p. 30623-6.
185. Eby, J.J., et al., *Actin cytoskeleton organization regulated by the PAK family of protein kinases*. Curr Biol, 1998. **8**(17): p. 967-70.
186. Hofken, T. and E. Schiebel, *A role for cell polarity proteins in mitotic exit*. EMBO J, 2002. **21**(18): p. 4851-62.
187. Ramer, S.W. and R.W. Davis, *A dominant truncation allele identifies a gene, STE20, that encodes a putative protein kinase necessary for mating in Saccharomyces cerevisiae*. Proc Natl Acad Sci U S A, 1993. **90**(2): p. 452-6.

188. Ahn, S.H., et al., *Sterile 20 kinase phosphorylates histone H2B at serine 10 during hydrogen peroxide-induced apoptosis in S. cerevisiae*. *Cell*, 2005. **120**(1): p. 25-36.
189. Wood, K., M. Tellier, and S. Murphy, *DOT1L and H3K79 Methylation in Transcription and Genomic Stability*. *Biomolecules*, 2018. **8**(1).
190. van Leeuwen, F., P.R. Gafken, and D.E. Gottschling, *Dot1p modulates silencing in yeast by methylation of the nucleosome core*. *Cell*, 2002. **109**(6): p. 745-56.
191. Siggers, K.A. and C.F. Lesser, *The Yeast Saccharomyces cerevisiae: a versatile model system for the identification and characterization of bacterial virulence proteins*. *Cell Host Microbe*, 2008. **4**(1): p. 8-15.
192. Dujon, B., *The yeast genome project: what did we learn?* *Trends Genet*, 1996. **12**(7): p. 263-70.
193. Heinicke, S., et al., *The Princeton Protein Orthology Database (P-POD): a comparative genomics analysis tool for biologists*. *PLoS One*, 2007. **2**(8): p. e766.
194. Baudin, A., et al., *A simple and efficient method for direct gene deletion in Saccharomyces cerevisiae*. *Nucleic Acids Res*, 1993. **21**(14): p. 3329-30.
195. Winzeler, E.A., et al., *Functional characterization of the S. cerevisiae genome by gene deletion and parallel analysis*. *Science*, 1999. **285**(5429): p. 901-6.
196. Dymond, J.S., *Preparation of genomic DNA from Saccharomyces cerevisiae*. *Methods Enzymol*, 2013. **529**: p. 153-60.
197. Brachmann, C.B., et al., *Designer deletion strains derived from Saccharomyces cerevisiae S288C: a useful set of strains and plasmids for PCR-mediated gene disruption and other applications*. *Yeast*, 1998. **14**(2): p. 115-32.
198. Froger, A. and J.E. Hall, *Transformation of plasmid DNA into E. coli using the heat shock method*. *J Vis Exp*, 2007(6): p. 253.
199. Gietz, R.D. and R.A. Woods, *Transformation of yeast by lithium acetate/single-stranded carrier DNA/polyethylene glycol method*. *Methods Enzymol*, 2002. **350**: p. 87-96.

200. Keogh, M.C., et al., *Kin28 is found within TFIIH and a Kin28-Ccl1-Tfb3 trimer complex with differential sensitivities to T-loop phosphorylation*. Mol Cell Biol, 2002. **22**(5): p. 1288-97.
201. Towbin, H., T. Staehelin, and J. Gordon, *Electrophoretic transfer of proteins from polyacrylamide gels to nitrocellulose sheets: procedure and some applications*. Proc Natl Acad Sci U S A, 1979. **76**(9): p. 4350-4.
202. Keogh, M.C., et al., *The Saccharomyces cerevisiae histone H2A variant Htz1 is acetylated by NuA4*. Genes Dev, 2006. **20**(6): p. 660-5.
203. Keogh, M.C., V. Podolny, and S. Buratowski, *Bur1 kinase is required for efficient transcription elongation by RNA polymerase II*. Mol Cell Biol, 2003. **23**(19): p. 7005-18.
204. Gorg, A., et al., *The current state of two-dimensional electrophoresis with immobilized pH gradients*. Electrophoresis, 2000. **21**(6): p. 1037-53.
205. Niu, W., G.T. Hart, and E.M. Marcotte, *High-throughput immunofluorescence microscopy using yeast spheroplast cell-based microarrays*. Methods Mol Biol, 2011. **706**: p. 83-95.
206. Bolte, S. and F.P. Cordelieres, *A guided tour into subcellular colocalization analysis in light microscopy*. J Microsc, 2006. **224**(Pt 3): p. 213-32.
207. Reese, J.C., H. Zhang, and Z. Zhang, *Isolation of highly purified yeast nuclei for nuclease mapping of chromatin structure*. Methods Mol Biol, 2008. **463**: p. 43-53.
208. Mizuno, T., Y. Masuda, and K. Irie, *The Saccharomyces cerevisiae AMPK, Snf1, Negatively Regulates the Hog1 MAPK Pathway in ER Stress Response*. PLoS Genet, 2015. **11**(9): p. e1005491.
209. Gartenberg, M.R. and J.S. Smith, *The Nuts and Bolts of Transcriptionally Silent Chromatin in Saccharomyces cerevisiae*. Genetics, 2016. **203**(4): p. 1563-99.
210. Rudner, A.D., et al., *A nonhistone protein-protein interaction required for assembly of the SIR complex and silent chromatin*. Mol Cell Biol, 2005. **25**(11): p. 4514-28.

211. Bokoch, G.M., *Biology of the p21-activated kinases*. Annu Rev Biochem, 2003. 72: p. 743-81.
212. Song, J., et al., *Molecular interactions of the Gbeta binding domain of the Ste20p/PAK family of protein kinases. An isolated but fully functional Gbeta binding domain from Ste20p is only partially folded as shown by heteronuclear NMR spectroscopy*. J Biol Chem, 2001. 276(44): p. 41205-12.
213. Ushinsky, S.C., et al., *Histone H1 in Saccharomyces cerevisiae*. Yeast, 1997. 13(2): p. 151-61.
214. Veron, M., et al., *Histone H1 of Saccharomyces cerevisiae inhibits transcriptional silencing*. Genetics, 2006. 173(2): p. 579-87.
215. Tosi, A., et al., *Structure and subunit topology of the INO80 chromatin remodeler and its nucleosome complex*. Cell, 2013. 154(6): p. 1207-19.
216. Deisenhofer, J., *Crystallographic refinement and atomic models of a human Fc fragment and its complex with fragment B of protein A from Staphylococcus aureus at 2.9- and 2.8-Å resolution*. Biochemistry, 1981. 20(9): p. 2361-70.
217. Bolte, S. and F.P. CordeliÈRes, *A guided tour into subcellular colocalization analysis in light microscopy*. Journal of Microscopy, 2006. 224(3): p. 213-232.
218. Manders, E.M.M., F.J. Verbeek, and J.A. Aten, *Measurement of co-localization of objects in dual-colour confocal images*. Journal of Microscopy, 1993. 169(3): p. 375-382.
219. Nelson, R.G. and W.L. Fangman, *Nucleosome organization of the yeast 2-micrometer DNA plasmid: a eukaryotic minichromosome*. Proc Natl Acad Sci U S A, 1979. 76(12): p. 6515-9.
220. Gasch, A.P., et al., *Genomic expression responses to DNA-damaging agents and the regulatory role of the yeast ATR homolog Mec1p*. Mol Biol Cell, 2001. 12(10): p. 2987-3003.
221. Fry, R.C., T.G. Sambandan, and C. Rha, *DNA damage and stress transcripts in Saccharomyces cerevisiae mutant sgs1*. Mech Ageing Dev, 2003. 124(7): p. 839-46.

222. Caba, E., et al., *Differentiating mechanisms of toxicity using global gene expression analysis in Saccharomyces cerevisiae*. *Mutat Res*, 2005. **575**(1-2): p. 34-46.
223. Takagi, Y., et al., *Ubiquitin ligase activity of TFIIH and the transcriptional response to DNA damage*. *Mol Cell*, 2005. **18**(2): p. 237-43.
224. Benton, M.G., et al., *Analyzing the dose-dependence of the Saccharomyces cerevisiae global transcriptional response to methyl methanesulfonate and ionizing radiation*. *BMC Genomics*, 2006. **7**: p. 305.
225. Hu, Z., P.J. Killion, and V.R. Iyer, *Genetic reconstruction of a functional transcriptional regulatory network*. *Nat Genet*, 2007. **39**(5): p. 683-7.
226. Morillo-Huesca, M., et al., *The SWR1 histone replacement complex causes genetic instability and genome-wide transcription misregulation in the absence of H2A.Z*. *PLoS One*, 2010. **5**(8): p. e12143.
227. Yoshida, T., et al., *Actin-related protein Arp6 influences H2A.Z-dependent and -independent gene expression and links ribosomal protein genes to nuclear pores*. *PLoS Genet*, 2010. **6**(4): p. e1000910.
228. Klopf, E., et al., *INO80 represses osmostress induced gene expression by resetting promoter proximal nucleosomes*. *Nucleic Acids Res*, 2017. **45**(7): p. 3752-3766.
229. Ranjan, A., et al., *Nucleosome-free region dominates histone acetylation in targeting SWR1 to promoters for H2A.Z replacement*. *Cell*, 2013. **154**(6): p. 1232-45.
230. Watanabe, S., et al., *A histone acetylation switch regulates H2A.Z deposition by the SWR-C remodeling enzyme*. *Science*, 2013. **340**(6129): p. 195-9.
231. Krogan, N.J., et al., *A Snf2 family ATPase complex required for recruitment of the histone H2A variant Htz1*. *Mol Cell*, 2003. **12**(6): p. 1565-76.
232. Poli, J., S.M. Gasser, and M. Papamichos-Chronakis, *The INO80 remodeller in transcription, replication and repair*. *Philos Trans R Soc Lond B Biol Sci*, 2017. **372**(1731).



233. Kashiwaba, S., et al., *The mammalian INO80 complex is recruited to DNA damage sites in an ARP8 dependent manner*. *Biochem Biophys Res Commun*, 2010. **402**(4): p. 619-25.
234. Yen, K., et al., *Genome-wide nucleosome specificity and directionality of chromatin remodelers*. *Cell*, 2012. **149**(7): p. 1461-73.
235. Seibel, N.M., et al., *Nuclear localization of enhanced green fluorescent protein homomultimers*. *Anal Biochem*, 2007. **368**(1): p. 95-9.
236. Burd, C.G., M. Babst, and S.D. Emr, *Novel pathways, membrane coats and PI kinase regulation in yeast lysosomal trafficking*. *Semin Cell Dev Biol*, 1998. **9**(5): p. 527-33.
237. Bonangelino, C.J., E.M. Chavez, and J.S. Bonifacino, *Genomic screen for vacuolar protein sorting genes in Saccharomyces cerevisiae*. *Mol Biol Cell*, 2002. **13**(7): p. 2486-501.
238. Copic, A., et al., *Genomewide analysis reveals novel pathways affecting endoplasmic reticulum homeostasis, protein modification and quality control*. *Genetics*, 2009. **182**(3): p. 757-69.
239. Alcasabas, A.A., et al., *Mrc1 transduces signals of DNA replication stress to activate Rad53*. *Nat Cell Biol*, 2001. **3**(11): p. 958-65.
240. Osborn, A.J. and S.J. Elledge, *Mrc1 is a replication fork component whose phosphorylation in response to DNA replication stress activates Rad53*. *Genes Dev*, 2003. **17**(14): p. 1755-67.
241. Park, E., et al., *RAD25 (SSL2), the yeast homolog of the human xeroderma pigmentosum group B DNA repair gene, is essential for viability*. *Proc Natl Acad Sci U S A*, 1992. **89**(23): p. 11416-20.
242. Qiu, H., et al., *The Saccharomyces cerevisiae DNA repair gene RAD25 is required for transcription by RNA polymerase II*. *Genes Dev*, 1993. **7**(11): p. 2161-71.
243. Wang, Z., et al., *Transcription factor b (TFIIH) is required during nucleotide-excision repair in yeast*. *Nature*, 1994. **368**(6466): p. 74-6.

244. Furuchi, T., et al., *Overexpression of Ssl2p confers resistance to adriamycin and actinomycin D in Saccharomyces cerevisiae*. *Biochem Biophys Res Commun*, 2004. **314**(3): p. 844-8.
245. Bridewell, D.J., G.J. Finlay, and B.C. Baguley, *Differential actions of aclarubicin and doxorubicin: the role of topoisomerase I*. *Oncol Res*, 1997. **9**(10): p. 535-42.
246. Nitiss, J.L., P. Pourquier, and Y. Pommier, *Aclacinomycin A stabilizes topoisomerase I covalent complexes*. *Cancer Res*, 1997. **57**(20): p. 4564-9.
247. Sundman-Engberg, B., U. Tidefelt, and C. Paul, *Toxicity of cytostatic drugs to normal bone marrow cells in vitro*. *Cancer Chemother Pharmacol*, 1998. **42**(1): p. 17-23.
248. Perry, R.P. and D.E. Kelley, *Inhibition of RNA synthesis by actinomycin D: characteristic dose-response of different RNA species*. *J Cell Physiol*, 1970. **76**(2): p. 127-39.
249. Pommier, Y., et al., *DNA topoisomerases and their poisoning by anticancer and antibacterial drugs*. *Chem Biol*, 2010. **17**(5): p. 421-33.
250. Tacar, O., P. Sriamornsak, and C.R. Dass, *Doxorubicin: an update on anticancer molecular action, toxicity and novel drug delivery systems*. *J Pharm Pharmacol*, 2013. **65**(2): p. 157-70.
251. Dellaire, G., R. Kepkay, and D.P. Bazett-Jones, *High resolution imaging of changes in the structure and spatial organization of chromatin, gamma-H2A.X and the MRN complex within etoposide-induced DNA repair foci*. *Cell Cycle*, 2009. **8**(22): p. 3750-69.
252. Fricker, M., et al., *Interphase nuclei of many mammalian cell types contain deep, dynamic, tubular membrane-bound invaginations of the nuclear envelope*. *J Cell Biol*, 1997. **136**(3): p. 531-44.
253. Legartova, S., et al., *Nuclear structures surrounding internal lamin invaginations*. *J Cell Biochem*, 2014. **115**(3): p. 476-87.

254. Azzi-Martin, L., et al., *Cytolethal distending toxin induces the formation of transient messenger-rich ribonucleoprotein nuclear invaginations in surviving cells*. PLoS Pathog, 2019. **15**(9): p. e1007921.
255. Furuchi, T., et al., *Functions of yeast helicase Ssl2p that are essential for viability are also involved in protection from the toxicity of adriamycin*. Nucleic Acids Res, 2004. **32**(8): p. 2578-85.
256. Kawashima, S., et al., *The INO80 complex is required for damage-induced recombination*. Biochem Biophys Res Commun, 2007. **355**(3): p. 835-41.
257. Sharma, U., D. Stefanova, and S.G. Holmes, *Histone variant H2A.Z functions in sister chromatid cohesion in Saccharomyces cerevisiae*. Mol Cell Biol, 2013. **33**(17): p. 3473-81.
258. Shroff, R., et al., *Distribution and dynamics of chromatin modification induced by a defined DNA double-strand break*. Curr Biol, 2004. **14**(19): p. 1703-11.
259. Strom, L., et al., *Postreplicative recruitment of cohesin to double-strand breaks is required for DNA repair*. Mol Cell, 2004. **16**(6): p. 1003-15.
260. Unal, E., et al., *DNA damage response pathway uses histone modification to assemble a double-strand break-specific cohesin domain*. Mol Cell, 2004. **16**(6): p. 991-1002.
261. Bennett, G., M. Papamichos-Chronakis, and C.L. Peterson, *DNA repair choice defines a common pathway for recruitment of chromatin regulators*. Nat Commun, 2013. **4**: p. 2084.
262. Srivastava, R., R. Srivastava, and S.H. Ahn, *The Epigenetic Pathways to Ribosomal DNA Silencing*. Microbiol Mol Biol Rev, 2016. **80**(3): p. 545-63.
263. Steffen, K.K., B.K. Kennedy, and M. Kaeberlein, *Measuring replicative life span in the budding yeast*. J Vis Exp, 2009(28).
264. Gotta, M., et al., *Localization of Sir2p: the nucleolus as a compartment for silent information regulators*. EMBO J, 1997. **16**(11): p. 3243-55.
265. Martin, S.G., et al., *Relocalization of telomeric Ku and SIR proteins in response to DNA strand breaks in yeast*. Cell, 1999. **97**(5): p. 621-33.

266. Mills, K.D., D.A. Sinclair, and L. Guarente, *MEC1-dependent redistribution of the Sir3 silencing protein from telomeres to DNA double-strand breaks*. Cell, 1999. **97**(5): p. 609-20.
267. bel, K.H.ü., *Yeast - Based Chemical Genomic Approaches*. 2009.
268. Dos Santos, S.C., et al., *Yeast toxicogenomics: genome-wide responses to chemical stresses with impact in environmental health, pharmacology, and biotechnology*. Front Genet, 2012. **3**: p. 63.
269. Alouf, J.E., *Bacterial protein toxins. An overview*. Methods Mol Biol, 2000. **145**: p. 1-26.
270. Carette, J.E., et al., *Global gene disruption in human cells to assign genes to phenotypes by deep sequencing*. Nat Biotechnol, 2011. **29**(6): p. 542-6.
271. Eshraghi, A., et al., *Cytolethal distending toxins require components of the ER-associated degradation pathway for host cell entry*. PLoS Pathog, 2014. **10**(7): p. e1004295.
272. Griac, P., *Sec14 related proteins in yeast*. Biochim Biophys Acta, 2007. **1771**(6): p. 737-45.
273. van den Hazel, H.B., et al., *PDR16 and PDR17, two homologous genes of Saccharomyces cerevisiae, affect lipid biosynthesis and resistance to multiple drugs*. J Biol Chem, 1999. **274**(4): p. 1934-41.
274. Wu, W.I., et al., *A new gene involved in the transport-dependent metabolism of phosphatidylserine, PSTB2/PDR17, shares sequence similarity with the gene encoding the phosphatidylinositol/phosphatidylcholine transfer protein, SEC14*. J Biol Chem, 2000. **275**(19): p. 14446-56.
275. Tamura, Y., et al., *Phosphatidylethanolamine biosynthesis in mitochondria: phosphatidylserine (PS) trafficking is independent of a PS decarboxylase and intermembrane space proteins UPS1P and UPS2P*. J Biol Chem, 2012. **287**(52): p. 43961-71.
276. Kirisako, T., et al., *Formation process of autophagosome is traced with Apg8/Aut7p in yeast*. J Cell Biol, 1999. **147**(2): p. 435-46.

277. Gonzalvez, F. and E. Gottlieb, *Cardiolipin: setting the beat of apoptosis*. *Apoptosis*, 2007. **12**(5): p. 877-85.
278. Nomura, K., et al., *Mitochondrial phospholipid hydroperoxide glutathione peroxidase inhibits the release of cytochrome c from mitochondria by suppressing the peroxidation of cardiolipin in hypoglycaemia-induced apoptosis*. *Biochem J*, 2000. **351**(Pt 1): p. 183-93.
279. Shidoji, Y., et al., *Loss of molecular interaction between cytochrome c and cardiolipin due to lipid peroxidation*. *Biochem Biophys Res Commun*, 1999. **264**(2): p. 343-7.





APPENDIX

จุฬาลงกรณ์มหาวิทยาลัย  
CHULALONGKORN UNIVERSITY

Figure S1

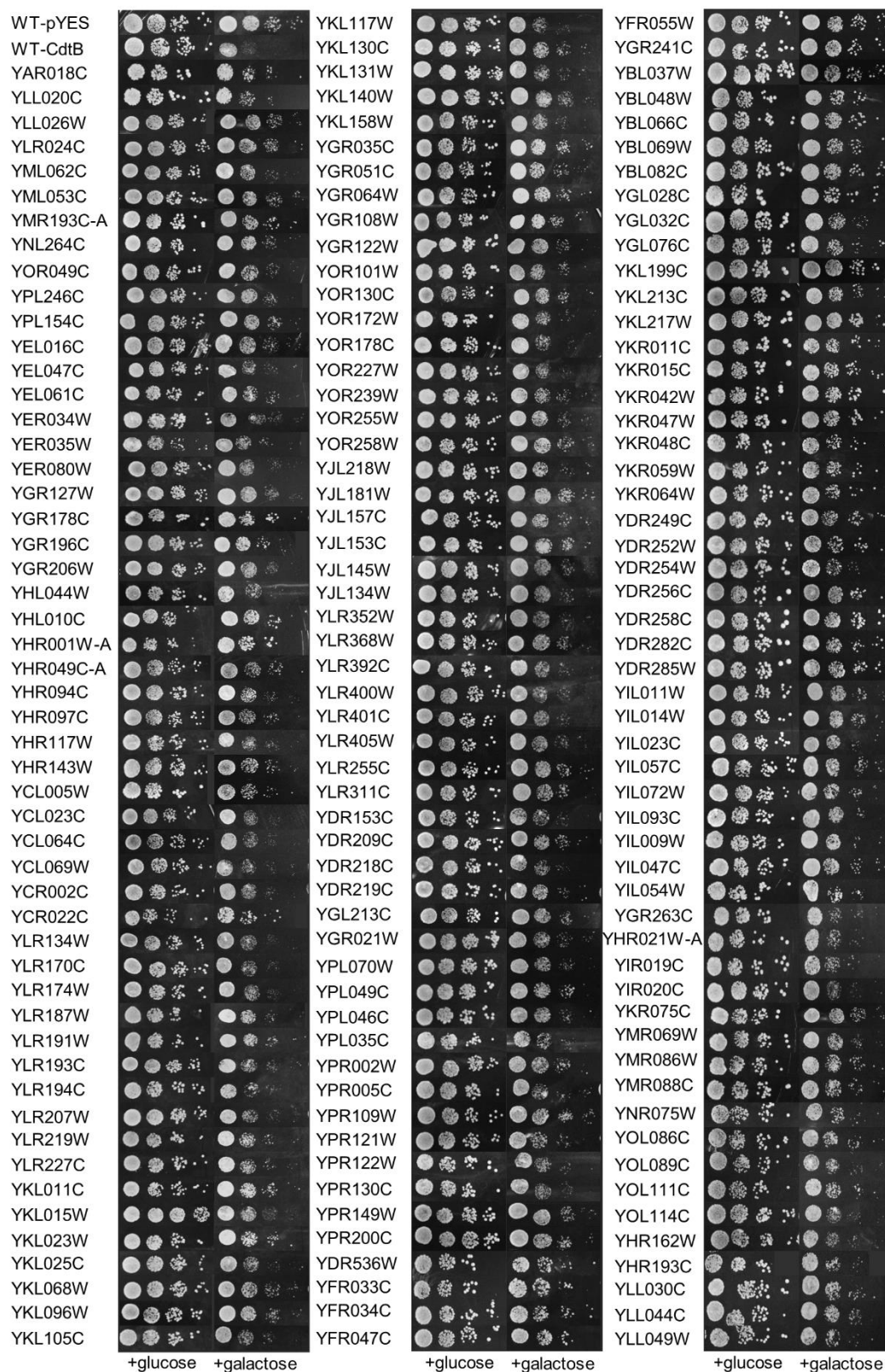
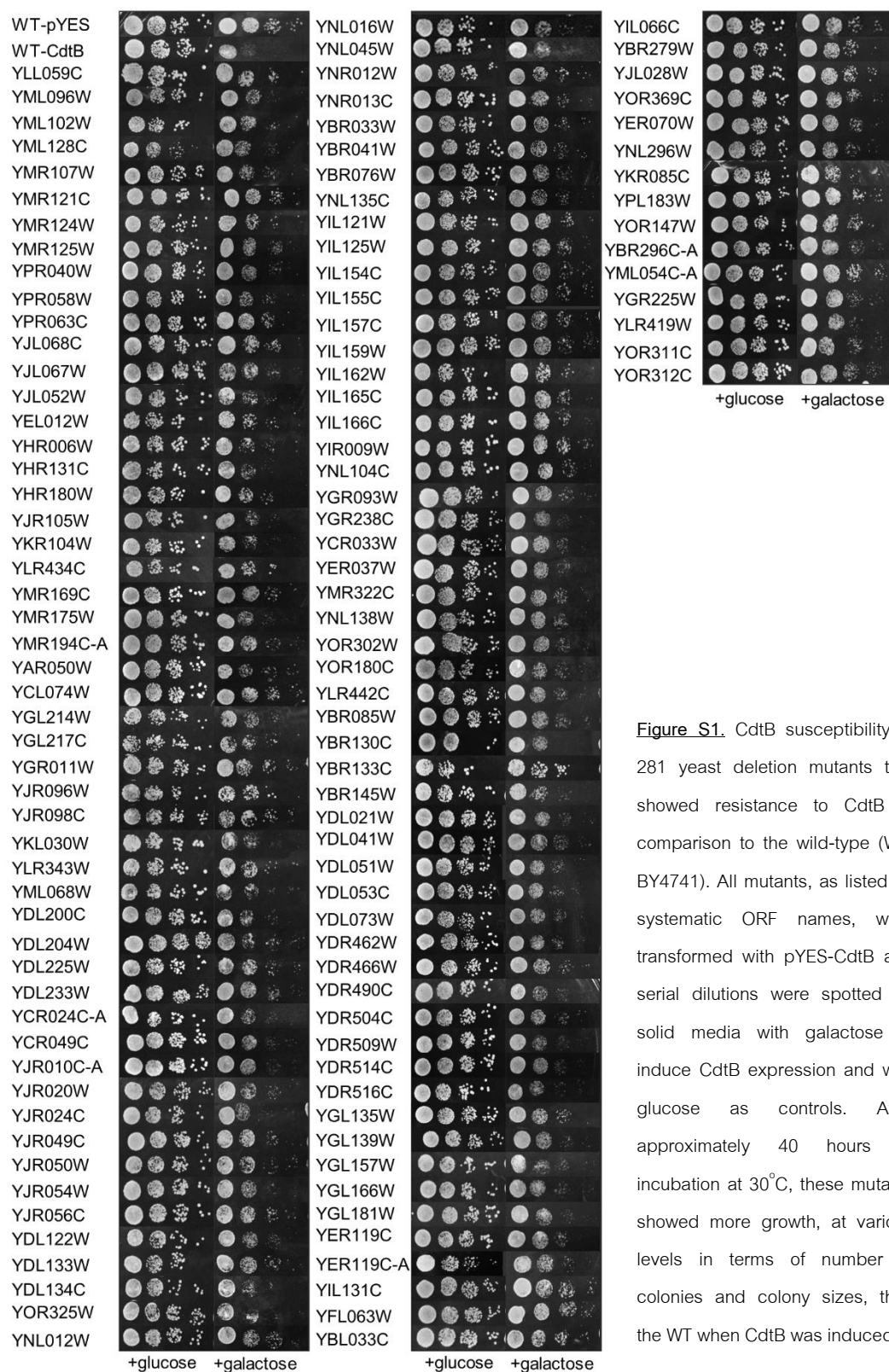


Figure S1 (continued)



**Figure S1.** CdtB susceptibility of 281 yeast deletion mutants that showed resistance to CdtB in comparison to the wild-type (WT; BY4741). All mutants, as listed by systematic ORF names, were transformed with pYES-CdtB and serial dilutions were spotted on solid media with galactose to induce CdtB expression and with glucose as controls. After approximately 40 hours of incubation at 30°C, these mutants showed more growth, at various levels in terms of number of colonies and colony sizes, than the WT when CdtB was induced.



#### Subleties of CdtB susceptibility protocol

- i. Inoculate fresh yeast colony which contain either pYES2-CdtB or empty vector from 2% glucose YNB -Ura plate into 5ml of 2% glucose YNB -Ura and incubate overnight at 30°C with 200 rpm shaking.
- ii. Next morning, samples were adjusted the OD<sub>600</sub> to 0.1 in 3ml of 2% sucrose YNB -Ura, then incubate for log phase at 30°C with 200 rpm shaking for 4-5 hours.
- iii. Measure the optical density and adjust to 0.1 OD<sub>600</sub> with sterile water in U-type 96-well plate. Afterward, 10-fold dilution was performed to each well for 4 times in 200 µl volume.
- iv. Samples were pipetted as 10 µl and spot on both 2% glucose and 2% galactose YNB -Ura agar and left for air dry.
- v. Spot plates were incubated in 30°C for 2-3 days.

#### Subleties of survival plating protocol

- i. Inoculate fresh yeast colony which contain either pYES2-CdtB or empty vector from 2% glucose YNB -Ura plate into 5ml of 2% glucose YNB -Ura and incubate overnight at 30°C with 200 rpm shaking.
- ii. Next morning, samples were adjusted the OD<sub>600</sub> to 0.1 in 3ml of 2% sucrose YNB -Ura, then incubate for log phase at 30°C with 200 rpm shaking for 4-5 hours.
- iii. Measure the optical density and adjust to 0.1 OD<sub>600</sub> with sterile water in U-type 96-well plate. Afterward, 10-fold dilution was performed to each well for 4-6 times in 200 µl volume.
- iv. Determine the number of cells in the well that may produce the colony counting range about 30-500 colonies with hemocytometer.
- v. Samples were pipette about 100 µl to plate on both 2% glucose and 2% galactose YNB -Ura agar.

- vi. Samples were incubated in 30°C for 4 days, then count all colonies on the plate.

#### Subleties of yeast whole cell extraction

- i. Inoculate a fresh yeast colony which contain either pYES2-CdtB or empty vector from 2% glucose YNB -Ura plate into 5ml of 2% glucose YNB -Ura and incubate overnight at 30°C with 200 rpm shaking.
- ii. Next morning, samples were adjusted the OD<sub>600</sub> to 0.1 in 10ml of 2% sucrose YNB -Ura, then incubate for log phase at 30°C with 200 rpm shaking for 4-5 hours.
- iii. Yeasts were washed with sterile water by centrifugation at 4,500 xg; RT; 5 min, then add new 10ml of 2% galactose YNB -Ura and incubate with the same condition for 6h.
- iv. Cells were collected and wash with sterile water, then discard all supernatant.
- v. Samples were resuspended with 200 µl lysis buffer (20mM HEPES pH7.6; 200 mM potassium acetate; 10% glycerol; 1mM EDTA) with proteinase inhibitors namely 0.1mM PMSF, 1 µM Pepstatin A, and 0.1mM 1,10-phenanthroline monohydrate.
- vi. Adding 0.5 mm glass beads to the sample's meniscus and incubate on ice for 2 min.
- vii. Samples were vortexed with the maximum speed for 1 min and rest on ice 1 min interval. Repeat for 3 times.
- viii. Stab the vial's bottom with 22g needle and place on a new vial tube. Afterward, spin these vials with 4,000 xg, 2min, 4°C.
- ix. The supernatants were collected after 14,000 xg, 10 min, 4°C centrifugation and determine protein concentration by Bradford assay.
- x. Samples can be kept at -80°C

### Subtleties of SDS-PAGE and antibody staining for CdtB protein expression detection

- i. 30  $\mu\text{g}$  of protein samples were mixed with 1x SDS loading buffer and boiled at  $100^{\circ}\text{C}$  for 10 min, then cool down at room temperature.
- ii. Denaturing acrylamide gel was prepared at 12.5% for resolving gel and 4% for stacking gel.
- iii. Samples were loaded into wells and applied electricity 100V for 1h 20min.
- iv. Semidry protein transfer method was use in this case. Nitrocellulose membrane was superimposed with acrylamide gel and applied electricity 20V for 1h.
- v. Membrane was blocked by 5% skim milk in PBST buffer (13.7 mM NaCl, 0.27 mM NaCl, 1 mM  $\text{Na}_2\text{HPO}_4$ , 0.2mM  $\text{KH}_2\text{PO}_4$ , 0.1% (v/v) Tween20) for 1h at room temperature.
- vi. Membrane was incubated with 1:5,000 Rabbit anti-CdtB serum in 5% skim milk in PBST buffer for 1h, then wash the membrane with PBST buffer for 3 times.
- vii. Membrane was incubated with 1:10,000 Goat anti-rabbit IgG polyclonal antibody, HRP conjugated (ENZO ADI-SAB-300) in 5% skim milk in PBST buffer for 1h, then wash the membrane with PBST buffer for 3 times.
- viii. ECL substrate (Pierce® ECL Western Blotting Substrate-Prod#32106) was mixed and overlay on the membrane, then the hypersensitive film (Amersham Hyperfilm™ ECL-28906838) was exposed to the membrane for detect the signal with various exposure time.
- ix. Hypersensitive film was developed and fixed in the reagents (Developer-Kodak GBX 4980553 and Fixer-Kodak GBX 4980561), then wash with water and let them dry at room temperature.

## VITA

|                       |   |
|-----------------------|---|
| NAME                  | Siriyod Denmongkolchai  |
| DATE OF BIRTH         | 7 September 1989  |
| PLACE OF BIRTH        | Bangkok   |
| INSTITUTIONS ATTENDED | I was graduated with bachelor's degree in medical technology from faculty of allied health science, Chulalongkorn University in 2012. I enrolled in interdisciplinary of medical microbiology, graduated school, Chulalongkorn University for philosophy degree in 2012. I am supported by Thailand Research Fund through the Royal Golden Jubilee Ph.D. Program (Grant No.PHD/1333/2554) to SD and OM. |
| PUBLICATION           | Genome-wide identification of host genes required for toxicity of bacterial cytolethal distending toxin in a yeast model.   |
| AWARD RECEIVED        | Outstanding poster presentation in RGJ-Ph.D. Congress 17 (June 8-11, 2016)  |